RNI No. MAHENG / 2017 / 74063
VOLUME 7 (Issue 1) January - June 2023

ISSN No. 2581-5911
BI-ANNUAL SUBSCRIPTION : Rs. 2000/-

G P GLOBALIZE RESEARCH JOURNAL OF CHEMISTRY

CODEN : GPGRAG

Abstracted in
Chemical Abstracts (CAS), USA

International Scientific Indexing (ISI)
Impact Factor 1.022

International Society for Research Activity Journal
Impact Factor 0.615

International Institute of Organized Research (I2OR)
Impact Factor 1.405

GAURANG PUBLISHING

GAURANG PUBLISHING GLOBALIZE
PRIVATE LIMITED

RNI No. MAHENG/2017/74063

ISSN (Print) No. 2581–5911
CODEN : GPGRAG

Volume 7 Issue 1 ❖ January – June 2023

G P GLOBALIZE RESEARCH JOURNAL OF CHEMISTRY

Abstracted in Chemical Abstracts (CAS), USA
International Scientific Indexing (ISI) Impact Factor 1.724
International Institute of Organized Research (I2OR) Impact Factor 1.405
ISRA Journal Impact Factor 0.615

Supported by **ASSOCIATION OF CHEMISTRY TEACHERS**, the National Registered Organisation of Chemistry Educators of India
Registration No. Maharashtra Government, Mumbai, 922, 2010 G.B.B.S.D. dated 08.04.2010.
Website: www.associationofchemistryteachers.org

GAURANG PUBLISHING GLOBALIZE PRIVATE LIMITED, MUMBAI
CIN No. U22130MH2016PTC287238
UAN - MH19D0008178

Published by:
Gaurang Publishing Globalize Private Limited, Mumbai
1, Plot 72, Pandit M.M.M. Marg, Tardeo, Mumbai 400 034.
Email: gpglobalize@gmail.com ❖ www.gpglobalize.in
Tel: +91 9969392245
CIN No. U22130MH2016PTC287238

ISSN (Print) No: 2581-5911
CODEN : GPGRAG

Printed at: Nil Creation, Girgaum, Mumbai - 400 004, India.

GP GLOBALIZE RESEARCH JOURNAL OF CHEMISTRY

An International Peer Reviewed Journal of Chemistry

RNI No: MAHEN/2017/74063 **ISSN (Print) No: 2581-5911**
ISI Impact Factor 1.724 (2022-2023) **CODEN : GPGRAG**

Printed and Published by Gaurang Rajan Pendurkar on behalf of Gaurang Publishing Globalize Private Limited and printed at NIL CREATION, Shop No. 7, 35/55, Bandu Gokhale Path, Mugbhat Cross Lane, Jivanji Maharaj Chawl (Shree Swami Samarth Nagar), Girgaon, Mumbai 400004 and published at Gaurang Publishing Globalize Private Limited 1, Plot 72, P M M M Marg, Tardeo, Mumbai-400034.

Editor-in-Chief : Dr. D.V. Prabhu.

G P GLOBALIZE RESEARCH JOURNAL OF CHEMISTRY

RNI No: MAHENG/2017/74063 **ISSN No. (Print): 2581-5911**
ISI Impact Factor 1.724 (2022-2023) **CODEN : GPGRAG**

GUIDELINES TO AUTHORS

GP Globalize Research Journal of Chemistry is an international peer reviewed journal which publishes full length research papers, short communications, review articles and book reviews covering all areas of Chemistry including Environmental Chemistry. G P Globalize Research Journal of Chemistry is a biannual journal published in English in print and online versions.

(1) Manuscript Preparation

a) Page Layout: A4 (21 cm x 29.7 cm) leaving 2.5 cm margin on all sides of the text. All the text should be in Times New Roman font, double spaced and pages should be numbered consecutively.

b) Use MS word (2003-2007) for text and TIFF, JPEG or Paint for figures.

c) The first page should contain title in bold, 14 point size, name/s of author/s in bold, 12 point size, affiliation/s-address, email id and contact number in 11 point size, abstract-up to 200 words in 11 point size, keywords-between 5 to 10 keywords in 11 point size.

d) Main Text- The paper should be divided into the following sections:

Introduction, Materials and Methods, Results and Discussion, Conclusions, Acknowledgement and References.

Tables and Figures of good resolution (600 dpi) should be numbered consecutively and given in the order of their appearance in the text and should not be given on separate pages.

e) References- References should be cited in the text as superscript numbers in order of appearance.

References at the end of the paper should be listed in serial order to match their order of appearance in the text. Names of journals should be in italics and volume number should be in bold.

Reference to papers e.g. Ganesh R.S., Pravin S. and Rao T.P., 2005, *Talanta,* **66,** 513.

Reference to books e.g. Lee J.D., 1984, A New Course in Inorganic Chemistry, 3rd ed., ELBS and Van Nostrand Reinhold (UK) Co. Ltd., p.268-269.

f) Abbreviations should be explained at first appearance in the text.

g) Nomenclature should be as per **IUPAC** guidelines.

h) SI units should be used throughout.

(2) Manuscript Submission

Manuscripts should be submitted online at dvprabhu48@gmail.com. The paper will be accepted for publication after review. All correspondence should be made to the Editor- in-Chief at dvprabhu48@gmail.com.

(3) Proofs

Galley proofs will be sent online to the corresponding author on request and should be returned to the Editorial office within seven working days.

(4) Plagiarism

GP Globalize Research Journal of Chemistry is committed to avoid plagiarism and ensure that only original research work is published. The journal follows a Zero Tolerance Policy on Plagiarism.

The Editorial Board and panel of reviewers will check and prevent plagiarism in the manuscripts submitted for publication.

(5) Copyright

Publication of a paper in GP Globalize Research Journal of Chemistry automatically transfers copyright to the publisher. Authors can share free eprints of their published papers with fellow researchers.

(6) Circulation and Subscription Rates

The Journal is published twice a year - January and July

Subscription rates are as follows:

Library/Institutional Charges (In India)	Rs. 2000/-
Individual Charges (In India)	Rs. 2000/-
Library/Institutional Charges (Outside India)	US $ 100
Individual Charges (Outside India)	US $ 100

Subscription Charges:
Review of research papers is done free of charge. There are no charges for processing and publication of papers. Subscription to the Journal is welcome.

GUIDELINES TO AUTHORS

Mode of Payment:

Demand draft/Multicity cheque payable at Mumbai in favour of **"Gaurang Publishing Globalize Pvt. Ltd. Mumbai"**

For Online Payment:

Name of the Bank	**:**	**Axis Bank**
Branch Name	**:**	**Tardeo, Mumbai (MH)**
Account No.	**:**	**916020066451552**
IFSC Code	**:**	**UTIB0001345**

For further details please contact:

Dr. D.V. Prabhu, Editor-in-Chief,
Email: dvprabhu48@gmail.com
Mobile: 09870 226 899

Mr. Rajan Pendurkar, Managing Editor,
Email: gpglobalize@gmail.com
Mobile: 09969 392 245

A Request to Authors

We thank you for sending your research paper to G P Globalize Research Journal of Chemistry (RNI No. MAHENG/2017/74063 ISSN No. (Print): 2581-5911, CODEN : GPGRAG).

Review, processing and publication of research papers is done free of charge.

You are requested to send a DD/Multicity Cheque for Rs. 2000/- in favour of ***"Gaurang Publishing Globalize Pvt. Ltd., Mumbai"*** *payable at Mumbai,* ***as subscription charges.***

We would appreciate if you help us in our efforts to promote academic excellence.

G P GLOBALIZE RESEARCH JOURNAL OF CHEMISTRY

RNI No: MAHENG/2017/74063 **ISSN No. (Print): 2581-5911**
ISI Impact Factor 1.724 (2022-2023) **CODEN : GPGRAG**

Volume 7 Issue 1 ❄ January - June 2023

CONTENTS

RNI No. MAHENG/2017/74063
ISSN No. (Print) 2581-5911
ISI Impact Factor 1.724

Silver(I) Assisted C-N bond Dissociation; Synthesis, Characterization, Solid-state Structure, and Molecular Docking Analysis of Silver(I)-1-methylbenzimidazole hexafluorophosphate

Priyanka Sahu[1], A. A. Isab[2] and Joydev Dinda[1*]
[1] Department of Chemistry, Utkal University, Bhubaneswar, Odisha, 751004, India
[2] Department of Chemistry, King Fahd University of Petroleum and Minerals, Dhahran, 31261, Saudi Arabia
Email: joydevdinda@gmail.com

Abstract
*Starting from 2-chloropyrimidine and 1-methylbenzimidazole, the proligand 2-(1-methylbenzimidazolium) pyrimidine hexafluorophosphate (**1**.HPF_6) and silver(I)-1-methylbenzimidazole hexafluorophosphate (**2**) were synthesized. The solid-state structure of **2** was elucidated using single-crystal X-ray diffraction analysis, which revealed a linear geometry in **2**, where two nitrogen atoms were coordinated to the silver atom in a linear fashion with a bond angle of about 176.5^0. It is expected that the unexpected formation of **2** is due to Ag(I) assisted C-N bond dissociation. The synthesized complex **2** is found to be consistent with molecular docking study that utilized DNA, BCL2, and human DNA topoisomerase II as the model receptors for analysis. The complex was also inspected by the SwissADME tool to predict its ADME parameters, pharmacokinetic properties, druglike nature, and medicinal chemistry friendliness.*

Keywords: 2-chloropyrimidine; 1-methylbenzimidazole; 2-(1-methylbenzimidazolium) pyrimidine hexafluorophosphate; silver(I)-azole; C-N bond dissociation, molecular docking, DNA, BCL2, human DNA topoisomerase II, SwissADME.

Introduction

Azoles,[1] are nitrogen, sulfur, and oxygen-containing heterocyclic compounds with a five or six-membered ring system that comprises imidazole,[2] triazole,[3] pyrazole,[4] thiadiazole,[5] oxadiazole,[5] isoxazole,[6] etc. and other aromatic rings. Azoles have always been considered a scaffold of choice in designing novel therapeutic agents. They are important heterocycles to develop novel therapeutic agents, mainly known as antifungal agents. Azole derivatives also have many other biological properties including antibacterial, antidiabetic, immunosuppressant, anti-inflammatory, and anticancer activities.[7] Azoles also exhibit α-glucosidase inhibition.[8] The imidazoles are used mostly as topical agents because of their severe toxicity when taken orally.[9] Triazoles have been regularly modified and are now used to treat fungal infections,[10] caused by both yeasts and molds. The most clinically useful imidazoles are clotrimazole, miconazole, and ketoconazole. Two important triazoles are itraconazole and fluconazole.[11] In general, the azole antifungal agents are thought to inhibit cytochrome P450–dependent enzymes involved in the biosynthesis of cell membrane sterols.[12,13] The benzimidazole and its

derivatives play a very important role as a therapeutic agent e.g., antiulcer and anthelmintic drugs. Apart from this, the benzimidazole derivatives exhibit pharmacological activities such as antimicrobial, antiviral, anticancer, anti-inflammatory, analgesic, etc.[14(a,b)] On the other hand, pyrimidines are present in thymine which is found in DNA, uracil, etc., and are biologically very important.[14(a,b)] So, pyrimidine fastened with benzimidazole will direct a new way of research that encourages us to design the ligand.

On the other hand, silver is a metal that has historically been used to maintain human health since ancient times. Silver metal has been used by many early civilizations in the purification of drinking water to kill pathogens. Throughout the 18th century and up to today, ionic silver compounds have been used as antimicrobial agents.[15] Physicians still use silver salts in wound dressings to prevent infections. The drawback of the current silver antimicrobial agents is that they do not kill over a sustained period. The slow release of silver ions from silver-azole complexes,[16] could obtain a slow release of silver ions into the wound and better prevent infection and promote healing. In addition, silver(I) complexes were also used to evaluate their functions as *in vitro* anticancer agents against human cancer lines by binding with DNA through the formation of disulfide bonds.[18] Silver(I) complexes also possess antibacterial and antifungal effects, characterized by minimum toxicity to human beings.[19]

Being inspired by the above recent findings of benzimidazole and silver, we designed a novel ligand and its respective silver(I) complex for studies. We docked the synthesized silver(I) complex with DNA, BCL2, and human DNA topoisomerase II to better understand how the complex could interact at the molecular level with CLL/lymphoma 2 (BCL-2) cells as well as with human topoisomerase II alpha bound to DNA, which may give a better insight into the potential of the complex towards antibacterial and anticancer studies. SwissADME studies have been performed to know whether the complex can be used as a potential drug in the future or not. It will also be helpful to know the various ADME parameters of the synthesized complex.

Materials and Methods

General procedure

The reagents 2-chloropyrimidine, 1-methylbenzimidazole, Ag_2O, and KPF_6 were purchased from Sigma Aldrich, UK, and used without further purification. All manipulations were carried out in an open atmosphere.

Synthesis of proligand, 1.HPF$_6$

The proligand was synthesized as per reported procedure.[17] 2-chloropyrimidine and 1-methylbenzimidazole were mixed (1:1 ratio) to undergo a neat reaction at about 110^{0}C for 20 hr. This resulted in **1**.HCl which was then converted to **1**·HPF$_6$ after being treated with KPF_6 by metathesis reaction.

Synthesis of silver(I)-1-methylbenzimidazole hexafluorophosphate

The proligand **1**·HPF$_6$ (250 mg, 0.67 mmol) and silver oxide (94 mg, 0.40 mmol) were taken in 10 mL dry acetonitrile and stirred at room temperature for 4 hr in dark. The solution was filtered through a plug of Celite to remove the unreacted Ag_2O and dark red solid mass. Then the solvent was evaporated at low temperature and high pressure to get a solid mass. Analytically pure compound was obtained by diffusion of Et_2O into saturated acetonitrile solution of the complex.

Crystal structure determinations

Single crystals of **2** suitable for X-ray data collection were grown by slow diffusion of diethyl ether into a saturated acetonitrile solution of the respective complex. The crystal data and details of the data collected for **2** are given in Table 1. The bond parameters are detailed in Tables 2 and 3. X-ray data were collected on a CCD

diffractometer (graphite monochromated Mo Ka radiation, k = 0.71073Å). The structure was solved by direct methods and refined on F2 using all reflections with SHELX-97. CCDC no of complex **2** is 2113386.

Molecular docking analysis

The molecular docking analysis was carried out using AUTODOCK 4.2.6 software accomplished by AUTODOCK TOOLS 4.0 (AD4.1_bound.dat). The receptor molecules were selected as PDB formats. [DNA (ID: 1bna), BCL2 (ID: 4lvt), Human-DNA Topoiso-merase II Alpha (ID: 4fm9)].

The graphical user interface AUTODOCK TOOLS was used to set up the chosen receptor molecules; water molecules were deleted from the crystal of the receptor molecule, gasteiger charge was computed, only polar hydrogens were added and non-polar hydrogens were merged to the carbon atom. Desired structures of compounds were saved in PDBQT format. A grid box size for complex **2** was set covering the active sites of the model receptor molecules. The generated grid parameter file and docking parameter file were saved and then modified for running the docking process. Fifty runs were generated by using Lamarckian genetic algorithm searches. Default settings were used with a maximum number of $2.5x10^6$ energy evaluations and an initial population of 50 randomly placed individuals. The running process was done with autogrid4.exe and autodock4.exe functions along with the generated gpf and dpf files to generate glg and dlg files respectively. The graphical interaction pictures were obtained by using Biovia Discovery Studio 2021 visualization software.

Drug-like nature study

SwissADME is a robust web tool to access the physicochemical properties, pharmacokinetics, drug-likeliness, and medical chemistry friendliness of a molecule to determine its proficiency to be used as a drug. Bioavailability Radar has been used for this purpose to calculate drug-likeness (lipophilicity, size, polarity, solubility, saturation, and flexibility). The chemical three-dimensional structure of complex **2** was used to analyze ADME parameters by using the SwissADME tool (http://www.swissadme.ch/).

Results and Discussion

Synthesis of proligand, 1.HPF_6 and the complex 2

Proligand **1**·HPF_6 was prepared by the neat reaction,[17] of 1-methylbenzimidazole and 2-chloropyrimidine. Anion metathesis was performed using a saturated aqueous solution of KPF_6 as shown in scheme 1. Proligand **1**·HPF_6 was floated in acetonitrile solution of Ag_2O in dark and stirred for 4 hr. A colourless solution was obtained along with a slight brick-red ppt (not identified). After filtration, the volume of the colourless solution was reduced and recrystallized from CH_3CN/Et_2O. The addition of diethyl ether to the concentrated solution afforded the respective compound **2**, which was subsequently collected and characterized using single-crystal X-ray diffraction analysis.

Scheme 1. Synthesis of 2-(1-methylbenzimidazolium) pyrimidine hexafluorophosphate and silver(I) complex, **2**.

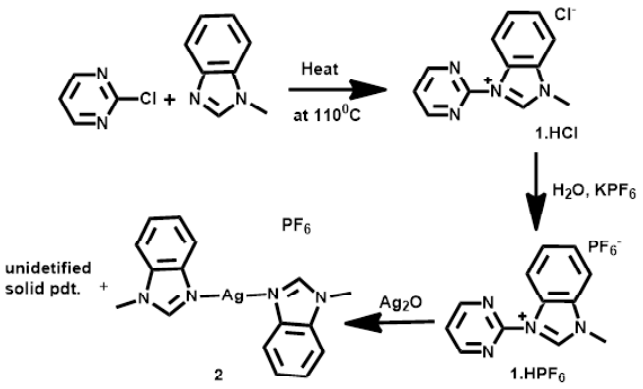

Solid-State Structure of 2

Single crystals of **2** suitable for X-ray diffraction were grown by slow diffusion of diethyl ether into a solution

of acetonitrile saturated with the complex; key crystallographic parameters are summarized in Table 1 and selected bond parameters (bond lengths and bond angles) are listed in Table 2 and 3.

Table 1. Crystallographic data of 2.

	2
Empirical formula	C_{16} H_{16} Ag F_6 N_4 P
Formula weight	517.17
Crystal system	orthorhombic
Space group	'P b c a'
Temperature (K)	296(2)
Cell dimensions	
a (Å)	23.8103(8)
b (Å)	12.9429(5)
c (Å)	24.6852(8)
α(°)	90
β(°)	90
γ(°)	90
Volume($Å^3$)	7607.3(5)
Z	16
Density (Mg m^{-3})	1.806
Absorption coefficient	1.210
F(000)	4096
Theta range for data collection	2.325-27.842
Index ranges	-31<=h<= 31, -17<=k<=16, -32<=l<= 32
Reflections collected	9467
Independent reflections	7512
GOF	1.158
Final R indices [I>2sigma(I)]	R1 = 0.0918, wR2 = 0.2446
R indices (all data)	R1 = 0.1071, wR2 = 0.2547

Table 2. Selected bond lengths (Å) of 2.

	Expt.
Ag(1)-N(2)	2.087(5)
Ag(1)-N(3)	2.087(5)
Ag(2)-N(5)	2.075(5)
Ag(2)- N(7)	2.076(6)
Ag(1)- Ag(2)	3.2479(8)

Table 3. Selected bond angles (°) of 2.

	Expt.
N(2)-Ag(1)-N(3)	176.5(2)
N(5)-Ag(2)-N(7)	172.7(2)
N(2)-Ag(1)-Ag(2)	94.00(15)
N(3)-Ag(1)-Ag(2)	82.62(15)
N(5)-Ag(2)-Ag(1)	73.27(15)
N(7)-Ag(2)-Ag(1)	102.39(16)
C(1)-N(2)-Ag(1)	126.7(5)
C(9)-N(3)-Ag(1)	125.0(4)
C(17)-N(5)-Ag(2)	127.0(5)
C(25)-N(7)-Ag(2)	123.3(5)
N(1)-C(1)-N(2)	112.3(7)
N(3)-C(9)-N(4)	112.4(6)
N(5)-C(17)-N(6)	111.4(7)
N(7)-C(25)-N(8)	112.2(7)

In the asymmetric unit of the single-crystal structure of the complex, two silver(I) units were present. Complex **2** adopted a linear geometry where two nitrogen atoms were coordinated to a silver atom (shown in Figure 1). In agreement with the linear geometry a bond angle of $176.5(2)^0$ was measured in the N(2)-Ag(1)-N(3) system. Similarly, an angle of $172.7(2)^0$ was measured for N(5)-Ag(2)-N(7) in another unit. Ag-N and Ag-Ag bond lengths were measured as 2.08Å and 3.25 Å respectively. The Ag-Ag bond lengths were measured at 3.25 Å shorter than the Vander Waals radii of Ag (1.72 Å). As shown in Figure 2, the packing diagram of **2** featured C-H•••π, π•••π and Ag•••Ag interactions that effectively formed stacked 1D layers of interconnected molecular units.

Molecular docking analysis

Molecular docking studies have played a significant role in understanding the molecular level interaction of ligand (small molecule) with receptors by placing the ligand in the binding site of the receptor. Here we consider DNA, BCL2, and human DNA topoisomerase II as receptors for the docking analysis. BCL-2 is a founding member of the BCL family of proteins that regulates cell death (apoptosis). Human DNA Topoisomerase (II) is an essential enzyme that regulates different fundamental

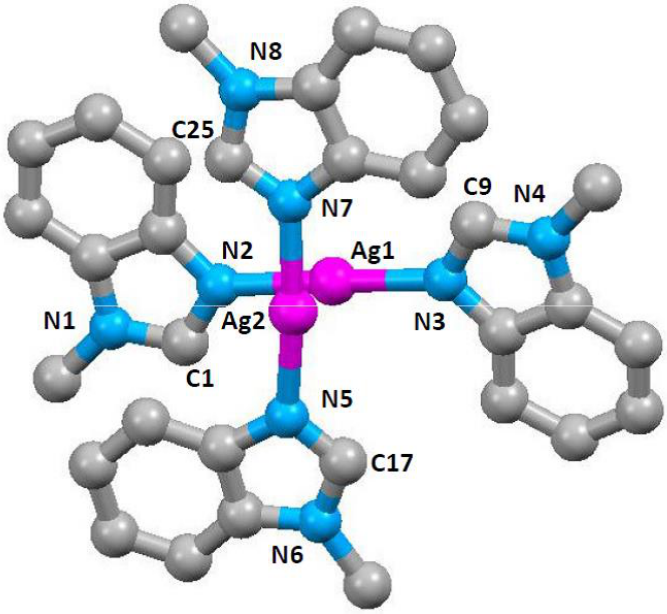

Fig. 1. Single crystal X-ray structure of complex 2. The H atoms and PF_6 have been omitted for clarity.

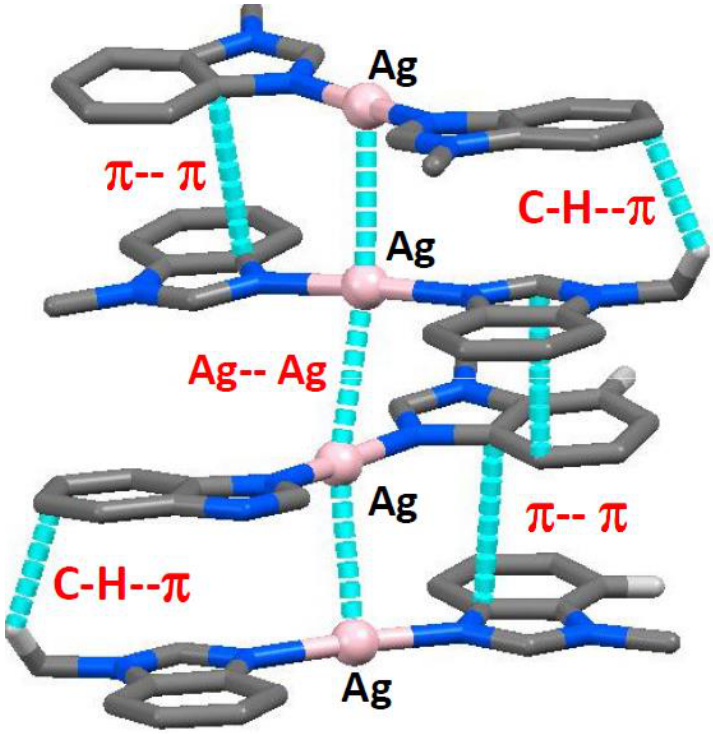

Fig. 2. Packing diagram found in the solid-state structure of 2 showing several C-H•••π, π•••π and Ag•••Ag interactions.

processes of DNA like DNA topology and chromosome organization.

The binding energies corresponding to the interaction of complex **2** with DNA, BCL2, and topoisomerase II are tabulated in Table 4, from which it is clear that the complex shows maximum affinity towards DNA among the three chosen receptors.

Table 4. Calculated binding energy (kcal.mol^{-1}) for the molecular complexes formed between complex 2 and DNA, BCL2, and topoisomerase II.

Complex	DNA	BCL2	Topoisomerase II
2	-7.89	-5.89	-7.06

The energetically most favorable conformations of complex **2** with DNA, BCL2, and topoisomerase II are shown in Figures 3, 4, and 5 respectively.

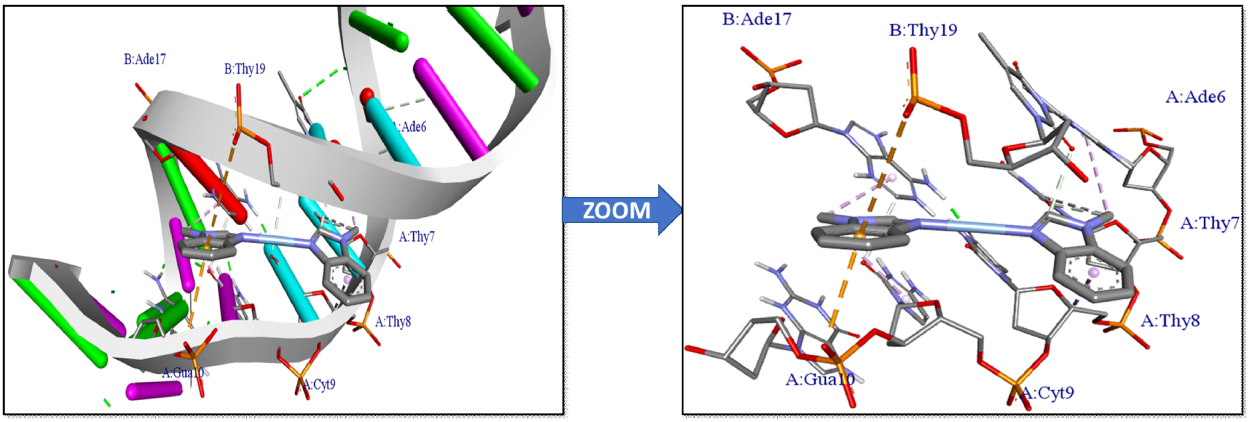

Fig. 3. Capped and stick model view of the interaction of complex 2 with DNA (PDB ID: 1bna).

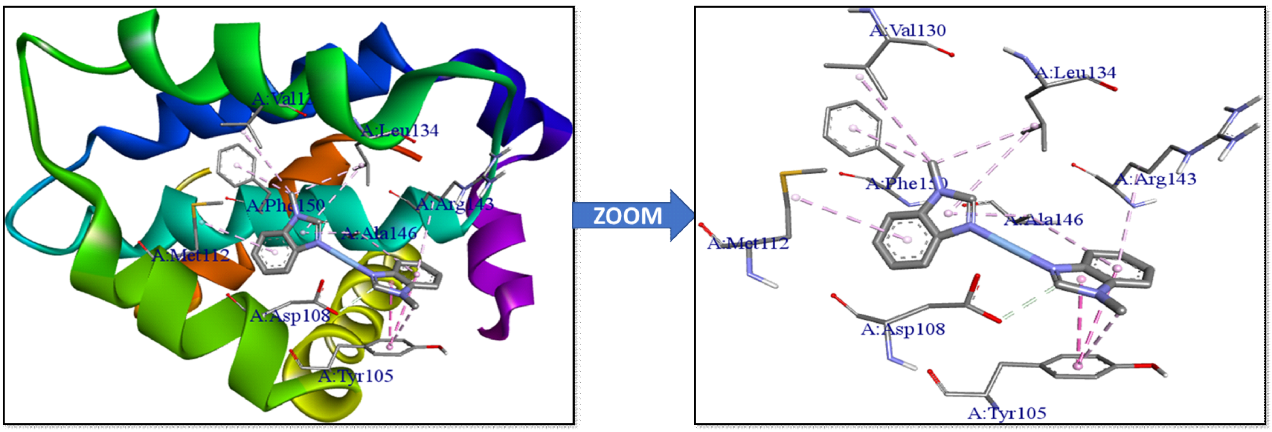

Fig. 4. Capped and stick model view of the interaction of complex 2 with BCL2 (PDB ID: 4lvt).

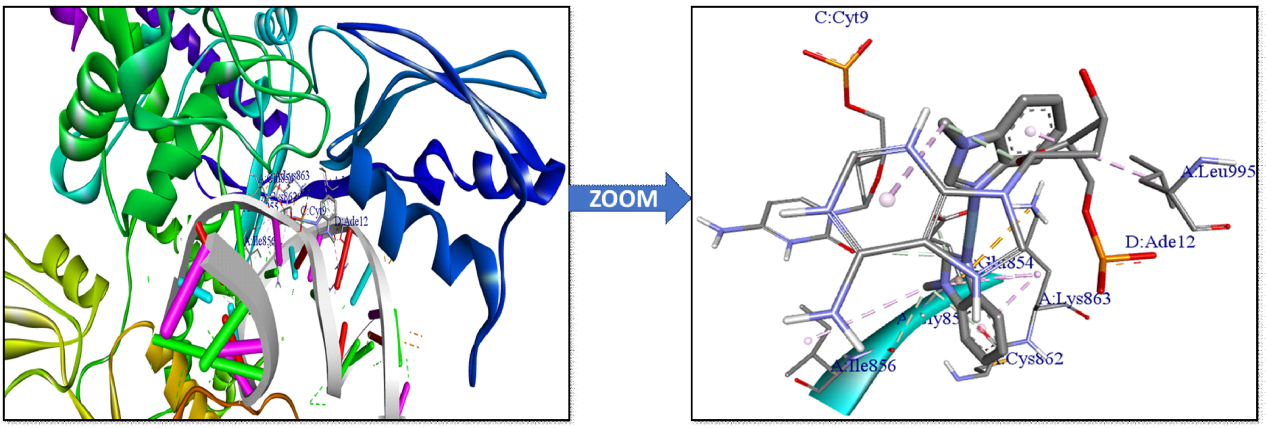

Fig. 5. Capped and stick model view of the interaction of complex 2 with human DNA topoisomerase II (PDB ID: 4fm9).

Complex **2** binds with DNA receptors through pi-anion (B: Thy19, A: Gua10), pi-alkyl (B: Ade17, A: Cyt9, A: Thy7, A: Thy8), pi-sigma (A: Thy8), and non-classical H-bond (B: Thy19) interactions.

Complex **2** binds with BCL2 receptor through pi-alkyl (A: Met112, A: Phe150, A: Val130, A: Leu134, A: Ala146, A: Arg143), pi-stacked (A: Tyr105) and non-classical H-bond (A: Asp108) interactions.

Complex **2** binds with human DNA topoisomerase II receptor through pi-alkyl (D: Ade12, A: Leu995, A: Lys863, A: Ile856), pi-cation (A: Lys863), and non-classical H-bond (D: Ade12, C: Cyt9, A: Glu854, A: Cys862) interactions. These are summarized in Table 5.

Table 5. The summary of binding energy, types of interaction, amino acids involved, and the respective bond lengths involved in the interaction of complex 2 with DNA, BCL2, and human DNA topoisomerase II.

Protein-Ligand	Binding affinity (kcal mol^{-1})	Type of interaction	Interacting AA chain(or nucleotide chain) name; AA(or nucleotide) name; AA(nucleotide) no.	Bond length (Å)
DNA-Complex **2**	-7.89	Pi-anion	B: Thy19	4.92
			A: Gua10	3.82
		Pi-alkyl	B: Ade17	4.58
			A: Cyt9	5.43
			A: Thy7	5.19
			A: Thy8	5.18
		Non-classical H-bond	B: Thy19	2.83
		Pi-sigma	A: Thy8	3.59

BCL2-Complex **2**	-5.89	Pi-alkyl	A: Met112	4.72
			A: Phe150	4.34
			A: Val130	4.82
			A: Leu134	4.42
			A: Leu134	5.41
			A: Ala146	4.20
			A: Ala146	5.25
			A: Arg143	5.39
		Pi-stacked	A: Tyr105	4.68
			A: Tyr105	4.06
		Non-classical H-bond	A: Asp108	2.64
Human DNA Topoisomerase II-Complex **2**	-7.06	Pi-alkyl	D: Ade12	4.97
			A: Leu995	5.25
			A: Lys863	4.61
			A: Lys863	3.94
			A: Lys863	3.75
			A: Ile856	5.41
		Non-classical H-bond	D: Ade12	3.02
			C: Cyt9	3.63
			A: Glu854	3.68
			A: Cys862	3.34
			A: Glu854	2.70
		Pi-cation	A: Lys863	4.24

Drug-like nature study

SwissADME tool has been used to investigate the drug-likeness property of complex **2** (shown in Figure 6). This tool interprets the relationship between pharmaco-kinetics and physicochemical parameters of the lead molecule. The complex has 2 rotatable bonds and 21 heavy atoms. The compound is with molar refractivity of 81.99 and a topological polar surface area of 19.72 Å². The average lipophilicity score of iLOGP, XLOGP3, WLOGP, MLOGP, and SILICOS-IT models for complex **2** was calculated as 1.692. The bioavailability score of the above molecules is 0.55. Complex **2** also possesses improved water solubility, which increases its efficacy for use as a drug molecule. It has high GI (gastro-intestinal) absorption and it can also work as BBB (blood-brain barrier) permeant. It can also act as a substrate for p-glycoprotein. (shown in Figure 7) It can permeate through the skin with the $\log k_p$ value of -6.22 cm/s.

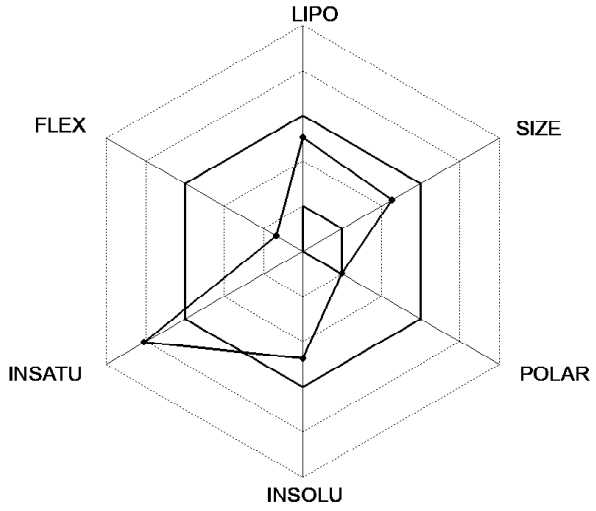

Fig. 6. The bioavailability radar illustrates a molecule's drug-likeness; the pink area represents the optimal range for each property of complex **2**.

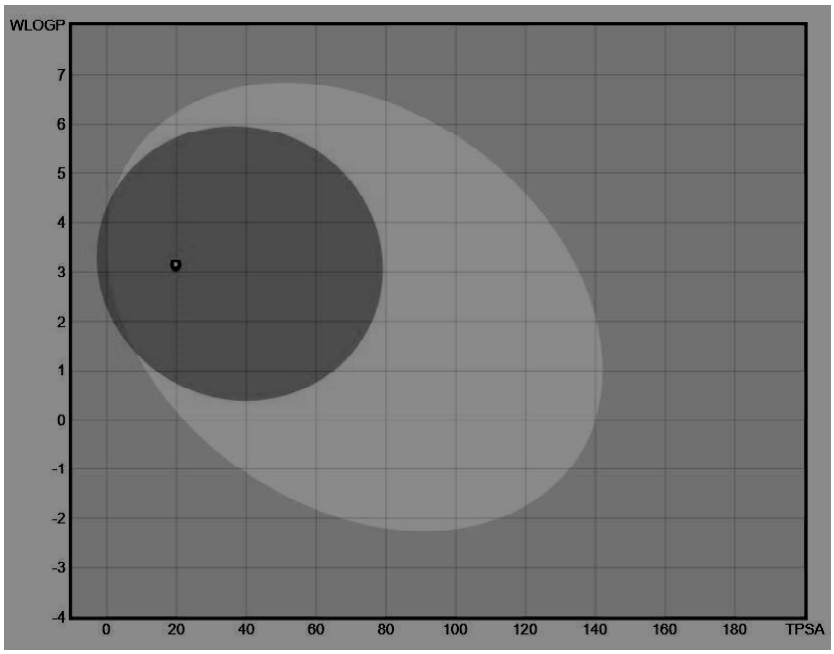

Fig. 7. The Boiled-Egg diagram of complex 2, yellow region for BBB permeation, white region for GI absorption, and blue dot indicated PGP^+.

Conclusions

In summary, we report a new complex of silver [silver(I)-1-methylbenzimidazole hexafluorophosphate] where the Ag-N bond was formed by C-N bond dissociation of 1-methylbenzimidazole and pyrimidine moieties. The resulting complex was characterized using single-crystal X-ray diffraction analysis. Analysis of single crystals revealed that the aforementioned complex adopted a linear geometry around the coordinated nitrogen atoms; features 1D polymeric networks that are held together through a series of C-H•••π, π•••π and Ag•••Ag interactions in the solid state. Molecular docking studies of the complex were performed by taking DNA, BCL2, and human DNA topoisomerase II as model receptors, where we found that our synthesized complex interacts with these receptors with different binding affinities through pi-anion, pi-cation, pi-alkyl, pi-stacked, non-classical H-bond like interactions thereby keeping its original linear geometry intact. Among the chosen receptors, the complex shows greater affinity towards DNA as compared to BCL2 and topoisomerase II. The SwissADME study of the complex revealed that the complex possesses good solubility, high GI absorbance, and good BBB permeation and can also act as a substrate for p-glycoprotein.

Acknowledgement

One of the authors (J. D.) is grateful to the Department of Chemistry of Utkal University, Bhubaneswar, India for providing valuable resources to do research.

References

1. Baidya M., Brotzel F. and Mayr H., 2010, Nucleophilicities and Lewis basicities of imidazoles, benzimidazoles, and benzotriazoles, *Org. Biomol. Chem*., **8**, 1929-1935.

2. Bellina F., Cauteruccio S. and Rossi R., 2007, Efficient and Practical Synthesis of 4(5)-Aryl-1H-imidazoles and 2,4(5)-Diaryl-1H-imidazoles via Highly

Selective Palladium-Catalyzed Arylation Reactions, *The Journal of Organic Chemistry*, **22**, 8543-8546.

3. Gonnet L., André-Barrès C., Guidetti B., Chamayou A., Menendez C., Baron M., Calvet R. and Baltas M., 2020, Study of the Two Steps and One-Pot Two-Step Mechanochemical Synthesis of Annulated 1,2,4-Triazoles, *ACS Sustainable Chemistry and Engineering*, **8**, 3114-3125.

4. Nieto S., Pérez J., Riera L., Riera V., Miguel D., Golen J. A. and Rheingold A. L., 2007, Pyrazole Complexes as Anion Receptors: Effects of Changing the Metal, the Pyrazole Substitution Pattern, and the Number of Pyrazole Ligands, *Inorganic Chemistry*, **8**, 3407-3418.

5. Ha J., Yang S. J. and Gong Y.D., 2018, Construction of 1,3,4-Oxadiazole and 1,3,4-Thiadiazole Library with a High Level of Skeletal Diversity Based on Branching Diversity-Oriented Synthesis on Solid-Phase Supports, *ACS Combinatorial Science*, **2**, 82-97.

6. Hibbs W., Koningsbruggen P. J., Arif A. M., Shum W. W. and Miller J. S., 2003, One- and Two-Step Spin-Crossover Behavior of [FeII(isoxazole)6]2+ and the Structure and Magnetic Properties of Triangular [FeIII3O(OAc)6(isoxazole)3][ClO4], *Inorganic Chemistry*, **18**, 5645-5653.

7. Wang W., Wang S., Dong G., Liu Y., Guo Z., Miao Z., Yao J., Zhang W. and Sheng C., 2011, Discovery of highly potent antifungal triazoles by structure-based lead fusion, *Med. Chem. Commun*., **2**, 1066-1072.

8. Khake S. M., Soni V., Gonnade R. G. and Punji B., 2014, Design and development of POCN-pincer palladium catalysts for C–H bond arylation of azoles with aryl iodides, *Dalton Trans*., **43**, 16084-16096.

9. Kaur I. P. and Kakkar S., 2010, Topical delivery of antifungal agents Expert Opinion on Drug Delivery, 1303-1327.

10. Kljun J., Scott A.J., Rižner T.L., Keiser J. and Turel I., 2014, Synthesis and biological characterization of organoruthenium complexes with 8-hydroxyquinolines, *Organometallics*, **7**, 1594-1601.

11. Fromtling R.A., 1988, Overview of medically important antifungal azole derivatives, *Clin. Microbial. Rev*., 187-217.

12. Yoshida Y., 1988, Cytochrome P450 of Fungi: Primary Target for Azole Antifungal Agents, *Current topics in Medical Mycology*, **2**, 388-418.

13. Vovk M.V., Pinchuk O.M., Sukach V.A., Tolmachov A.O. and Gakh A.A., 2009, Polyfluoro- and perfluoroalkoxyenaminones in syntheses of nitrogen containing heterocycles, ACS Symposium Series, 307-345.

14. (a) Singla P., Luxami V. and Paul K., 2014, Benzimidazole-biologically attractive scaffold for protein kinase inhibitors, *RSC Adv*., 4, 12422-12440; (b) Lagoja I. M., 2005, Pyrimidine as Constituent of Natural Biologically Active Compounds, *Chemistry and Biodiversity*, **2**, 1-50.

15. Melaiye A., Simons R.S., Milsted A., Pingitore F., Wesdemiotis C., Tessier C. A. and Youngs W. J., 2004, Formation of Water-Soluble Pincer Silver(I)"Carbene Complexes; *A Novel Antimicrobial Agent Journal of Medicinal Chemistry*, **4**, 973-977.

16. Kljun J., Scott A. J., Rižner T. L., Keiser J. and Turel I., 2016, Pyrithione-based ruthenium complexes as inhibitors of aldo–keto reductase 1C enzymes and anticancer agents, *RSC*., **7**, 1594-1601.

17. Behera P. K., Maity L., Kisan H. K, Dutta B., Isab A. A., Chandra S. K. and Dinda J., 2021, Gold(I) and gold(III) complexes supported by a pyrazine / pyrimidine wingtip N-heterocyclic carbene: Synthesis, Structure and DFT studies*, J. Mol. Structure*., **1223**, 129253.

RNI No. MAHENG/2017/74063
ISSN No. (Print) 2581-5911
ISI Impact Factor 1.724

Green Synthesis and Studies on Solid Dispersion of Paracetamol-Caffeine Binary Drug System

H. Shekhar and Raj Laxmi
Department of Chemistry, V.K.S. University, Ara – 802301, India
Email: hshe2503@rediffmail.com; laxmiraj19852010@gmail.com

Abstract
The present communication aims at some thermodynamic and interfacial investigations of Paracetamol (PCM) and Caffine (CF) binary drug dispersion. Partial and Integral thermodynamic quantities such as, excess Gibbs energy (g^E), excess enthalpy (h^E), excess entropy (s^E) of eutectic and non-eutectic mixtures were calculated using activity coefficient data. The positive value of excess free energy indicates positive deviation from ideal behaviour and refers to stronger association between like molecules during the formation of the binary mix. However, the negative value of free energy of mixing (ΔG^M) suggests that the mixing for eutectic and non-eutectic is spontaneous. The interfacial properties such as interfacial energy (σ), roughness parameter (a), grain boundary energy of parent components, eutectics and non-eutectics have been studied using enthalpy of fusion data. The size of critical nucleus at different undercoolings in nanoscale, may be a big challenge for the pharmaceutical world.

Keywords: *Binary drug, Excess thermodynamic quantities, mixing functions, Critical radius and Interfacial Energy.*

Introduction

The green approach adopted for the present synthesis of Paracetamol (PCM)-Caffeine(CF) drug products is ecofriendly, very simple and involves the elimination/ reduction of the use or generation of hazardous substances[1-3]. Biopharmaceutical Classification System (BCS) class II drugs and their products suffer from poor water solubility which results in their incomplete absorption. Extensive research[4-6] has been reported on various solid dispersion techniques for drug development involving poor water soluble drugs which are highly permeable to biological membranes. The formulation of drugs as solid dispersion form offers a variety of processes and a number of excipients/co-formers/carriers that allow flexibility during formulating oral delivery systems for poorly water soluble drugs. With a view to improve solubility and oral bioavailability of drugs, solid dispersions have been used to produce a homogenous distribution of a small amount of drug in solid state to minimize the therapeutic dose, reduce particle size, increase surface area and porosity of drug and convert the crystalline structure of drug into amorphous form. The eutectic mixture of less soluble sulphathiazole with hydrophilic excipient urea is a more soluble form of the drug. Researches on NSAID (Non-Steroidal Anti-inflammatory Drugs) combined drugs[7-10] have been utilised for analgesic, decongestant and anti-histaminic functions, pain and fever. The compatibility between drugs and carriers has gained great prominence because they allow predicting possible interaction and incompatibilities in the final product. PCM is welled

tolerated and lacks side effects[11-13] and is commonly used for the relief of headaches, minor aches, simple pain as well as severe pain and fever. Caffeine is a pharmacologically active substance. It is usually used in common beverages and headache or pain remedies. Caffeine toxicity[14-16] may lead to nervousness, irritability, elevated respiration, insomnia and sensory and gastrointestinal disturbances. Long exposure of caffeine implicates the liver and renal system and musculature. The most important mechanism of action of caffeine is the antagonism of adenosine receptors. It blocks adenosine receptors and competitively inhibits the action of adenosine in people. It responses the release of norepinephrine, dopamine and serotonin in the brain and the increase of circulating catecholamines and reverse the inhibitory effect of adenosine. The present binary drug system PCM-CF has been aimed at highlighting thermodynamic excess and mixing functions, interfacial energy, driving force of solidification and critical nucleus size and interface morphology.

Materials and Methods

Manually prepared binary mixtures of different ratios of drug (PCM) and excipient (CF) by repeated heating and chilling in ice were taken for measuring the solid-liquid equilibrium data and their thaw and melting temperatures were determined in a Toshniwal melting point apparatus using a precision thermometer which could read correctly up to ± 0.1^0C. The enthalpy of fusion value[17] of Paracetamol and Caffine was determined by DTA method.

Results and Discussion

Equilibrium Study

The solid liquid equilibrium (SLE) data of PCM-CF system leads to the formation of an eutectic(E)[18] and non-eutectics solid dispersion (A1-A11). The melting point of PCM (M.P. - 168.7^0C) decreases on the addition of second component CF (M.P. – 235.6^0C) which is shown in Table 1. Using mixture law, the values of heats of fusion of binary solid dispersions A1-A11 and E have been reported in Table 1. Thermo-dynamic quantities, activity coefficient and activity have been calculated using the equation[19].

$$-\ln\chi_i\gamma_i = \frac{\triangle H_i}{R}\left(\frac{1}{T_e}-\frac{1}{T_i}\right) \quad (1)$$

where χ_j and γ_i is mole fraction and activity coefficient of the component *i* respectively in the liquid phase respectively, Ti is the melting point of component and Te is the melting temperature of alloy respectively.

Mixing Functions

The thermodynamic mixing functions (partial and integral) such as molar free energy of mixing (ΔG^M), molar entropy of mixing (ΔS^M) and molar enthalpy of mixing (ΔH^M) of the binary solid dispersions were determined with the help of the values of activity of the component and by using the following equations.

$$\Delta G^M = RT(\chi_{PCM}\ Ina_{PCM} + \chi_{CF} Ina_{CF}) \quad (2)$$

$$\Delta S^M = R(\chi_{PCM}\ In\chi_{PCM} + \chi_{CF} In\chi_{CF}) \quad (3)$$

$$\Delta H^M = RT(\chi_{PCM}\ In\chi_{PCM} + \chi_{CF} In\chi_{CF}) \quad (4)$$

where partial molar free energy of thermodynamic mixing function, G^{-M}_i or mixing chemical potential (μ^{-M}_i) has been determined by the equation:

$$G^{-M}_i = \mu^{-M}_i = RT\ Ina_j \quad (5)$$

The value of molar free energy of mixing of solid dispersions was negative[20] which suggests that there is spontaneous mixing in all cases. (Table 2)

Excess Functions

Excess function is very helpful in prediction of the nature of the interactions between the components forming the eutectic and non-eutectic solid dispersions. In view of this, the excess thermodynamic functions such as integral excess integral free energy (g^E), excess integral entropy

(s^E) and excess integral enthalpy (h^E) were determined using the equations:

$$g^h = RT\ (\chi_{PCM}\ In\gamma_{PCM} + \chi_{CF} In\gamma_{CF}) \quad (6)$$

$$S^E = -R\left(\chi_{PCM}\, In\gamma_{PCM} + \chi_{CF} In\gamma_{CF} + \chi_{PCM}\, T\frac{\delta In\gamma_{PCM}}{\delta T} + \chi_{CF}\frac{\delta In\gamma_{CF}}{\delta T}\right) \quad (7)$$

$$g^h = RT\ (\chi_{PCM}\frac{\delta In\gamma_{PCM}}{\delta T} + \chi_{CF}\frac{\delta In\gamma_{CF}}{\delta T} \quad (8)$$

The value of excess chemical potential (μi^{-E}) or excess chemical potential(μi^{-E}) function (gi^{-E}) was determined by the equation,

$$g^{-}i^{M} = \mu^{-}i^{M} = RT\ ln\gamma_I \quad (9)$$

The positive value of the excess free energy manifests an appreciable deviation from ideal behaviour. The thermodynamic data (Table 3) reported here indicates the stronger interaction between like molecules in the binary product.

The Solid-Liquid Interfacial Energy(σ)

Past researches show that the computation value of solid-liquid intertacial energy (σ) from melting enthalpy change[23] was in good agreement with the observed experimental values. The interfacial energy of binary solid dispersions[24] which is a well accepted technique to evaluate the value of Turnbull empirical relationship is expressed as,

$$\sigma = \frac{C\Delta H}{(N)^{1/3}\ (V_m)^{2/3}} \quad (10)$$

where the value of the coefficient *C* lies between 0.33 to 0.35 for non-metallic system, Vm is molar volume and N is the Avogadro's constant. The value of σ for Paracetamol, Caffeine and solid dispersions is mentioned in Table 1. Further it has also been determined by Gibb Thomson equation:

$$\tau = r\Delta T = \frac{TV_m\sigma}{\Delta H} = \frac{\sigma}{\Delta S_V} \quad (10)$$

where r is the is the radius grooves of interface at the dispersion in equilibrium temperature (ΔT). The value of Gibb Thomson coefficient τ for PCM, CF and their solid dispersions was reported in Table-1. The Gunduz and Hunt method[25] for materials having known grain boundary shape supports the value of τ determined in the present case. The interfacial grain boundary energy (σ_{gb}) at the grain boundary groove in anisotropic interface was evaluated through a numerical method[26] without applying the temperature gradient for the grain boundary groove shape. The grain boundary energy can be obtained by the equation,

$$\sigma_{gb} = 2\sigma\cos\theta) \quad (12)$$

At zero contact angle (q=0), the grain boundary energy could be double with respect to s value of the solid-liquid already observed. The value of s_{gb} for solid PCM and CF was found to be 9.07×10^{-2} and $5.44\times10^{-2}Jm^{-2}$ respectively and the value for all solid dispersions is reported in Table 1.

The Driving Force of Nucleation (ΔG_V)

The driving force for liquid-solid transition and equilibrium cumulatively proceeds due to the difference in Gibb's energy between the two phases. The Gibbs free energy arises during the solidification of crystalline solid and occurs due to change in enthalpy, entropy and specific volume and non-equilibrium lies. The solidification phenomena have been previously stated on the basis of kinetic characteristics of nucleation, thermodynamic features and diffusion model. The driving force of nucleation from liquid to solid during solidification (ΔG_V) could be determined by the equation[27].

$$\Delta Gv = \Delta Sv\ \Delta T \quad (13)$$

The effective entropy change ΔSv is opposed by the increase in surface free energy due to the creation of a new solid-liquid interface. .The effective entropy change per unit volume (ΔSv) is given by

$$\Delta S_V = \frac{\Delta H}{T} \cdot \frac{1}{V_m} \quad (14)$$

The value of ΔS_V is reported in Table 1 and entropy of fusion per unit volume (ΔS_V) for PCM and CF was found to be 543 and 253 $kJK^{-1}m^{-3}$ respectively. The solid phase nucleates as a small spherical cluster of radius arising due to random motion of atoms within liquid. The value of ΔG_V for the solid dispersions and pure components are shown in Table 4. It is obvious that the critical free energy of nucleation (ΔG*) is responsible for the formation of the critical nucleus of the materials. It can be evaluated by equation:

$$\Delta G^* = \frac{16\pi\ \sigma^3}{3\ \Delta G_V^2} \quad (15)$$

The value of ΔG* for solid dispersions and pure components has been found in the range of 10^{-15} to 10^{-16} J per molecule and reported in Table 5.

The Critical Radius (r*)

During solid-liquid equilibrium, the rapidly dispersed transient and unstable embryos in supercooled liquid become saturated and emerge as a stable embryo of critical size with radius r* for leading nucleation.The value of r* was determined by using the following equation[28]:

$$r^* = \frac{2\sigma}{\Delta G_v} = \frac{2\sigma T}{\Delta H_V\ \Delta T} \quad (16)$$

The values of r* for the components and eutectic and non eutectic solid dispersion was calculated at different undercoolings (ΔT) and are given in Table 6. It was obvious that the size of the critical nucleus decreases with increase in the undercooling of the melt. The existence of embryo of different sizes can be expected in the liquid at any temperature. The value of r* for pure components (PCM and CF) and solid dispersions lies between 47 to 215 nm.

Interfacial Morphology

Interfacial growth morphology of a substance during phase transformation could be predicted from the value of the entropy of fusion and is due to a combined effect of thermodynamics, kinetics, crystal structures and interfacial structures. The Hunt and Jackson[30] relation manifests the type of growth from a binary melt and is shown as:

$$\alpha = \xi\ \frac{\Delta H}{RT} = \xi \frac{\Delta S}{R} \quad (17)$$

where ΔS/R (Jackson's roughness parameter α) is the entropy of fusion (dimensionless) forecasting the nature of the growth morphology of binary interface and ξ is a crystallographic factor depending upon the geometry of the molecule and has a value less than or equal to 1. The α values reported in Table 1 for all binary products have been found to be greater than 2 and suggests the faceted growth[31] in the entire solid dispersions.

Conclusions

A eutectic solid dispersion is formed in the present PCM-CF binary drug system. The positive value of g^E and the negative value of DGM for eutectic and non-eutectic solid dispersions suggest stronger interaction leads between like molecules and there is spontaneous mixing of PCM and CF in all the binary products.

Acknowledgement

The authors are thankful to the Head, Department of Chemistry, V K S University Ara 802301, India for providing research facilities and help.

References

1. Abbasi, Mohan. 2017. â-Cyclodextrin as an Efûcient and Recyclable Supramolecular Catalyst for the Synthesis of Heterocyclic Compounds. *J. Chines. Chemical Soc*. **64**, 896-917.
2. Shekhar, H., Kumar, Manoj., Singh, Rakesh Kumar. and Poomalai, P. 2013. Studies on banana fiber reinforced high density polyethylene (HDPE)/ polyamide(PA)-66blend composite. *Wuolpecker Journal of Food Technology* **1**, 062-073.
3. William, Alexander-J.M. and Ward, B. 1999. Paracetamol revisited: At review of the pharmacokinetics and pharmacodynamics. *Acute Pain* **2(3)**, 139-149.
4. Chaulang, Ganesh, Patel, Piyush, Hardikar, Sharwaree, Kelkar, Mukul, Bhosale, Ashok and Bhise, Sagar. 2009. Formulation and Evaluation of Solid Dispersions of Furosemide in Sodium Starch Glycolate, *Tropical Journal of Pharmaceutical Researh* **8**, 43-51.
5. Liua, Dan, Fei, Xueping, Wang, Siling, Jiang, Tongying and Su, Desen. 2006. Increasing solubility and dissolution rate of drugs via eutectic mixtures, itraconazole-poloxamer188 system, *A. J. Pharm. Sci*. **4:** 213-221.
6. Ajibola, V.A., Babatunde, O.A. and Suleiman, S. 2009. The Effect of Storage Method on the Vitamin C Content in some Tropical Fruit Juices, *Trends Appl Sci Res*. **4(2)**, 79-84.
7. Sairam, K., Saravanan, K.S., Banerjee, R. and K.P. Mohankumar. 2003. Non-Steroidal Anti-Inflammatory Drug Sodium Salicylate, but Not Diclofenac or Celecoxib, Protects against 1-Methyl-4-phenyl Pyridinium-Induced Dopaminergic Neurotoxicity in Rats, *Brain Research* **966**, 245-252.
8. Casper, D.,Yaparpalvi, U., Remepel, N., and Werner, P. 2000. Ibuprofen Protects Dopaminergic Neurons against Glutamate Toxicity in Vitro, *Neuroscience Letters* **289**, 201-204.
9. Shekhar, H. and Laxmi, Raj. 2017. Some Thermodynamics Studies on Paracetamol and Ascorbic Acid Drug System, *Journal of Applicable Chemistry* **6(5)**, 868-876.
10. Orhan, H. and Sahin, G. 2001. In Vitro Effects of NSAIDS and Paracetamol on Oxidative Stress-Related Parameters of Human Erythrocytes*, Experimental and Toxicologic Pathology* **53**, 133-140.
11. Marta, J.B. and Jerzy, Z.N. 2014. Paracetamol: Mechanism of action,applications and safty concern,*Acta Polonica Pharmaceutica – Drug Research* **71**, 11-23.
12. Aktas, A. Hakan and Filiz Kitis. 2014. Spectrophotometric Simultaneous Determination of Caffeine and Paracetamol in Commercial Pharmaceutical,*Croat. Chem. Acta* **87**, 69-74.
13. Rosivaldo, B.S., Taina, B.G.,et. al. 2014. A Structure and Antioxidant Activity Study of Paracetamol and Salicylic Acid, *Pharmacology& Pharmacy* **5**, 1185-1191.
14. Golonka, Iwona, Kawacki, Andrzej and Witold, Musial. 2015. Stability Studies of a Mixture of Paracetamol and Ascorbic Acid at Elevated Temperature, *Tropical Journal of Pharmaceutical Research* **14**, 1315-1321.
15. Silva, L.A.D., Wouk, Jessica. et al. 2017. Mechanisms and biological effects of Caffeine on substrate metabolism homeostasis: A systematic review*, Journal of Applied Pharmaceutical Science* **7**, 215-221.
16. Anderson, L.F. et al. 2006. Consumption of coffee is associated with reduced risk of death attributed to infiammatory and cardiovascular diseases in the lowa

Womens Health Study, *Am J. Clin Nutr* **83**, 1039-1046.

17. Shekhar, H. and Kant, Vishnu. 2015. Transparent Binary Material of Phenothiazine-Benzamide Binary SSystems-Future for Light emitting Sources, *Internation Journal of Chemistry* **4**, 351-361.

18. Shekhar, H. and Kumar, Manoj. 2016. Phase Diagram, Thermodynamic Stability and Interfacial Studies on solid dispersions of Phenothiazine-Acetanilide drug system, *Asian J, of Organic and Medicinal Chemistry* **1**, 26-32.

19. Darken, L.S. 1987. Thermodynamics binary metallic solutions. *Trans Met Soc AIMS*. **239**, 80-89.

20. Shekhar, H. and Kant, Vishnu. 2013. Thermodynamic Studies on Solid Dispersions, of Nicotinamide - Khellin Drug System. *Mol. Cryst. Liq. Cryst* **577**, 103-115.

21. Sharma, B.L., Tandon, S., Gupta, S. 2009. Characteristics of the binary faceted eutectic; benzoic Acid-Salicylic Acid system. *Cryst. Res. Technol*. **44**, 258-268.

22. Shamsuddin, M., Singh, S.B. and Nasar, A. 1998. Thermodynamic investigations of liquid gallium-cadmium alloys. *Thermochemka Acta*., **318**, 11-19.

23. Singh, N.B. and Glicksman, M.E. 1998, Determination of the mean solid-liquid interface energy of pivalic acid. *J, Cryst Growth.* **98**, 573-580.

24. Turnbull, D., 1960, Formation of Crystal Nuclei in Liquid Metals. *J. Chem. Phys*. **21**, 1022-1027.

25. Gunduz, M. and Hunt, J.D., 1989, Solid-Liquid surface energy in the AI-Mg system. *Acta Metall*. **37**, 1839-1845.

26. Akbulut, S., Ocak, Y., Keslioglu, K. and Marasli, N. 2009. Determination of Interfacial Energies in the Aminomethylpropanediol-neopentylglycol Organic Alloy. *Applied Surface Science*. **255**, 3594-99.

27. Hunt, J.D. and Lu, S.Z., 1994, Hand Book of Crystal Growth. Ed. DTJ Hurie Elsevier Amsterdam. p.112.

28. Chadwick, G.A., 1972, Metallography of Phase Transformation. Butterworths; London, p-61.

29. Wilcox, W.R. 1974. The relation between classical nucleation theory and the solubility of small particles. *Journal of crystal growth*. **26**, 153-154.

30. Hunt, J.D. and Jackson, K.A. 1966. Binary Eutectic Solidification. *Trans Metall SocAIME* **236**, 843-852,

31. Gupta, P., Agrawal, T., Das, S.S. and Singh, N.B. 2012. Phase equilibria and molecular interaction studies on (naphthols + vanillin) systems. *J. Chem. Thermody.,* **48**, 291-299.

Table 1: Phase Composition, melting temperature, values of entropy of fusion per unit volume (ΔS_V), heat of fusion (ΔH), interfacial energy (σ), grain boundary energy (σ_{gb}), Gibbs-Thomson coefficient (τ) and roughness parameter(α)

Alloy	χ_{PCM}	MP	ΔH (J/mol)	ΔS (J/mol/K)	α	$\sigma\times10^2$	$\sigma_{gb}\times10^2$(J/m^2)	ΔS_v (KJ/m^3/K)	ΔH_v	$\tau\times10^6$(Km)
A1	0.183	215	21601.59	44.265	5.324	30.561	61.122	296.995	144.934	10.290
A2	0.33	194	22590.90	48.374	5.818	33.223	66.446	340.314	158.927	9.762
A3	0.46	172	23465.80	52.732	6.342	35.577	71.154	387.191	172.300	9.188
A4	0.50	165	23735.00	54.189	6.517	36.302	72.604	403.239	176.619	9.002
A5	0.56	155	24138.80	56.399	6.783	37.388	74.776	428.240	183.287	8.730
E	0.619	141	24535.87	59.265	7.128	38.456	76.912	459.118	190.075	8.376
A6	0.665	143	24845.45	59.724	7.183	39.289	78.578	470.031	195.533	8.358
A7	0.726	150	25255.98	59.706	7.181	40.394	80.788	479.919	203.006	8.416
A8	0.790	156	25686.70	59.875	7.201	41.553	83.106	492.179	211.145	8.442
A9	0.835	160	25989.55	60.022	7.219	42.368	84.736	501.297	217.062	8.451
A10	0.876	162	26265.48	60.380	7.262	43.110	86.220	511.714	222.596	8.424
A11	0.920	164	26561.60	60.780	7.310	43.907	87.814	523.324	228.693	8.390
PCM	0.00	168.7	27100.00	61.353	7.379	45.356	90.712	543.853	240.220	8.339
CF	0.00	235.6	20370.00	40.051	4.817	27.248	54.496	253.670	129.017	10.741

Table 2 : Value of partial and integral missing of Gibbs free energy (ΔG^M), enthalpy (ΔH^M) and entropy (ΔS^M) of PCM–CF system

Alloy	ΔG_{PCM}-^{M} J/mol	ΔG_{CF}-M J/mol	ΔG^M J/mol	ΔH_{PCM}-^{M} J/mol	ΔH_{CF}-^{M} J/mol	ΔH^M J/mol	ΔS_{PCM}-^{M} J/mol/K	ΔS_{CF}-^{M} J/mol/K	ΔS^M J/mol/K
A1	-1.2171	-6.9013	-5.861	6886.179	815.303	1926.985	14.119	1.680	3.956
A2	-2.9515	-4.2709	-3.835	4301.962	1553.055	2460.194	9.217	3.329	5.272
A3	-3.2568	-5.9232	-4.696	2870.990	2275.333	2549.335	6.456	5.122	5.735
A4	-1.8211	-5.4659	-3.643	2523.581	2519.940	2521.760	5.762	5.762	5.762
A5	-3.4174	-4.2700	-3.792	2060.308	2917.881	2437.640	4.820	6.825	5.702
E	-3.2368	-7.4760	-4.851	1648.716	3314.642	2283.433	3.987	8.022	5.524
A6	-4.0465	-5.8831	-4.661	1407.659	3776.817	2201.326	3.391	9.092	5.300
A7	-4.1322	-6.4041	-4.754	1121.866	4547.250	2060.421	2.662	10.763	4.881
A8	-5.1396	-5.9242	-5.304	838.175	5560.494	1829.861	1.959	12.975	4.272
A9	-1.6239	-6.9155	-2.497	647.993	6479.931	1610.262	1.499	14.980	3.723
A10	-1.8086	-5.6454	-2.284	477.389	7544.206	1353.674	1.100	17.355	3.115
A11	-3.1983	-6.3980	-3.454	301.557	9181.141	1011.923	0.693	20.998	2.317

Table 3 : Value of partial and integral excess Gibbs free energy (g^E), enthalpy (h^E) and entropy (s^E) of PCM-CF system

Alloy	g_{PCM}^{-E} J/mol	g_{CF}^{-E} J/mol	g^E J/mol	h_{PCM}^{-E} J/mol	h_{CF}^{-E} J/mol	h^E J/mol	s_{PCM}^{-E} J/mol/K	s_{CF}^{-E} J/mol/K	s^E J/mol/K
A1	6886.179	815.303	1926.985	81078.104	3864.029	17994.204	152.026	6.246	32.923
A2	4301.962	1553.055	2460.194	30391.913	6692.564	14513.349	50.386	11.005	24.000
A3	2870.990	2275.333	2549.335	8690.745	10118.502	9461.733	13.781	17.625	15.856
A4	2523.581	2519.940	2521.760	4799.806	11529.711	8164.758	5.196	20.570	12.886
A5	2060.308	2917.881	2437.640	96.281	14243.323	6320.979	-4.588	26.461	9.073
E	1648.716	3314.642	2283.433	-4079.165	17030.011	3963.431	-13.835	33.128	4.057
A6	1407.659	3776.817	2201.326	-5464.083	22578.749	3930.265	-16.518	45.196	4.156
A7	1121.866	4547.250	2060.421	-6609.327	-16293.854	-9262.887	-18.277	-49.269	-26.768
A8	838.175	5560.494	1829.861	-7731.374	17156.741	-9710.701	-19.975	-52.953	-26.900
A9	647.993	6479.931	1610.262	-8431.927	17797.878	-9977.308	-20.969	-56.068	26.760
A10	477.389	7544.206	1353.674	-9140.860	-18417.647	-10291.181	-22.110	-59.682	-26.768
A11	301.557	9181.141	1011.923	-9842.094	-19098.638	-10582.617	-23.212	-64.68	-26.530

Table 4 : Value of volume free energy change (ΔG_v) during solidification for PCM-CF system of different undercoolings (ΔT)

Alloy	ΔG_V(J/m^3)					
$\Delta T \rightarrow$	**1.0**	**1.5**	**2.0**	**2.5**	**3.0**	**3.5**
A1	0.297	0.445	0.594	0.742	0.891	1.039
A2	0.340	0.51.	0.680	0.850	1.020	1.190
A3	0.387	0.580	0.774	0.967	1.161	1.354
A4	0.403	0.604	0.806	1.007	1.209	1.410
A5	0.428	0.642	0.856	1.070	1.284	1.498
E	0.459	0.688	0.918	1.147	1.377	1.606
A6	0.470	0.705	0.940	1.175	1.410	1.645
A7	0.480	0.720	0.960	1.200	1.440	1.680
A8	0.492	0.738	0.984	1.230	1.476	1.722
A9	0.501	0.751	1.002	1.252	1.503	1.753
A10	0.511	0.766	1.022	1.277	1.533	1.788
A11	0.523	0.784	1.046	1.307	1.569	1.830
PCM	0.544	0.816	1.088	1.360	1.632	1.904
CF	0.253	0.379	0.506	0.632	0.759	0.885

Table 5 : Value of critical free energy of nucleation (ΔG*) for alloys of PCM-CF system at different undercoolings (ΔT)

Alloy	$\Delta G^* \times 10^{16}$ (J/m^3)					
ΔT→	**1.0**	**1.5**	**2.0**	**2.5**	**3.0**	**3.5**
A1	54.219	24.097	13.554	8.675	6.024	4.426
A2	53.052	23.575	13.263	8.488	5.894	4.330
A3	50.327	22.347	12.581	8.052	5.591	4.108
A4	49.283	21.903	12.320	7.885	5.475	4.023
A5	47.749	21.222	11.937	7.639	5.305	3.897
E	45.205	20.091	11.301	7.232	5.022	3.690
A6	45.994	20.442	11.498	7.359	5.110	3.754
A7	47.947	21.309	11.986	7.671	5.327	3.914
A8	49.662	22.056	11.406	7.940	5.514	4.051
A9	50.707	22.536	12.676	8.113	5.634	4.139
A10	51.265	22.784	12.816	8.202	5.696	4.184
A11	51.785	23.015	12.964	8.285	5.753	4.227
PCM	52.855	23.491	13.213	8.456	5.872	4.314
CF	52.676	23.411	13.169	8.428	5.852	4.300

Table 6 : Critical size of nucleus (r*) at different undercoolings (ΔT)

Alloy	r^* (nm)					
ΔT→	**1.0**	**1.5**	**2.0**	**2.5**	**3.0**	**3.5**
A1	205.80	137.20	102.90	82.32	68.60	58.80
A2	195.24	130.16	97.62	78.09	65.08	55.78
A3	183.76	122.50	91.88	73.50	61.25	52.50
A4	180.04	120.02	90.02	72.01	60.01	51.44
A5	174.60	116.40	87.30	69.84	58.20	49.88
E	167.52	111.68	83.76	67.00	55.84	47.86
A6	167.60	111.40	83.58	66.86	55.72	47.76
A7	168.32	112.21	84.16	67.32	56.10	48.09
A8	168.84	112.56	84.42	67.53	56.28	48.24
A9	169.02	112.68	84.51	67.60	56.34	48.29
A10	168.48	112.32	84.24	67.39	56.16	48.13
A11	167.80	111.86	83.90	67.12	55.93	47.94
PCM	166.78	111.18	83.39	66.71	55.59	47.65
CF	214.82	143.21	107.41	85.92	71.60	61.37

RNI No. MAHENG/2017/74063
ISSN No. (Print) 2581-5911
ISI Impact Factor 1.724

Oxidation Kinetics and Mechanism of DL methionine, a Sulphur containing Amino acid by Tetramethylguanidinium Chlorochromate

Yashasvi Inaniyan, Heena Kansara, Pramila Naga and Priyanka Purohit*
Chemical Kinetics Lab., Department of Chemistry,
J.N.V. University, Jodhpur, 342 005, India.
Email: drpkvs27@yahoo.com

Abstract
The oxidation of DL-methionine (Met) by Tetramethylguanidinium chlororochromate (TMGCC) in dimethylsulphoxide (DMSO) leads to the formation of the corresponding sulphoxide. The reaction is of first order with respect to TMGCC. Michaelis-Menten type kinetics was observed with respect to methionine. The reaction is catalysed by hydrogen ions. The hydrogen-ion dependence has the form: $k_{obs} = a + b [H^+]$. The oxidation of methionine was studied in nineteen different organic solvents. The solvent effect was analyzed by Kamlet's and Swain's multiparametric equations. Solvent effect indicated the importance of the cation-solvating power of the solvent. A suitable mechanism has also been postulated.

Keywords: *Halochromate, Kinetics, Mechanism, Methionine, Oxidation.*

Introduction

Selective oxidation of organic compounds under non-aqueous conditions is an important reaction in synthetic organic chemistry. For this, a number of different chromium (VI) derivatives have been reported[1-4]. Recently tetramethylguanidinium chlorochromate (TMGCC) has been reported as an efficient reagent for the oxidation of organic substrates under solvent-free conditions and microwave irradiation[5]. Our group has also been interested in the kinetic and mechanistic aspects of the oxidation by complexed Cr(VI) species and several reports on mechanistic aspects of organic functions have already been published from our laboratory[6-9]. It is, known however, that the mode of oxidation depends upon the nature of counter-ion attached to the chromium anion. Methionine (Met), a sulphur-containing essential amino acid, is reported to behave differently from other amino acids, towards many oxidants[10,11], due to electron-rich sulphur center which is easily oxidizable. There seems to be no report on the oxidation aspects of TMGCC. Therefore, in continuation of our earlier work on halochromates, we report here the kinetics of oxidation of DL-methionine by TMGCC in dimethylsulphoxide (DMSO) as solvent. A suitable mechanism has also been proposed.

Materials and Methods

Materials: TMGCC was prepared by the reported method[5] and its purity checked by an iodometric method. Methionime (Merck) was used as supplied. Due to the non-aqueous nature of the solvent, toluene-*p* sulphonic acid (TsOH) was used as a source of hydrogen ions. Other solvents were purified by the usual methods[12].

Product Analysis: Product analysis was carried out under kinetic conditions. The oxidation of Met by TMGCC resulted in the formation of the corresponding sulphoxide, which was determined by the reported method[13]. The yield of sulphoxide was 96±4%. The oxidation state of chromium in completely reduced reaction mixtures, as determined iodometrically, was 3.95±0.10.

Kinetic measurements: The pseudo first order conditions were attained by maintaining a large excess (×10 or more) of the Met over TMGCC. The solvent was DMSO, unless specified otherwise. The reactions were followed, at constant temperatures (±0.1 K), by monitoring the decrease in [TMGCC] spectrophotometrically at 358 nm. No other reactant or product has any significant absorption at this wavelength. The pseudo first order rate constant, k_{obs}, was evaluated from the linear (r = 0.990 0.999) plots of log [TMGCC] against time for upto 80% reaction. Duplicate kinetic runs showed that the rate constants were reproducible to within ±3%. All experiments, other than those for studying the effect of hydrogen ions, were carried out in the absence of TsOH. The second order rate constant, k_2, was evaluated from the relation $k_2 = k_{obs}/[Met]$. Simple and multivariate linear regression analyses were carried out by the least squares method on a personal computer.

Results and Discussion

Stoichiometry: The oxidation of methionine by TMGCC resulted in the formation of the corresponding sulfoxides. The overall reaction may therefore, be represented as Equation 1.

$$\text{Me-S-R} + \text{CrO}_2\text{ClO}^-\text{H}_2\text{N}^+\text{C}[\text{N}(\text{CH}_3)_2]_2 \longrightarrow \text{Me-S-R} + \underset{\underset{\text{O}}{||}}{\text{CrOClO}^-\text{H}_2\text{N}^+\text{C}}[\text{N}(\text{CH}_3)_2]_2 \qquad (1)$$

where R is $CH_2CH_2CH(NH_2)COOH$

TMGCC undergoes a two electron change. This is in accord with the earlier observations with structurally similar halochromates. It has already been proved earlier that both pyridinium fluorochromate (PFC)[14] and pyridinium chlorochromate (PCC)[15] act as two electron oxidants and are reduced to chromium (IV) species , by determining the oxidation state of chromium by magnetic succeptibility, ESR and IR studies.

Kinetic Dependence: The reactions were found to be first order with respect to TMGCC (Figure 1). In individual kinetic runs, plots of log [TMGCC] *versus* time were linear ($r^2 > 0.995$). Further, it was found that the observed rate constant, k_{obs}, does not depend on the initial concentration of TMGCC. The order with respect to methionine was less than one (Table 1). A plot of $1/k_{obs}$ *versus* 1/[Met] was linear with an intercept on the rate ordinate (Figure 2). Thus Michaelis Menten type kinetics were observed with respect to Met. This leads to the postulation of following overall mechanism (Equations 2 and 3) and the rate law (4).

Table 1. Rate constants for the oxidation of DL-methionine by TMGCC at 298 K

10^3 [TMGCC] (mol dm^{-3})	[Met] (mol dm^{-3})	[TsOH] (mol dm^{-3})	10^4 k_{obs} (mol dm^{-3})
1.0	0.10	0.00	3.36
1.0	0.20	0.00	4.97
1.0	0.40	0.00	6.57
1.0	0.60	0.00	7.38
1.0	0.80	0.00	7.83
1.0	1.00	0.00	8.15
1.0	1.50	0.00	8.55
1.0	3.00	0.00	9.09
2.0	0.40	0.00	6.39
4.0	0.40	0.00	6.66
6.0	0.40	0.00	6.48
8.0	0.40	0.00	6.55
1.0	0.20	0.00	7.47*
[a] contained 0.001 M acrylonitrile			

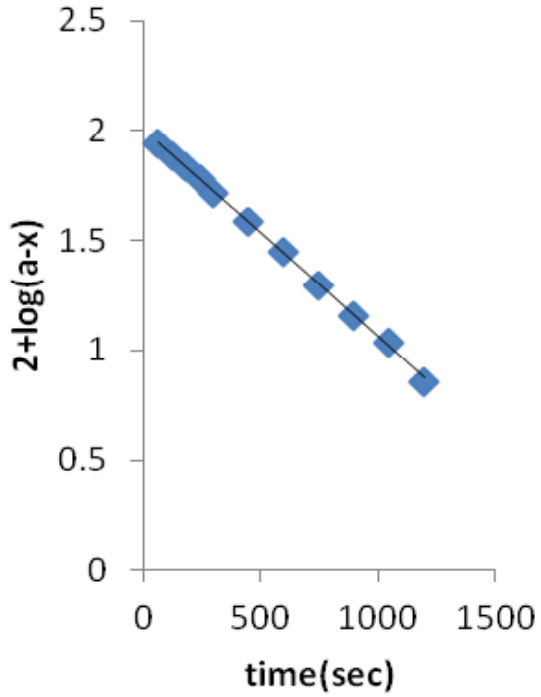

Fig. 1. Oxidation of DL-Met by TMGCC: A typical Kinetic Run

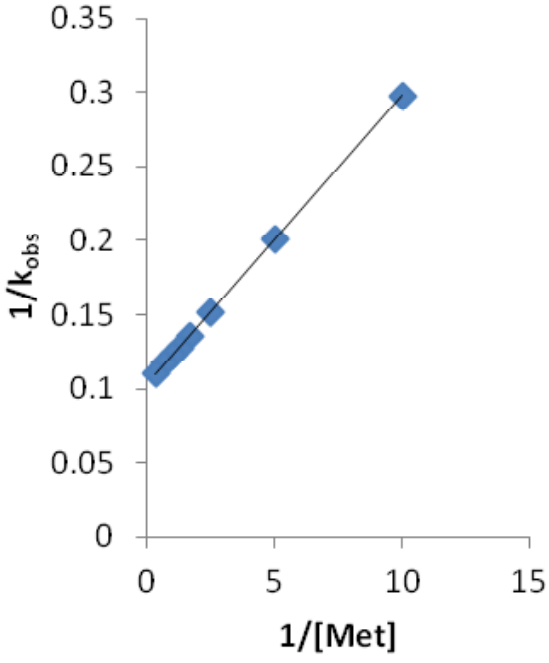

Fig. 2. Oxidation of DL-Met by TMGCC: A double reciprocal plot

$$\text{Met} + \text{TMGCC} \underset{k_2}{\overset{K}{\leftrightarrows}} [\text{Complex}] \quad (2)$$

$$[\text{Complex}] \xrightarrow{k_2} \text{Products} \quad (3)$$

$$\text{Rate} = k_2 K [\text{Met}] [\text{TMGCC}] / (1 + K[\text{Met}]) \quad (4)$$

The dependence of k_{obs} on the concentration of methionine was studied at different temperatures and the values of K and k_2 were evaluated from the double reciprocal plots. The thermodynamic parameters for the complex formation and activation parameters of the disproportionation of the complexes, at 298 K, were calculated from the values of K and k_2 respectively at different temperatures (Tables 2 and 3).

Table 2. Formation constant and thermodynamic parameters for the oxidation of TMGCC–Met complexes

K / (dm^3 mol^{-1})				$-\Delta H^*$	$-\Delta S^*$	$-\Delta G^*$
288	298	308	318K	(kJ mol^{-1})	(J mol^1 K^{-1})	(kJ mol^{-1})
6.03	5.35	4.50	3.78	14.4±0.6	27±2	6.59±0.5

Table 3. Rate constants and activation parameters for the decomposition of TMGCC–Met Complexes

$10^4 k_2$ / (dm^3 mol^{-1} s^{-1})				$-\Delta H^*$	$-\Delta S^*$	$-\Delta G^*$
288	298	308	318K	(kJ mol^{-1})	(J mol^1 K^{-1})	(kJ mol^{-1})
4.41	9.63	21.6	45.9	57.1±0.7	111±2	90.1±0.5

Test for free radicals: The oxidation of Met, in an atmosphere of nitrogen, failed to induce the polymerization of acrylonitrile. Further, the addition of acrylonitrile had no effect on the rate of oxidation (Table 1). Therefore, a one-electron oxidation, giving rise to free radicals, is unlikely. To further confirm the absence of free radicals in the reaction pathway, the reaction was carried out in the presence of 0.05 mol dm^{-3} of 2,6-di-t-butyl-4-methylphenol (butylated hydroxytoluene or BHT). It was observed that BHT was recovered unchanged, almost quantitatively.

Effect of Hydrogen Ion: The reaction was studied at different acidities by adding varying amount of toluene-p-sulphonic acid (TsOH) to the reaction mixtures. The reaction is catalyzed by hydrogen ions (Table 4). The hydrogen ion dependence has the form $k_{obs} = a + b [H^+]$. The values of *a* and *b* are 6.86±0.21′10^{-4} s^{1} and 12.4±0.35′10^{-4} mol^{1} dm^3 s^{1} respectively (r^2 = 0.9968).

Table 4. Dependence of reaction rate on hydrogen-ion concentration

[TMGCC] = 0.001 mol dm^{-3};	[Met] = 1.0 mol dm^{-3};		Temp. = 298 K			
[H$^+$]/mol dm^{-3}	0.10	0.20	0.40	0.60	0.80	1.00
Met	3.96	4.68	5.85	7.11	8.37	9.54

Solvent Effect: The oxidation of Met was studied in nineteen organic solvents. The choice of solvents was limited due to the solubility of TMGCC and its reaction with primary and secondary alcohols. There was no reaction with the chosen solvents. The kinetics are similar in the all the solvents. The values of K and k_2 are recorded in Table 5.

Table 5. Effect of solvents on the oxidation of DL-methionine by TMGCC at 298 K

Solvents	K (dm^{-3} mol^{-1})	10^5 k_{obs} (s^{-1})	Solvents	K (dm^{-3} mol^{-1})	10^5 k_{obs} (s^{-1})
Chloroform	5.58	77.6	Toluene	6.10	18.6
1,2-Dichloroethane	6.30	87.1	Acetophenone	5.58	83.2
Dichloromethane	5.49	72.4	THF	6.03	33.9
DMSO	5.25	216	t-Butylalcohol	6.31	41.7
Acetone	5.67	63.1	1,4-Dioxane	5.98	38.9
DMF	6.12	117	1,2-Dimethoxyethane	5.95	22.9
Butanone	6.03	51.3	CS_2	5.76	11.2
Nitrobenzene	5.94	95.5	Acetic Acid	6.04	45.7
Benzene	5.76	22.4	Ethyl Acetate	5.89	30.9
Cyclohexane	6.00	2.81			

A perusal of the data shows that the formation constants do not vary much with the nature of the solvents. However, the rate constants, k_2 varied considerably with the solvents. The rate constants for oxidation, k_2, in eighteen solvents (CS_2 was not considered, as the complete range of the solvent parameters was not available) were correlated in terms of the linear solvation energy relationship Equation 5 of Kamlet et al.[16]

$$\log k_2 = A_0 + p\pi^* + b\beta + a\alpha \quad (5)$$

In this equation, π^* represents the solvent polarity, β the hydrogen bond acceptor basicities and α is the hydrogen bond donor acidity. A_0 is the intercept term. It may be mentioned here that out of the 18 solvents, 12 have a value of zero for α. The results of correlation analyses in terms of equation (5), a biparametric equation involving π^* and β, and separately with π^* and β are given below.

$$\log k_2 = -4.48 + 1.59\ (\pm 0.16)\ \pi^* + 0.15\ (\pm 0.13)\ \beta + 0.29\ (\pm 0.12)\ \alpha \quad (6)$$
$R^2 = 0.8966;\ sd = 0.14;\ n = 18;\ \psi = 0.35$

$$\log k_2 = -4.41 + 1.49\ (\pm 0.17)\ \pi^* + 0.25\ (\pm 0.14)\ \beta \quad (7)$$
$R^2 = 0.8568;\ sd = 0.16;\ n = 18;\ \psi = 0.40$

$$\log k_2 = -4.35 + 1.57\ (\pm 0.18)\ \pi^* \quad (8)$$
$r^2 = 0.8260;\ sd = 0.45;\ n = 18;\ \psi = 0.43$

$$\log k_2 = -3.54 + 0.52\ (\pm 0.33)\ \beta \quad (9)$$
$r^2 = 0.1367;\ sd = 0.39;\ n = 18;\ \psi = 0.96$

Here n is the number of data points and ψ is the Exner's statistical parameter.[17]

Kamlet's[16] triparametric equation explains *ca.* 89% of the effect of solvent on the oxidation. However, by Exner's[17] criterion the correlation is not even satisfactory (*cf.* Eqn. 7). The major contribution is of solvent polarity. It alone accounted for *ca.* 83% of the data. Both β and α play relatively minor roles.

The data on the solvent effect were analysed in terms of Swain's equation[18] of cation and anion solvating concept of the solvents as well.

$$\log k_2 = aA + bB + C \quad (10)$$

Here A represents the anion solvating power of the solvent and B the cation solvating power. C is the intercept term. (A + B) is postulated to represent the solvent polarity. The rates in different solvents were analysed in terms of equation (10), separately with A and B and with (A + B).

$$\log k_2 = 1.19\ (\pm 0.04)\ A + 1.45\ (\pm 0.03)\ B - 3.65 \quad (11)$$
$R^2 = 0.9960$; sd = 0.03; n = 19; $\psi = 0.07$

$$\log k_2 = 0.99\ (\pm 0.48)\ A - 2.65 \quad (12)$$
$r^2 = 0.2013$; sd = 0.50; n = 19; $\psi = 0.92$

$$\log k_2 = 1.36\ (\pm 0.21)\ B - 3.26 \quad (13)$$
$r^2 = 0.7054$; sd = 0.24; n = 19; $\psi = 0.56$

$$\log k_2 = 1.37 \pm 0.04\ (A + B) - 3.64 \quad (14)$$
$r^2 = 0.9867$; sd = 0.50; n = 19; $\psi = 0.12$

The rates of oxidation of methionine in different solvents show an excellent correlation with Swain's equation with both the cation and anion solvating powers playing significant roles, though the contribution of the cation solvation is slightly more than that of the anion solvation. The solvent polarity, represented by (A + B), also accounted for *ca.* 98% of the data. However, the correlations individually with A and B were poor. In view of the fact that solvent polarity is able to account for *ca.* 98% of the data, an attempt was made to correlate the rate with the relative permittivity of the solvent. However, a plot of log k_2 against the inverse of the relative permittivity is not linear ($r^2 = 0.4958$; sd = 0.31; $\psi = 0.73$).

The observed solvent effect points to a transition state more polar than the reactant state. Further, the formation of a dipolar transition state, similar to those of S_N2 reactions, is indicated by the major role of both anion- and cation-solvating powers. However, the solvent effect may also be explained assuming that the oxidant and the intermediate complex exist as ion-pair in non-polar solvent like cyclohexane and be considerably dissociated in more polar solvents.

Mechanism

In view of the absence of any effect of radical scavenger, acrylonitrile, on the reaction rate and recovery of unchanged BHT, it is unlikely that a one-electron oxidation giving rise to free radicals, is operative in this oxidation reaction. The observed Michaelis – Menten type of kinetics observed with respect to methionine, suggests the formation of 1:1 complex of TMGCC and Met in a rapid pre-equilibrium. With the present set of data, it is difficult to state the definite nature of the intermediate complex. The experimental results can be accounted for in terms of electrophilic attack of methionine-sulphur at the metal *via* an intermediate complex. Transfer of an unshared pair of electrons to an empty d orbital of the metal resulted in the formation of a coordinate bond. The formation of intermediate is likely to undergo a further rapid reaction in which the incipient.

It is of interest to compare here the mode of oxidation of methionine by PFC,[19] pyridinium chlorochromate (PCC),[20] pyridinium bromochromate (PBC)[21] and TMGCC. The oxidation by PFC and PBC presented a similar kinetic picture, i.e. the reactions are of first order with respect to the reductants. While in the oxidation by

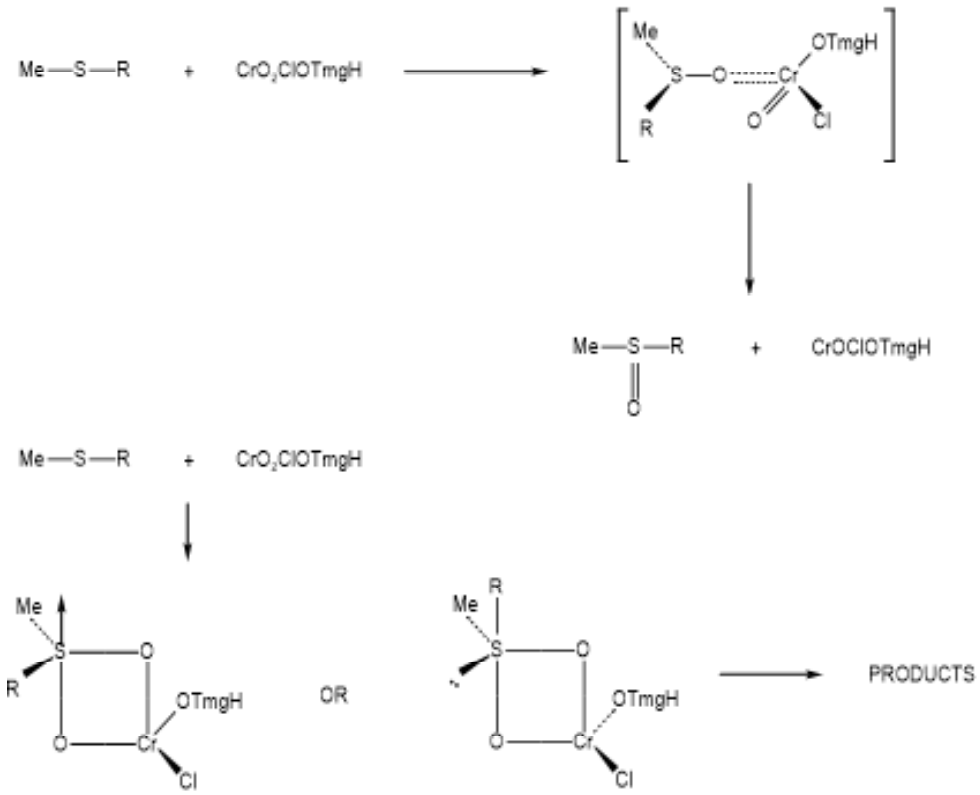

PCC and TMGCC, Michaelis Menten type kinetics was observed with respect to the reductants. It is possible that the values of the formation constants for the reductant PFC/PBC complexes are very low. This resulted in the observation of second order kinetics. No explanation of the difference is available presently. Solvent effects and the dependence of the hydrogen ions are of similar nature in all these reactions, for which essentially similar mechanisms have been proposed.

Conclusions

The oxidation of DL-methionine involves a rate-determining electrophilic attack of methionine sulfur at the metal ion *via* an intermediate complex. Both deprotonated and protonated forms of TMGCC are reactive oxidizing species.

Acknowledgement

Thanks are due to the UGC, New Delhi for financial support in the form of UGC-One time grant to PP and CSIR-NET-JRF to PN, and to Department of Chemistry, JNV University, Jodhpur for lab facilities.

References

1. Cainelli G. and Cardillo G., 1984, Chromium Oxidations in Organic Chemistry, (Springer-Verlag, Berlin) 19.
2. Firouzabadi H. and Sharifi A., 1992, *Synthesis*, 999.
3. Li M. and Johnson M.E., 1995, *Synth..Communn.*, **25**, 533.
4. Mahanti M.K. and Banerji K.K., 2002, *J. Indian Chem. Soc.*, **79**, 31.

5. Sendil K., Ozgun H.B. and Ustun E., 2016, *Journal of Chemistry*, 1.

6. Sharma G., Banerji J., Purohit P., Sharma P.K. and Banerji K.K., 2014, *Eur. Chem. Bull.*, **3(11)** 1081.

7. Ranga V., Rao A., Soni U., Purohit P., Sharma P.K., 2016, *J. Indian Chem. Soc.*, **93(10)** 1377.

8. Sharma R., Soni D., Kamla, Purohit P., Sharma P.K., 2019, *J. Emer. Tech. Innov. Res.*, **6(5)** 136.

9. Kamla, Naga P., Purohit P., Sharma V., 2021 *Rasayan J. Chem.*, (Special Issue) 217.

10. Mahadevappa D.S., Ananda S., Gouda N.M.M. and Rangappa K.S., 1985, *J. Chem. Soc., Perkin Trans.* **2**, 39 and references cited therein.

11. Mittal S., Sharma V. and Banerji K.K., 1986, *J. Chem. Research*(S) 264.

12. Perrin D.D., Armarego W.L. and Perrin D.R., 1966, Purification of Organic Compounds, Pergamon Press, Oxford.

13. Mitchell J., 1953, *Organic Analysis*, Interscience, New York, **1**, 375.

14. Bhattacharjee M.N., Choudhuri M.K., Purakayastha S., 1987, *Tetrahedron*, **43**, 5389.

15. Brown H.C., Rao G.C. and S.U. Kulkarni, 1979, *J. Org. Chem.*, **44**, 2809.

16. Kamlet M.J., Abboud J.L.M., Abraham M.H. and Taft R.W., 1983, *J. Org. Chem.*, **48,** 2877.

17. Exner O., *Collect Chem. Czech. Commun.*, 1966, **31**, 3222.

18. Swain C.G., Swain M.S., Pqwel A.L. and Alunni S., 1983, *J. Am. Chem. Soc.*, **105**, 502.

19. Sharma V., Sharma P.K. and Banerji K.K., 1996, *J. Chem. Research (S)*, 290.

20. Sharma V., Sharma P.K. and Banerji K.K., 1997, *J. Indian Chem. Soc.*, **74**, 607.

21. Sharma V., Sharma P.K. and Banerji K.K., 1997, *Indian J. Chem.*, **36A**, 418.

RNI No. MAHENG/2017/74063
ISSN No. (Print) 2581-5911
ISI Impact Factor 1.724

Sudha Jain and Reetu Sangwan
G P Globalize Research Journal of Chemistry
Vol 7 Issue 1 2023 : pp 28 - 44

Synthesis and Biological Evaluation of Theobromine Analogs Based on Purine Alkaloids

Reetu Sangwan[1] and Sudha Jain [1*]
[a]Department of Chemistry, University of Lucknow, Lucknow-226001, UP, India
Email: ritnikrana@gmail.com, jainsudha2954@gmail.com

ABSTRACT
*Methylxanthines are a group of phytochemicals derived from the purine base xanthine and obtained from plant secondary metabolism and used in daily diet in common products such as coffee, tea, energetic drinks and chocolate. Theobromine is another relevant methylxanthine commonly available in the aforementioned sources. Herein, we explore the synthesis of theobromine analogs **(4a-4l)** at N1 reactive site in three steps predicted by retrosynthetic analysis. All the synthesized analogs were screened for antioxidant (free radical scavenging activity) and antibacterial activity from which only four analogs **4b** with 3,4-dimethoxybenzyl substituent, **4d** with -OCH_2Ph substituent, **4h** with 2,3,4-trimethoxybenzyl substituent and **4l** with 4-nitrobenzyl substituent showed the free radical scavenging activity with % inhibition 98.55%, 99.13%, 97.91% and 97.87% as compared to standard BHT (99.35%) at 1000 μg/mL concentration and only two compounds **4k** with -OBz and **4l** with 4-nitrobenzyl substituent were found to be moderately active against all five bacterial strains.*

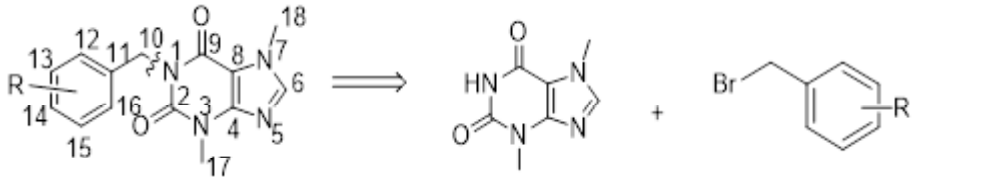

Reterosynthetic analysis of theobromine analogs

Introduction

Purine the N-heterocycle, abundantly found in nature was firstly synthesized by Emil Fischer, as a colorless crystalline weak base from uric acid in 1899.[1] A large number of purine alkaloids isolated from natural sources act as leads for new pharmacologically active compounds.[2-4] The purine alkaloids known by their trivial names are adenine, guanine, hypoxanthine, isoguanine, and uric acid.[5,6] Other important group of naturally occurring purine alkaloids are xanthine, which includes caffeine, theobromine, theophylline, hypoxanthine, paraxanthine, heteroxanthine etc.[7-10] The most important naturally occurring xanthines are caffeine, theobromine, and theophylline. The methylxanthines are found in limited number of plant species such as tea (*Camellia sinensis* L.), coffee (*Coffea* sp.) and cacao (*Theobroma cacao* L.).[11,12] Theobromine, one of the major xanthine

alkaloids, is also found in a variety of other foodstuffs such as tea leaves, guarana and cola nuts.[13] It is also known as the "food of the God" because in Greek the word "theo" means "God" and "broma" means "food". It is reported in literature that if theobromine has been consumed through chocolate consumption, it decreases the plasma low-density lipoprotein (LDL) cholesterol and increases high-density lipoprotein (HDL) cholesterol.[14-19] Theobromine is used as dilator for the coronary and peripheral arteries[20], antiangiogenic[21], antitumour agent[22], vasodilator[23], anti-inflammatory agents[24,25], diuretic[26], antioxidant[27-29], anticarcinogenic effect[30], as a skin moisturant[31] and antitussive[32].

There is a special interest in the synthesis of new theobromine derivatives because of their widespread biological and physiological properties. As it is clear from the structure of theobromine that it has two major reacting sites one at N1 position and other is C6 position. Although many theobromine with substitution variations at the 1-, 3-, 7-, and 6-position have been synthesized, to the best of our knowledge there is not even a single compound reported with simple aromatic substitution at the 1N-position of theobromine compound. It was therefore thought worthwhile, to carry out the synthesis of 1N-substituted theobromine derivatives **(4a-4l)** for the evaluation of *in vitro* anti-oxidant (free radical scavenging activity using DPPH) taking BHT as standard of all the synthesized compounds **(4a -4l)** along with antibacterial activity following cup-plate method using Muller- Hinton Agar for bacteria against standard drug streptomycin.

Materials and Methods

Melting points were determined in a melting point apparatus. The IR spectra were recorded on a Perkin-Elmer RX-1 (4000-450 cm^{-1}) spectrophotometer using KBr pellets. ^{1}H NMR and ^{13}C NMR (Nuclear Magnetic Resonance) spectra were recorded on Bruker 300 MHz instrument using $CDCl_3$ as a solvent. Chemical shifts are reported in parts per million (ppm) using Tetramethylsilane (TMS) as internal standard. Solvents and reagents were used without further purification, unless otherwise specified. The Positive Electron Spray Ionization (ESI) High resolution mass spectra of compounds were recorded on Agilent 6520(Q-TOF) mass spectrometer. Ultra violet (UV) spectra were recorded on UV–visible Double-Beam Spectrophotometer (systronic-2203) instrument using chloroform as a solvent. Thin layer chromatograms (TLCs) were visualized in an iodine chamber and carried out on pre coated silica gel plates 60 F254 or RP-18 F254 plates (Merck). TLC was carried out on pre coated silica gel plates 60 F254 (Merck) for monitoring of reactions. Spots were visualized by UV light or by iodine chamber. Column Chromatography was performed using silica gel (230-400 and 100-200 mesh size). 1, 1-Dipheny1-2-picryl-hydrazyl (DPPH) was purchased from Sigma-Aldrich Merck to determine the antioxidant activity of synthesized compounds in terms of free radical scavenging activities. Theobromine and benzyl bromides **3a** and **3l** were purchased from Aldrich Chemical Co.

Synthesis of Benzyl bromide (3b-3l)

- **3, 4-Dimethoxybenzyl bromide (3b)**

$NaBH_4$ (65.0mg 1.7mmol) was added in portions to a stirred solution of 3,4-dimethoxybenzaldehyde (**1b**) (1.0 gm 3mmol) in 10 mL of CH_3OH/THF (1:1) in ice-water bath and stirring was continued for 30 min (TLC monitored). After completion of reaction, the solvent was evaporated. Then 1M HCl was poured into the mixture to neutralize excess $NaBH_4$. The resulting solution was extracted with DCM (2×20ml). The DCM layer was washed with brine solution (2×2mL), dried (anhyd. Na_2SO_4), and filtered to afford the corresponding benzyl alcohol (**2b**). The benzyl alcohol (**2b**) so obtained was used in the next step without purification. Phosphorus tribromide (3.16mmol) was added dropwise to a stirred solution of substituted benzyl alcohol in DCM (30ml) and cooled at 0°C. After 40 min of vigorous stirring at 0°C, the reaction mixture was slowly quenched

with ice water. The DCM layer was separated and aqueous layer was further extracted with DCM (2× 20ml). The combined organic layer was washed twice with H_2O, dried (anhyd. Na_2SO_4) and evaporated under reduced pressure to give 3, 4-Dimethoxybenzyl bromide **(3b).**

Yield: 76%; Bright yellow oil; ^1H ($CDCl_3$, 300 MHz; δ, ppm): 6.97-6.88 (2H, m, Ar-H), 6.1 (1H, m, Ar-H), 4.48 (2H, s, CH_2), 3.84(3H, s, OCH_3). ^{13}C ($CDCl_3$, 75 MHz; δ, ppm): 149.98, 149.86, 148.85, 131.02, 121.35, 113.86, 111.82, 55.73, 34.24; ESI-MS *m/z* 334 $[M+H]^+$; $C_{15}H_{11}O_4Br$.

➢ **2-Bromo-3-(bromomethyl)-6-methoxyphenyl benzoate (3c)**

The compound **3c** was prepared in a similar manner as described earlier for the synthesis of **(3b)** using (**2c)** which was obtained by the $NaBH_4$ reduction of (**1c).** Yield: 86%; Yellow solid; m.p. 44-46^{0}C; ^1H ($CDCl_3$, 300 MHz; δ, ppm): 8.32(2H, m, J=8.3, Ar-H), 7.50-7.60(3H, m, J=8.3, Ar-H), 6.91(1H, d, Ar-H), 6.88(1H, d, Ar-H), 4.36(2H, s, CH_2), 3.83(3H, s, OCH_3). ^{13}C ($CDCl_3$, 75 MHz; δ, ppm): 165.2, 154.1, 138.6, 133.9, 130.3, 128.6, 122.0, 113.5, 11.1, 55.8, 33.4 ESI-MS *m/z* 334 $[M+H]^+$; $C_{15}H_{11}O_4Br$.

➢ **4-Benzyloxybenzyl bromide (3d)**

The compound **3d** was prepared in a similar manner as described earlier for the synthesis of **(3b)** using **2d** which was obtained by the $NaBH_4$ reduction of **1d.** Yield: 96%; Off-white solid; m.p. 51-53°C; ^1H ($CDCl_3$, 300 MHz; δ, ppm): 6.98-7.49 (9H, m, Ar-H), 5.11 (2H, s, -O**C**H_2Ph), 4.55 (2H, s, CH_2Br); ^{13}C ($CDCl_3$, 75 MHz; δ, ppm): 159.02, 136.80, 130.03, 128.94, 128.12, 114.53, 2.87, 33.60; ESI-MS *m/z* 273 $[M+H]^+$, $C_{14}H_{13}BrO$.

➢ **4-Methoxybenzyl bromide (3e)**

The compound **3e** was prepared in a similar manner as described earlier for the synthesis of **(3b)** using **2e** which was obtained by the $NaBH_4$ reduction of **1e.** Yield: 91%; light yellow oil; ^1H ($CDCl_3$, 300 MHz; δ, ppm): 7.27-7.29(2H, d, J = 8 Hz, Ar-H), 6.87-6.89 (2H, d, J=8 Hz, Ar-H), 4.61 (2H, s, -CH_2Br), 3.80 (3H, s, -OCH_3); ^{13}C ($CDCl_3$, 75 MHz; δ, ppm): 159.8, 130.02, 129.35, 114.86, 55.73, 34.24; ESI-MS *m/z* 199 $[M+H]^+$, C_8H_9BrO.

➢ **4-(Bromomethyl)-2-methoxyphenyl benzoate (3f)**

The compound **3f** was prepared in a similar manner as described earlier for the synthesis of **(3b)** using **2f** which was obtained by the $NaBH_4$ reduction of **1f.** Yield: 92%; light yellow oil; ^1H ($CDCl_3$, 300 MHz; δ, ppm): 8.22(2H, m, J=8.2, Ar-H), 7.60-7.2(3H, m, J=8.2, Ar-H), 6.86-7.14(3H, m, Ar-H), 4.56(2H, s, CH_2Br), 3.83(3H, s, OCH_3); ^{13}C ($CDCl_3$, 75 MHz; δ, ppm): 165.2, 151.6, 138.6, 135.8, 133.9, 130.2, 122.9, 121.7, 113.5, 55.8, 33.6 ESI-MS *m/z* 322 $[M+H]^+$; $C_{15}H_{13}O_3Br$.

➢ **4-(Bromomethyl)phenyl benzoate(3g)**

The compound **3g** was prepared in a similar manner as described earlier for the synthesis of **(3b)** using **2g** which was obtained by the $NaBH_4$ reduction of **1g.** Yield: 91%; light yellow oil; ^1H ($CDCl_3$, 300 MHz; δ, ppm): 8.22(2H, m, J=8.2, Ar-H), 7.60-7.2(3H, m, J=8.2, Ar-H), 7.30(2H, m, J=8.0, Ar-H), 7.25(2H, m, J=8.0, Ar-H), 4.56(2H, s, CH_2Br). ^{13}C ($CDCl_3$, 75 MHz; δ, ppm): 165.2, 149.6, 134.8, 133.9, 130.3, 129.4, 128.6, 121.9, 113.5, 33.6 ESI-MS *m/z* 291 $[M+H]^+$; $C_{14}H_{11}O_2Br$.

➢ **2, 3, 4-Trimethoxybenzyl bromide (3h)**

The compound **3h** was prepared in a similar manner as described earlier for the synthesis of **(3b)** using **2h** which was obtained by the $NaBH_4$ reduction of **1h.** Yield: 84%; Yellow oil; ^1H ($CDCl_3$, 300 MHz; δ, ppm): 6.62-6.59 (2H, d, J=1.2Hz, Ar-H), 6.38-6.36 (2H, d, J= 8Hz, Ar-H), 4.59 (2H, s, CH_2Br), 3.86 (6H, s, -OCH_3), 3.84 (3H, s, - OCH_3). ^{13}C ($CDCl_3$, 75 MHz; δ, ppm): 154.12(-**C**-OCH3), 150.48, 143.16, 138.57, 136.43, 107.00, 61.04, 61.4, 56.36, 32.42; ESI-MS *m/z* 260 $[M+H]^+$, $C_{10}H_{13}O_3Br$.

➢ **2-Methoxybenzyl bromide (3i)**

The compound **3i** was prepared in a similar manner as described earlier for the synthesis of **(3b)** using **2i** which was obtained by the $NaBH_4$ reduction of **1i.** Yield: 89%;

light Yellow Oil; ^{1}H ($CDCl_3$, 300 MHz; δ, ppm): 7.29-7.23 (2H, m, Ar-H), 6.96-6.86 (2H, m, Ar-H), 4.67 (2H, s, $-CH_2Br$), 3.84(3H, s, $-OCH_3$). ^{13}C ($CDCl_3$, 75 MHz; δ, ppm): 158.60, 131.02, 127.26, 121.35, 112.86, 56.73, 29.4; ESI-MS *m/z* 260 $[M+H]^+$, $C_8H_9O_3Br$.

➢ **3, 4-Dibenzyloxybenzyl bromide (3j)**

The compound **3j** was prepared in a similar manner as described earlier for the synthesis of **(3b)** using **2j** which was obtained by the $NaBH_4$ reduction of **1j.** Yield: 86%; Light yellow oil; ^{1}H ($CDCl_3$, 300 MHz; δ, ppm): 7.31-7.41 (4H, m, Ar-H), 7.38 (6H, m, Ar-H), 6.90 (1H, s, Ar-H), 6.76 (1H, d, J= 8.4, Ar-H), 6.68 (1H, d, J= 8.4, Ar-H), 5.01.(2H, s, -O**C**H$_2$Ph), 5.00 (2H, s, -O**C**H$_2$Ph) 4.40(2H, s, CH$_2$Br). ^{13}C ($CDCl_3$, 75 MHz; δ, ppm): 150.20, 136.78, 131.3, 128.84, 127.80, 127.15, 123.37, 114.40, 112.77, 77.45, 34.00; ESI-MS *m/z* 382 $[M+H]^+$, $C_{21}H_{19}O_2Br$.

➢ **4-(Bromomethyl)-1,2-phenylene dibenzoate (3k)**

The compound **3k** was prepared in a similar manner as described earlier for the synthesis of **(3b)** using **2k** which was obtained by the $NaBH_4$ reduction of **1k.** Yield: 88%; Light yellow oil; ^{1}H ($CDCl_3$, 300 MHz; δ, ppm): 7.60-8.22 (10H, m, Ar-H), 7.46 (1H, s, Ar-H), 7.32 (1H, d, J= 8.4, Ar-H), 7.20 (1H, d, J= 8.4, Ar-H), 4.46(2H, s, CH$_2$Br). ^{13}C ($CDCl_3$, 75 MHz; δ, ppm):165.21, 146.0, 135.23, 133.90, 130.30, 128.67, 122.34, 120.89, 33.36 ESI-MS *m/z* 411 $[M+H]^+$, $C_{21}H_{15}O_4Br$.

Synthesis of Theobromine analogs (4a-4l)

We have attempted five methods for the synthesis of theobromine analogs. The detailed description about these method are as follows:

Method 1: In a 100 mL round bottom flask, theobromine **(**540 mg, 3 mmol) was stirred in DMSO in presence of NaOH at 20°C. Then benzyl bromide **(3a)** (1 ml) was added drop wise to the reaction mixture. The reaction mixture was stirred for 8 hrs. After completion of reaction (TLC monitored in UV lamp), the reaction mixture was poured into ice cold water. The precipitate was filtered and purified by column chromatography using $CHCl_3$: Methanol (9:1) as an eluent to afford the product 1-benzyl-3,7-dimethyl-1H-purine-2,6(3H,7H)-dione **(4a)**. Yield: ~ 60%.

Method 2: In a 100 mL round bottom flask, theobromine **(**540 mg, 3 mmol) was refluxed in ethanol in presence of KOH. Then benzyl bromide **(3a)** (1 ml) was added drop wise to the reaction mixture. The reaction mixture was refluxed for 12 hrs. After completion of reaction (TLC monitored in UV lamp), the reaction mixture was poured into ice cold water. The precipitate was filtered and purified by column chromatography using $CHCl_3$: Methanol (9:1) as an eluent to afford the product 1-benzyl-3,7-dimethyl-1H-purine-2,6(3H,7H)-dione **(4a)**. Yield: ~ 65%.

Method 3: In a 100 mL round bottom flask, theobromine **(**540 mg, 3 mmol) was stirred in DMF in presence of K_2CO_3 at room temperature. Then benzyl bromide **(3a)** (1 ml) was added drop wise to the reaction mixture. The reaction mixture was stirred for 24 hrs. After completion of reaction (TLC monitored in UV lamp), the reaction mixture was poured into ice cold water. The precipitate was filtered and purified by column chromatography using $CHCl_3$:Methanol (9:1) as an eluent to afford the product 1-benzyl-3,7-dimethyl-1H-purine-2,6(3H,7H)-dione **(4a)**. Yield: ~ 56%.

Method 4: In a 100 mL round bottom flask, theobromine **(**540 mg, 3 mmol) was refluxed in THF in presence of K_2CO_3 and KI. Then benzyl bromide **(3a)** (1 ml) was added drop wise to the reaction mixture. The reaction mixture was refluxed for 6 hrs. After completion of reaction (TLC monitored in UV lamp), the reaction mixture was poured into ice cold water. The precipitate was filtered and purified by column chromatography using $CHCl_3$:Methanol (9:1) as an eluent to afford the product 1-benzyl-3,7-dimethyl-1H-purine-2,6(3H,7H)-dione **(4a)**. Yield: ~ 59%.

Method 5: In a 100 mL round bottom flask, NaOMe (300 mg) in MeOH (20 ml) was stirred well at room

temperature. Then theobromine **(**540 mg, 3 mmol) added and reaction mixture was stirred vigorously so that the theobromine properly dissolved in MeOH. Then benzyl bromide **(3a)** (1 ml) was added drop wise to the reaction mixture with the help of pressure equalized dropping funnel. After completion of reaction (TLC monitored in UV lamp), the solvent evaporated under reduced pressure, extracted with DCM (2x10 ml), washed with brine and dried (anhyd. Na_2SO_4) to afford the product 1-benzyl-3,7-dimethyl-1H-purine-2,6(3H,7H)-dione **(4a)**. Yield: ~ 90%

➢ **1-Benzyl-3,7-dimethyl-1H-purine-2,6(3H,7H)-dione (4a)**

The compound **4a** was synthesized by following the method 5 described above. The pure compound **4a** was obtained as a white solid, m.p. 282-285R"C; Yield: ~ 90%; TLC Solvent System: 9:1 ($CHCl_3$: MeOH), Rf value: 0.2; IR (KBr; υ_{max}, cm^{-1}) 3107.32 (-CH Stretching), 125.07 (C=O Stretching), 1658.78 (C=O Stretching), 1598.99 (C=N Stretching), 1028.06 (C-N Stretching), 104.42 (C-N Stretching), 1126.43 (C-N Stretching). ^1H ($CDCl_3$, 300 MHz; δ, ppm): 7.513 (1H, s, =CH, H-6, H-6), 7.25-7.48 (5H, m, Ar-H), 5.200 (2H, s, CH_2, H-10), 3.98(3H, s, CH_3, H-17), 3.578(3H, s, CH_3, H-18). ^{13}C ($CDCl_3$, 75 MHz; δ, ppm): 155.41 (C=O), 151.76 (C=O), 149.00 (C-4), 141.74 (C-16), 137.44 (C-11), 129.2 (C-12), 128.96 (C-13), 128.56 (C-14), 127.1 (C-15), 121.11 (C-16), 107.81 (C-8), 44.56 (C-10), 33.80 (C-17), 31.11 (C-18). HRMS *m/z* 23 $[M+H]^+$; Anal. Calcd. for $C_{14}H_{14}N_4O_2$: C 62.21, H 5.22, N 20.73, O 11.84.

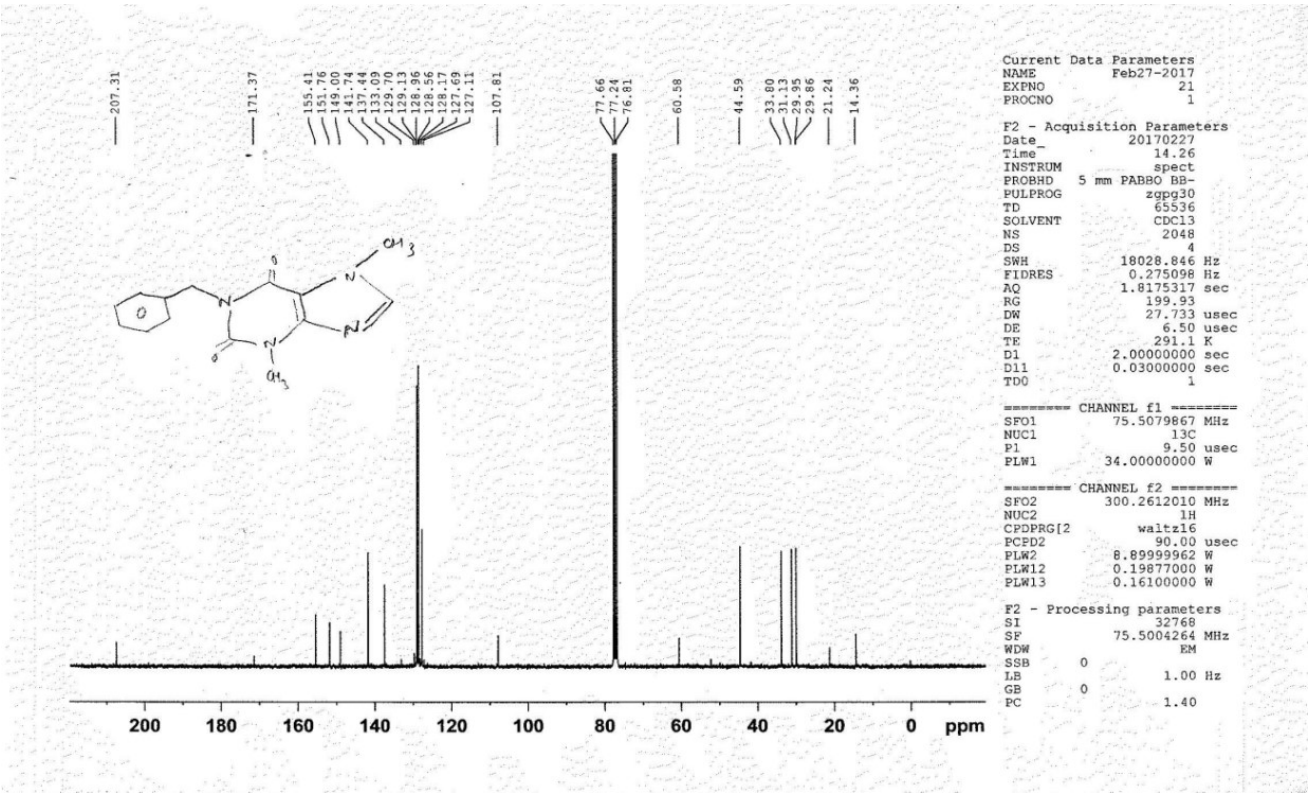

^{13}C NMR Spectra of 4a

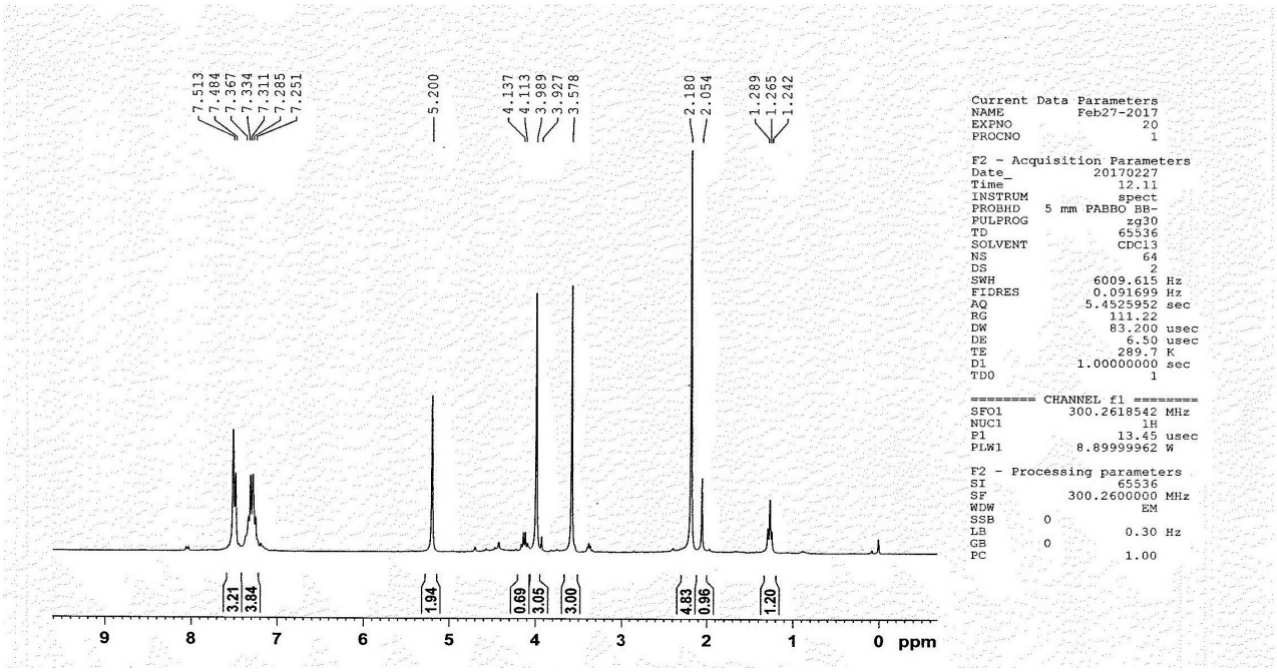

^{1}H NMR Spectra of 4a

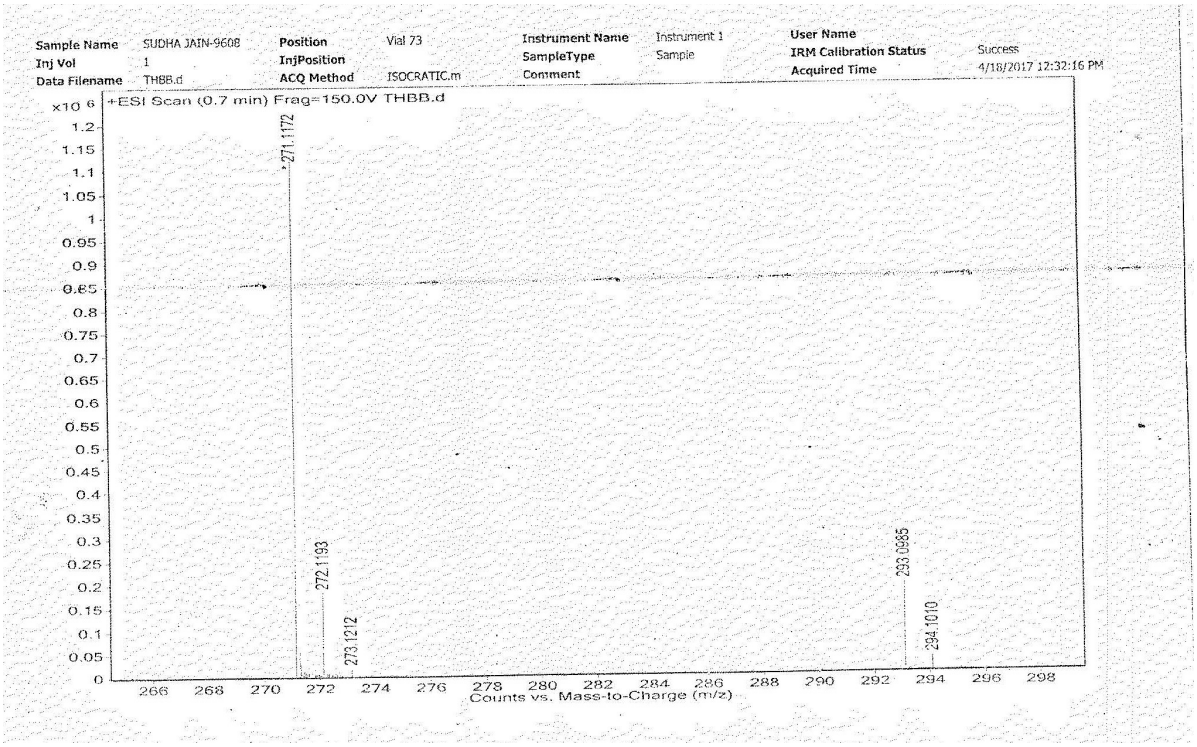

Mass Spectra of 4a

All the other compounds **(4b-4l)** were synthesized by a similar procedure. The data of the theobromine analogs is as follows:

➢ **1-1-(3,4-Dimethoxybenzyl)-3,7-dimethyl-1H-purine 2,6(3H,7H)-dione (4b)**

This was prepared in a similar procedure as described earlier for the synthesis of **4a** by the reaction of **3b** with theobromine**.** The pure compound **4b** was obtained as a white solid, m.p. 290-293$^{R"}$C; Yield: ~ 85%; TLC Solvent System: 9:1 ($CHCl_3$: MeOH), Rf value: 0.60; IR (KBr; υ_{max}, cm^{-1}) 2931.80 (-CH Stretching), 113.50 (C=O Stretching), 1660.3 (C=O Stretching), 1606.2 (C=N Stretching), 1263.37 (C-N Stretching), 1220.94 (C-N Stretching), 1150.4 (C-O Stretching), 1145.4 (C-N Stretching). ^{1}H ($CDCl_3$, 300 MHz; δ, ppm): 7.98 (1H, s, =CH, H-6, H-6), 7.03 (1H, s, Ar-H, H-12), 6.76 (1H, d, J= 6.9, Ar-H, H-15), 6.81(1H, d, J= 6.9, Ar-H, H-16), 5.21 (2H, s, CH_2, H-10), 3.98(3H, s, CH_3, H-17), 3.83(6H, s, OCH_3, H-19, H-20), 3.578(3H, s, CH_3, H-18). ^{13}C ($CDCl_3$, 75 MHz; δ, ppm): 155.31 (C=O), 152.66 (C=O), 149.56 (C-13), 148.01 (C-4), 147.80 (C-14), 143.35 (C-6), 139.54 (C-11), 122.56 (C-15), 112.67 (C-16), 109.23 (C-12), 107.81 (C-8), 56.1 (OCH_3), 44.56 (C-10), 33.80 (C-17), 31.11 (C-18). ESI-MS *m/z* 331 $[M+H]^+$; Anal. Calcd. for $C_{16}H_{18}N_4O_4$: C 58.17, H 5.49, N 16.96, O 19.37.

➢ **2-Bromo-3-((3,7-dimethyl-2,6-dioxo-2,3,6,7-tetrahydro-1H-purin-1-yl)methyl)-6-methoxyphenyl benzoate (4c)**

This was prepared in a similar procedure as described earlier for the synthesis of **4a** by the reaction of **3c** with theobromine**.** The pure compound **4c** was obtained as a off white solid, m.p. 332-335°C; Yield: ~ 76%; TLC Solvent System: 9:1 ($CHCl_3$: MeOH), Rf value: 0.65; IR (KBr; υ_{max}, cm^{-1}) 2951.2 (-CH Stretching), 1755.42 (C=O Stretching), 1733.50 (C=O Stretching), 110.3 (C=O Stretching), 1650.2 (C=N Stretching), 1163.37 (C-N Stretching), 1120.94 (C-N Stretching), 1115.4 (C-N Stretching), 650.87 (C-Br). ^{1}H ($CDCl_3$, 300 MHz; δ, ppm): 7.97 (1H, s, =CH, H-6), 7.60-8.22 (5H, m, Ar-H, C-21 to C-26), 6.91 (1H, d, J= 7.0, Ar-H, C-15), 6.88(1H, d, J= 7.0, Ar-H, C-16), 5.18 (2H, s, CH_2, C-10), 3.4(3H, s, CH_3, , C-17), 3.83(3H, s, OCH_3, C-19), 3.36(3H, s, CH_3, C-18). ^{13}C ($CDCl_3$, 75 MHz; δ, ppm): 165.20 (C=O), 154.81 (C-2), 151.9 (C-14), 151.36 (C-9), 148.41 (C-4), 143.35 (C-6), 139.54 (C-13), 138.12 (C-11), 133.90, 130.68,130.3, 128.56, 126.90 (C-16), 119.78 (C-12), 111.67 (C-15), 109.23 (C-8), 56.4 (OCH_3), 44.76 (C-10), 34.80 (C-17), 30.11 (C-18). ESI-MS *m/z* 499 $[M+H]^+$; Anal. Calcd. for $C_{22}H_{19}BrN_4O_5$: C 52.92, H 3.84, Br 16.00, N 11.22, O 16.02.

➢ **1-(4-(Benzyloxy)benzyl)-3,7-dimethyl-1H-purine-2,6(3H,7H)-dione (4d)**

This was prepared in a similar procedure as described earlier for the synthesis of **4a** by the reaction of **3d** with theobromine**.** The pure compound **4d** was obtained as a yellow solid, m.p. 295-298°C; Yield: ~ 82%; TLC Solvent System: 9:1 ($CHCl_3$: MeOH), Rf value: 0.60; IR (KBr; υ_{max}, cm^{-1}) 2955.90 (-CH stretching), 133.50 (C=O stretching), 1680.81 (C=O stretching), 1630.60 (C=N stretching), 1250.67 (C-O stretching), 1253.37 (C-N stretching), 1120.94 (C-N stretching), 1118.4 (C-N stretching), . ^{1}H ($CDCl_3$, 300 MHz; δ, ppm): 7.97 (1H, s, =CH, H-6), 7.38-7.47 (5H, m, Ar-H, OBn, C-21 to C-25), 6.87 (2H, dd, J= 7.8, Ar-H, C-13, C-15), 7.25(2H, dd, J= 7.8, Ar-H, C-12, C-16), 5.28 (2H, s, CH_2, C-10), 5.01 (2H, s, CH_2, OCH_2Ph, C-19), 3.4(3H, s, CH_3, C-17), 3.36(3H, s, CH_3, C-18). ^{13}C ($CDCl_3$, 75 MHz; ä, ppm): 157.01 (C=O), 154.81 (C=O), 151.36 (C-14), 148.41 (C-4), 143.35 (C-6), 136.44, 133.90, 128.89 (C-11), 130.58 (C-12, C-16), 127.16, 114.14 (C-13, C-15), 108.23 (C-8), 2.90 (OCH_2Ph), 46.76 (C-10), 34.80 (C-17), 30.11 (C-18). ESI-MS *m/z* 377 $[M+H]^+$; Anal. Calcd. for $C_{21}H_{20}N_4O_3$: C 67.01, H 5.36, N 14.88, O 12.75.

➢ **1-(4-Methoxybenzyl)-3,7-dimethyl-1H-purine-2,6(3H,7H)-dione (4e)**

This was prepared in a similar procedure as described earlier for the synthesis of **4a** by the reaction of **3e** with

theobromine**.** The pure compound **4e** was obtained as a yellow solid, m.p. 285-287˚C; Yield: ~ 86%; TLC Solvent System: 9:1 ($CHCl_3$: MeOH), Rf value: 0.2; IR (KBr; υ_{max}, cm^{-1}) 2999.30 (-CH stretching), 111.57 (C=O stretching), 1662.64 (C=O stretching), 1606.2 (C=N stretching), 1296.17 (C-O stretching), 1247.94 (C-N stretching), 1178.51 (C-N stretching), 1112.92 (C-N stretching), . ^1H ($CDCl_3$, 300 MHz; δ, ppm): 7.19 (1H, s, =C<u>H</u>, H-6), 6.4-6.83 (2H, dd, J= 7.5, Ar-H, C-13, C-15), 7.46-7.64(2H, dd, J= 7.5, Ar-H, C-12, C-16), 4.84 (2H, s, CH_2, C-10), 3.79(3H, s, CH_3, C-17), 3.49(3H, s, CH_3, C-18), 3.94 (3H, s, O<u>C</u>H_3). ^{13}C ($CDCl_3$, 75 MHz; δ, ppm): 167.83 (C-14), 154.81 (C=O), 151.36 (C=O), 148.41(C-4), 143.35 (C-6), 132.43, 130.93 (C-12, C-16), 119.42 (C-13, C-15), 128.82 (C-11), 113.78 (C-8), 57.84 (O<u>C</u>H_3), 55.30 (C-10), 38.2 (C-17), 30.35 (C-18). ESI-MS *m/z* 301 $[M+H]^+$; Anal. Calcd. for $C_{15}H_{16}N_4O_3$: C 59.99, H 5.37, N 18.66, O 15.98.

➢ **4-((3,7-Dimethyl-2,6-dioxo-2,3,6,7-tetrahydro-1H-purin-1-yl)methyl)-2-methoxyphenyl benzoate (4f)**

This was prepared in a similar procedure as described earlier for the synthesis of **4a** by the reaction of **3f** with theobromine**.** The pure compound **4f** was obtained as a yellow solid, m.p. 310-311˚C; Yield: ~ 89%; TLC Solvent System: 9:1 ($CHCl_3$: MeOH), Rf value: 0.45; IR (KBr; υ_{max}, cm^{-1}) 3010.90 (-CH stretching), 143.50 (C=O stretching), 110.81 (C=O stretching), 1660.60 (C=O stretching), 1650.2 (C=N stretching), 1230.67 (C-O stretching), 1233.37 (C-N stretching), 1180.94 (C-N stretching), 1178.4 (C-N stretching), ^1H ($CDCl_3$, 300 MHz; δ, ppm): 7.36 (1H, s, =C<u>H</u>, H-6), 7.28-7.41 (5H, m, Ar-H, C-22 to C-26), 6.74-6.88(3H, m, Ar-<u>H</u>), 5.16 (2H, s, CH_2, H-10), 3.83 (3H, s, H-19), 3.95(3H, s, CH_3, H-17), 3.32(3H, s, CH_3, H-18). ^{13}C ($CDCl_3$, 75 MHz; ä, ppm): 167.75 (O(<u>C</u>=O)Ph), 154.8 (C=O), 150.43 (C=O), 149.83 (C-4), 147.97 (C-13), 146.49 (C-6), 137.51 (C-11), 133.94, 131.79, 131.52, 131.46 (C-14), 128.60, 127.87 (C-15), 127.46 (C-16), 111.82 (C-12), 111.63 (C-8), 56.25 (C-10), 37.41 (C-17), 30.41 (C-18). ESI-MS *m/z* 421 $[M+H]^+$; Anal. Calcd. for $C_{22}H_{20}N_4O_5$: C 62.85, H 4.79, N 13.33, O 19.03

➢ **4-((3,7-Dimethyl-2,6-dioxo-2,3,6,7-tetrahydro-1H-purin-1-yl)methyl)phenyl benzoate (4g)**

This was prepared in a similar procedure as described earlier for the synthesis of **4a** by the reaction of **3g** with theobromine**.** The pure compound **4g** was obtained as a yellow solid, m.p. 298-299R"C; Yield: ~ 80%; TLC Solvent System: 9:1 ($CHCl_3$: MeOH), Rf value: 0.55; IR (KBr; υ_{max}, cm^{-1}) 2995.90 (-CH stretching), 143.40 (C=O stretching), 113.50 (C=O stretching), 162.31 (C=O stretching), 1640.80 (C=N stretching), 1330.57 (C-O stretching), 1273.37 (C-N stretching), 1210.94 (C-N stretching), 1198.4 (C-N stretching), . ^1H ($CDCl_3$, 300 MHz; δ, ppm): 7.19 (1H, s, =C<u>H</u>, H-6), 7.45-7.65 (9H, m, Ar-<u>H</u>), 4.43 (2H, s, CH_2, C-10), 3.90(3H, s, CH_3, C-17), 3.47(3H, s, CH_3, C-18). ^{13}C ($CDCl_3$, 75 MHz; δ, ppm): 167.82 (C=O), 154.41 (C=O), 150.43 (C=O), 149.83 (C-4), 147.97 (C-14), 146.49 (C-11), 143.35 (C-6), 132.43, 130.93, 128.82, 127.87, 127.46 (C-12, C-16), 120.76 (C-13, C-15), 48.17 (C-10), 38.3 (C-17), 30.35 (C-18). ESI-MS *m/z* 391 $[M+H]^+$; Anal. Calcd. for $C_{21}H_{18}N_4O_4$: C 64.61, H 4.65, N 14.35, O 16.39.

➢ **3,7-Dimethyl-1-(2,3,4-trimethoxybenzyl)-1H-purine-2,6(3H,7H)-dione (4h)**

This was prepared in a similar procedure as described earlier for the synthesis of **4a** by the reaction of **3h** with theobromine**.** The pure compound **4h** was obtained as a yellow solid, m.p. 302-304˚C; Yield: ~ 92%; TLC Solvent System: 9:1 ($CHCl_3$: MeOH), Rf value: 0.65; IR (KBr; υ_{max}, cm^{-1}) 2933.30 (-CH Stretching), 115.50 (C=O Stretching), 1662.3 (C=O Stretching), 1636.2 (C=N Stretching), 1273.37 (C-N Stretching), 1250.94 (C-N Stretching), 1150.4 (C-O Stretching), 1140.4 (C-N Stretching), . ^1H ($CDCl_3$, 300 MHz; δ, ppm): 7.98 (1H, s, =C<u>H</u>, H-6), 6.57 (1H, d, J= 7.9, Ar-<u>H</u>, H-15), 6.32(1H, d, J= 7.9, Ar-<u>H</u>, H-16), 5.18 (2H, s, CH_2, H-10), 3.4(3H, s, CH_3, C-17), 3.83(9H, s, 3x OCH_3, H-19, H-20, H-21), 3.26(3H, s, CH_3, C-18). ^{13}C ($CDCl_3$, 75 MHz; δ, ppm): 151.96 (C=O), 151.10 (C=O), 149.36 (C-14), 148.41

(C-4), 148.30 (C-13), 143.35 (C-6), 142.23 (C-12), 122.45 (C-16), 108.67 (C-8), 104.56 (C-15), 120.26 (C-11), 60.80 (2 x O<u>C</u>H3), 56.1 (O<u>C</u>H3), 41.56 (C-10), 33.80 (C-17), 30.11 (C-18). ESI-MS *m/z* 361$[M+H]^+$; Anal. Calcd. for $C_{17}H_{20}N_4O_5$: C 56.66, H 5.59, N 15.55, O 22.20.

➢ **1-(2-Methoxybenzyl)-3,7-dimethyl-1H-purine-2,6(3H,7H)-dione (4i)**

This was prepared in a similar procedure as described earlier for the synthesis of **4a** by the reaction of **3i** with theobromine**.** The pure compound **4i** was obtained as a yellow solid, m.p. 302-304°C; Yield: ~ 92%; TLC Solvent System: 9:1 ($CHCl_3$: MeOH), Rf value: 0.65; IR (KBr; υ_{max}, cm^{-1}) 3113.11 (-C-H Stretching), 111.57 (C=O Stretching), 1674.21 (C=O Stretching), 1666.50 (C=N Stretching), 1286.52 (C-N Stretching), 1247.94 (C-N Stretching), 1186.22 (C-O Stretching), 1099.43 (C-N Stretching), . ^{1}H ($CDCl_3$, 300 MHz; δ, ppm): 7.19 (1H, s, =C<u>H</u>, H-6), 7.45 (4H, m, Ar-<u>H</u>), 4.43 (2H, s, CH_2, C-10), 3.77(3H, s, CH_3, C-17), 3.90 (3H, s, OC<u>H</u>$_3$), 3.53(3H, s, CH_3, C-18). ^{13}C ($CDCl_3$, 75 MHz; δ, ppm): 166.63 (C=O), 150.43 (C=O), 149.83 (C-4), 147.97 (C-12), 146.49 (C-6), 131.24 (C-11), 129.4 (C-14), 127.63 (C-16), 120.80 (C-15), 112.56 (C-13), 108.67 (C-8), 66.98 (O<u>C</u>H$_3$), 37.52 (C-10), 29.16 (C-17), 27.74 (C-18). ESI-MS *m/z* 301$[M+H]^+$; Anal. Calcd. for $C_{15}H_{16}N_4O_3$: C 59.99, H 5.37, N 18.66, O 15.98.

➢ **1-(3,4-Bis(benzyloxy)benzyl)-3,7-dimethyl-1H-purine-2,6(3H,7H)-dione (4j)**

This was prepared in a similar procedure as described earlier for the synthesis of **4a** by the reaction of **3j** with theobromine**.** The pure compound **4j** was obtained as a yellow solid, m.p. 320-321°C; Yield: ~ 79%; TLC Solvent System: 9:1 ($CHCl_3$: MeOH), Rf value: 0.55; IR (KBr; υ_{max}, cm^{-1}) 3155.90 (-C-H stretching), 143.50 (C=O stretching), 1685.81 (C=O stretching), 1638.60 (C=N stretching), 1255.67 (C-O stretching), 1255.87 (C-N stretching), 1130.64 (C-N stretching), 1218.4 (C-N stretching). ^{1}H ($CDCl_3$, 300 MHz; δ, ppm): 7.17 (1H, s, =C<u>H</u>, H-6), 7.38-7.47 (10H, m, Ar-<u>H</u>), 6.76-7.03 (3H, m, Ar-<u>H</u>), 5.16 (4H, s, CH_2, H-10), 5.01 (4H, s, C<u>H</u>$_2$, 2 x OC<u>H</u>$_2$Ph), 3.4(3H, s, CH_3, H-17), 3.36(3H, s, CH_3, H-18). ^{13}C ($CDCl_3$, 75 MHz; δ, ppm): 154.61 (C=O), 151.26 (C=O), 149.6 (C-13), 148.51 (C-4), 147.25 (C-14), 143.34 (C-6), 136.44, 134.90 (C-11), 128.98, 127.66, 127.16, 122.87 (C-16), 112.23 (C-15), 109.89 (C-12), 108.23 (C-8), 3.90 (2 x O<u>C</u>H$_2$Ph), 46.76 (C-10), 34.80 (C-17), 30.11 (C-18). ESI-MS *m/z* 483 $[M+H]^+$; Anal. Calcd. for $C_{28}H_{26}N_4O_4$: C 1.2, H 5.43, N 11.61, O 13.26.

➢ **4-((3,7-Dimethyl-2,6-dioxo-2,3,6,7-tetrahydro-1H-purin-1-yl)methyl)-1,2-phenylene dibenzoate (4k)**

This was prepared in a similar procedure as described earlier for the synthesis of **4a** by the reaction of **3k** with theobromine**.** The pure compound **4k** was obtained as a yellow solid, m.p. 315-316$^{R°}$C; Yield: ~68%; TLC Solvent System: 9:1 ($CHCl_3$: MeOH), Rf value: 0.40; IR (KBr; υ_{max}, cm^{-1}) 2945.90 (-C-H stretching), 1783.50 (C=O stretching), 1678.81 (C=O stretching), 162.80 (C=O stretching), 110.60 (C=N stretching), 1235.67 (C-O stretching), 1215.87 (C-N stretching), 112.64 (C-N stretching), 1118.4 (C-N stretching). ^{1}H ($CDCl_3$, 300 MHz; δ, ppm): 7.97 (1H, s, =C<u>H</u>, H-6), 7.60-8.22 (10H, m, Ar-<u>H</u>), 7.22-7.46 (3H, m, Ar-<u>H</u>), 5.01 (2H, s, C<u>H</u>$_2$, C-10), 3.4(3H, s, C<u>H</u>$_3$, H-17), 3.36(3H, s, C<u>H</u>$_3$, H-18). ^{13}C ($CDCl_3$, 75 MHz; δ, ppm): 165.24 (C=O), 154.61 (C=O), 151.26 (C=O), 148.45 (C-4), 145.51 (C-13), 143.78 (C-14), 143.34 (C-6), 138.44 (C-11), 133.90 (C-20, C-20'), 130.34(C-21, C-21', C-25, C-25'), 130.2 (C-22, C-22', C-23, C-23'), 128.98 (C-24, C-24'), 122.87 (C-16), 120.67 (C-15), 112.23 (C-12), 108.23 (C-8), 46.76 (C-10), 34.80 (C-17), 30.11 (C-18). ESI-MS *m/z* 510 $[M+H]^+$; Anal. Calcd. for $C_{28}H_{22}N_4O_6$: C 65.88, H 4.34, N 10.97, O 18.80

➢ **3,7-Dimethyl-1-(4-nitrobenzyl)-1H-purine-2,6(3H,7H)-dione(4l)**

This was prepared in a similar procedure as described earlier for the synthesis of **4a** by the reaction of **3l** with theobromine**.** The pure compound **4l** was obtained as a

yellow solid, m.p. 330-332$^{R^{\circ}}$C; Yield: ~75%; TLC Solvent System: 9:1 ($CHCl_3$: MeOH), Rf value: 0.35; IR (KBr; υ_{max}, cm^{-1}) 3145.90 (-C-H stretching), 1789.50 (C=O stretching), 1688.81 (C=O stretching), 1640.60 (C=N stretching), 1536.45 (-NO_2 stretching), 1366.45 (-NO_2 stretching), 1225.87 (C-N stretching), 112.64 (C-N stretching), 1118.4 (C-N stretching). ^{1}H ($CDCl_3$, 300 MHz; δ, ppm): 7.98 (1H, s, =C<u>H</u>, H-6), 8.14 (2H, dd, J=8.4, Ar-<u>H</u>), 7.95(2H, dd, J=8.4, Ar-<u>H</u>), 5.01 (2H, s, CH_2, H-10), 3.4(3H, s, CH_3, H-17), 3.36(3H, s, CH_3, H-18). ^{13}C ($CDCl_3$, 75 MHz; δ, ppm): 154.61 (C=O), 151.26 (C=O), 148.51 (C-4), 145.34 (C-14; <u>C</u>-NO_2), 143.44 (C-6), 142.90 (C-11), 127.98 (C-12, C-16), 123.87 (C-13, C-15), 108.23 (C-8), 46.76 (C-10), 34.80 (C-17), 30.11 (C-18). ESI-MS *m/z* 315 $[M+H]^+$; Anal. Calcd. for $C_{14}H_{13}N_5O_4$: C 53.33, H 4.16, N 22.21, O 20.30.

Result and Discussion

Synthesis of theobromine analogs (4a-4l)

The synthesis of theobromine analogs **(4a-4l)** was done in three steps as:

Step 1: Synthesis of substituted benzyl alcohols (2b-2l)

The substituted benzaldehyde **(1b)** was treated with sodium borohydride ($NaBH_4$) in dry THF/MeOH (1:1) at 0°C. The reaction mixture was stirred for 30 minutes. Usual workup afforded the corresponding benzyl alcohols **(2b).**

Similarly all the benzyl alcohols **(2c-2l)** were synthesized by following the above procedure in good yields (76% -91%). **(Scheme 1).**

Step 2: Synthesis of substituted benzyl bromides (3b-3l)

To a stirred solution of benzyl alcohol **(2b)** in dry DCM, phosphorustribromide (PBr_3) was added dropwise. The reaction mixture was stirred at 0°C for 40 mins. Usual workup afforded the corresponding benzyl bromides **(3b)** in good yield (76%). **(Table 1, Scheme 1).**

Similarly all the benzyl bromides **(3c-3l)** were synthesized by following the above procedure. **(Scheme 1).**

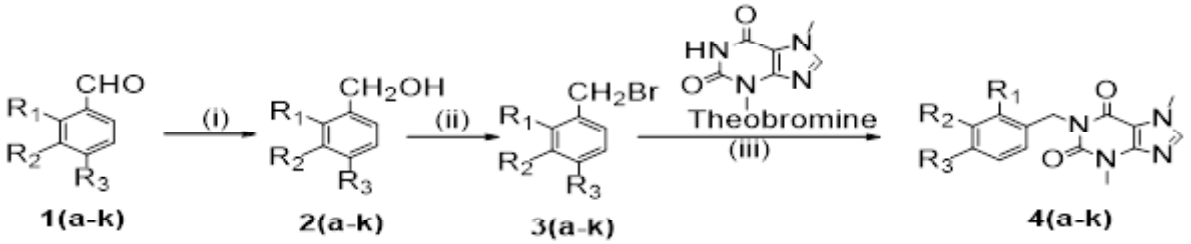

1a, 2a, 3a, 4a	R_1, R_2, R_3 = H;
1b, 2b, 3b, 4b	R_1 = H, R_2 , R_3= -OMe;
1c, 2c, 3c, 4c	R_1 = Br, R_2 = -OBz, R_3 = -OMe;
1d, 2d, 3d, 4d	R_1, R_2 = H, R_3 = -OBn;
1e, 2e, 3e, 4e	R_1, R_2 = H, R_3 = -OMe;
1f, 2f, 3f,4f	R_1 = H, R_2 = -OMe, R_3 = -OBz;
1g, 2g, 3g, 4g	R_1, R_2 = H, R_3 = -OBz;
1h, 2h, 3h,4h	R_1, R_2, R_3 = -OMe;
1i,2i, 3i, 4i	R_1 = -OMe, R_2, R_3 = H;
1j, 2j, 3j, 4j	R_1 = H, R_2, R_3 = -OCH_2Ph;
1k,2k, 3k, 4k	R_1 = H, R_2 , R_3= -OBz;
1l, 2l, 3l, 4l	R_1, R_2 = H, R_3 = -NO_2;

Scheme 1: (i) $NaBH_4$, THF/MeOH (1:1) (ii) PBr_3/DCM at 0°C,(iii)NaOMe/MeOH/r.t

Table 1: Benzyl bromides (3a-3l)

S. No	Benzyl bromides	R_1	R_1	R_3	Yield (%)	M.P. (°C)
1.	**3a***	H	H	H	-	-
2.	**3b**	H	OMe	OMe	76	Oil
3.	**3c**	Br	OBz	OMe	86	44-46
4.	**3d**	H	H	OCH_2Ph	96	51-53
5.	**3e**	H	H	OMe	91	Oil
6.	**3f**	H	OMe	OBz	92	-
7.	**3g**	H	H	OBz	91	-
8.	**3h**	OMe	OMe	OMe	84	Oil
9.	**3i**	OMe	H	H	89	Oil
10.	**3j**	H	OCH_2Ph	OCH_2Ph	86	Oil
11.	**3k**	H	OBz	OBz	88	-
12.	**3l***	H	H	NO_2	-	-

**purchased from Aldrich Chemical Co.*

Step 3: Synthesis of theobromine analogs (4a-4l)
The Theobromine was stirred separately with substituted benzyl bromides **(3a-3l)** in presence of freshly prepared sodium methoxide (NaOMe) base in methanol at room temperature. Workup of the reaction mixture in the usual manner gave the corresponding theobromine analogs **(4a-4l)** in ~80 % yields **(Table 3, Scheme 1).**

Optimization of reaction conditions for N-benzylation of theobromine
We have attempted a number of reported methods with different bases such as NaOH[33,34], KOH[35], K_2CO_3[36,37]or Cs_2CO_3[38,39] for N-benzylation of theobromine with various benzyl bromides. But with all the bases used, the reaction time was between 4-24 hours and poor yields, however with the use of NaOMe as base the reaction time reduced to 3 hours only with almost 75-90% yield. During the reaction, the solubility of theobromine increased in methanol in presence of NaOMe as base before undergoing the benzylation process which enhances the utilization of theobromine in reaction mixture. The results of the N-benzylation reaction performed under different reaction conditions are recorded in Table 2.

Table 2: Optimization of reaction Parameters

S. No.	Reactants	Reaction conditions	Reaction time	Yield (%)
1.	**Theobromine + 3a**	in DMSO at 20°C with NaOH	4–8 hours	60%
2.	**Theobromine + 3a**	in EtOH refluxed with KOH	12 hours	65%
3.	**Theobromine + 3a**	in DMF and K_2CO_3 at r.t.	24 hours	56%
4.	**Theobromine + 3a**	in THF with K_2CO_3 & KI as base under reflux	6 hours	59%
5.	**Theobromine +3a**	**in MeOH with NaOMe as base at r.t.**	**3 hours**	**80%**

As it is clear from the Table 2, the best reaction condition to synthesize the theobromine analogs was NaOMe as base in methanol as solvent. Therefore, all the twelve theobromine analogs **(4a-4l)** were prepared by N-alkylation of theobromine with various benzyl bromides **(3a-3l) (Scheme 1)**. The theobromine analogs synthesized by following the above methodology, with their yields and m.ps are recorded in Table 3.

The structures of all 1N-substituted theobromine analogs (**4a-4l)** and the precursors were fully established by their spectral data (IR, ^{1}H, ^{13}C NMR and MASS) except benzyl alcohols, which were used in subsequent reactions without purification.

Biological Activity

All the theobromine analogs (**4a-4l)** were evaluated for their *in vitro* antioxidant (free radical scavenging activity) and antibacterial activity. The results are summarized in Table 4 and 5.

Table 3: Theobromine Analogs (4a-4l)

S. No.	Compounds	R_1	R_2	R_3	Yield (%)	M. P. (°C)
1.	**4a**	H	H	H	90	282-285
2.	**4b**	H	OMe	OMe	85	290-293
3.	**4c**	Br	OBz	OMe	76	332-335
4.	**4d**	H	H	OCH_2Ph	82	295-298
5.	**4e**	H	H	OMe	86	285-287
6.	**4f**	H	OMe	OBz	89	310-311
7.	**4g**	H	H	OBz	80	298-299
8.	**4h**	OMe	OMe	OMe	92	302-304
9.	**4i**	OMe	H	H	92	281-282
10.	**4j**	H	OCH_2Ph	OCH_2Ph	79	320-321
11.	**4k**	H	OBz	OBz	68	315-316
12.	**4l**	H	H	NO_2	75	330-332

Experiment 1: Determination of free radical scavenging activity by 1, 1-diphenyl-2-picrylhydrazyl (DPPH) method (Table 4, Graph 1).

All the synthesized 1-aryl-3,7-dimethyl-1H-purine-2,6(3H,7H)-dione analogs **(4a-4l)** were separately dissolved in methanol to prepare samples of different concentrations (1000 µg/mL, 500 µg/mL, 250 µg/mL, 100 µg/mL). To determine the DPPH free radical scavenging activity the absorbance of each prepared samples (sample with DPPH) was recorded at 517 nm by UV spectro-photometer. The % inhibition and IC_{50} were calculated by the following formula:

$$\text{DPPH radical scavenging activity (\%)} = \frac{A_{control} - A_{sample}}{A_{control}} \times 100$$

where, $A_{control}$ was the absorbance of the control and A_{sample} was the absorbance in the presence of the sample.

The antioxidant activity in terms of percentage of DPPH scavenging activities were determined using BHT (butylated hydroxyl toluene) as standard. The results are listed in Table 4 and Graph 1.

The absorbance at 517 nm for free radical scavenging activity by DPPH was compared with the standard BHT at 517 nm at four concentrations viz. 1000 µg/mL, 500 µg/mL, 250 µg/mL and 100 µg/mL. The standard BHT has shown an increase in absorbance as the concentration decreases. The absorbance obtained for BHT at the concentrations 1000 µg/mL, 500 µg/mL, 250 µg/mL and

100 µg/mL were 0.014, 0.021, 0.026 and 0.0202 respectively **(Table-4)**.

Among all the 12 samples (**4a-4l**) at concentration 1000 µg/mL only four samples **4b, 4d, 4h** and **4l** have shown comparable absorption value (0.0386, 0.023, 0.0557 and 0.0567 respectively) with the standard BHT (0.014). At concentration 500 ìg/mL, three samples **4b, 4d** and **4l** have shown absorption values **0.0592**, **0.0977** and **0.0731** respectively as compared to the standard BHT (0.021). Similarly at concentration 250 µg/mL, only two samples **4b** and **4d** have shown absorption values **0.0858** and **0.0854** respectively comparable with the standard BHT (0.026). Similarly at concentration 100 µg/mL, one sample **4l** has shown absorption value **0.0876** comparable with the standard BHT (0.020). All the results of absorption values at different concentrations are listed in Table 4.

The study of percentage of DPPH scavenging activity in 12 samples **(4a-4l)** has also been carried out and demonstrated that the four samples **4b, 4d, 4h** and **4l** have the highest value of % inhibition at concentrations 1000 µg/mL (98.55, 99.13, 97.91, 97.87 respectively) comparable with the standard BHT at concentration 1000 µg/mL (99.35). The compound **4b** also exhibited the % inhibition values at 97.78 and 96.78 at concentrations 500µg/mL and 250µg/mL respectively comparable with standard BHT which showed the % inhibition 98.99 and 99.02 at 500µg/mL and 250µg/mL respectively. Similarly compound **4l** have % inhibition values 97.26 and 96.80 at concentrations 500µg/mL and 250µg/mL respectively comparable with standard BHT **(Table-4, Graph-1)**.

The results therefore demonstrated that amongst all the synthesized compounds only **4l** with **nitro** substituent showed values of absorption and % inhibition comparable with BHT at all concentrations. The free radical scavenging activity and % inhibition are related to the concentration of compounds and the most suitable concentration of the synthesized compounds are 250 µg/mL -1000 ìg/mL as compared to standard BHT.

Table 4: Absorbance (517 nm) and % Inhibition at different concentrations for free radical scavenging activity by DPPH in compounds 4a-4l and BHT

Sample	Concentration (µg/ml)							
	1000		500		250		100	
	Absorbance (517 nm)	% Inhibition	Absorbance (517 nm)	% Inhibition	Absorbance (517 nm)	% Inhibition	Absorbance (517 nm)	% Inhibition
4a	0.3268	87.75	0.3261	87.78	0.3275	87.73	0.2853	89.31
4b	**0.0386**	**98.55**	**0.0592**	**97.78**	**0.0858**	**96.78**	0.256	92.50
4c	0.342	87.18	0.2183	91.82	0.2441	90.85	0.2682	89.95
4d	**0.023**	**99.13**	0.0977	96.34	0.103	96.14	0.1846	93.08
4e	0.1936	92.74	0.1134	95.75	0.2366	91.13	0.2584	90.32
4f	0.035	97.32	0.2357	91.17	0.2676	89.97	0.2859	89.29
4g	0.047	97.27	0.1842	93.09	0.2285	91.	0.3208	87.98
4h	**0.0557**	**97.91**	0.1599	94.01	0.1668	93.75	0.1749	93.44
4i	0.118	95.57	0.2081	92.20	0.241	90.97	0.2689	89.92
4j	0.2181	91.82	0.286	89.28	0.3574	86.61	0.2846	89.33
4k	0.2244	91.59	0.374	85.87	0.4109	84.60	0.4497	83.15
4l	**0.0567**	**97.87**	**0.0731**	**97.26**	**0.0854**	**96.80**	**0.0876**	**96.3**
BHT	**0.014**	**99.35**	**0.021**	**98.99**	**0.026**	**99.02**	**0.0202**	**99.24**

Experiment 2: Determination of antibacterial activity of theobromine analogs (4a-4l) (Table 5, Graph 2).

All the theobromine analogs **4a-4l** were evaluated for their antibacterial activity and the results are summarized in Table 5.

Antibacterial Activity- The antibacterial activity was evaluated against five pathogenic bacterial strains *viz. Agrobacterium tumefaciens* (gram -ve), *Erwinia chrysanthemi* (gram -ve), *Xanthomonas phaseoli* (gram -ve), *Escherichia coli* (gram -ve) and *Bacillus subtilis* (gram +ve) with standard antimicrobial agent streptomycin.

The antimicrobial activity was carried out against the above mentioned organisms by following the cup-plate method using Muller-Hinton Agar medium for bacteria. The compounds were screened for their antibacterial activity at 200 µg/mL concentration level using DMSO as solvent.

The zone of inhibitions of the synthesized compounds against five pathogenic (Gram positive and Gram negative) bacteria are presented in Table 5.

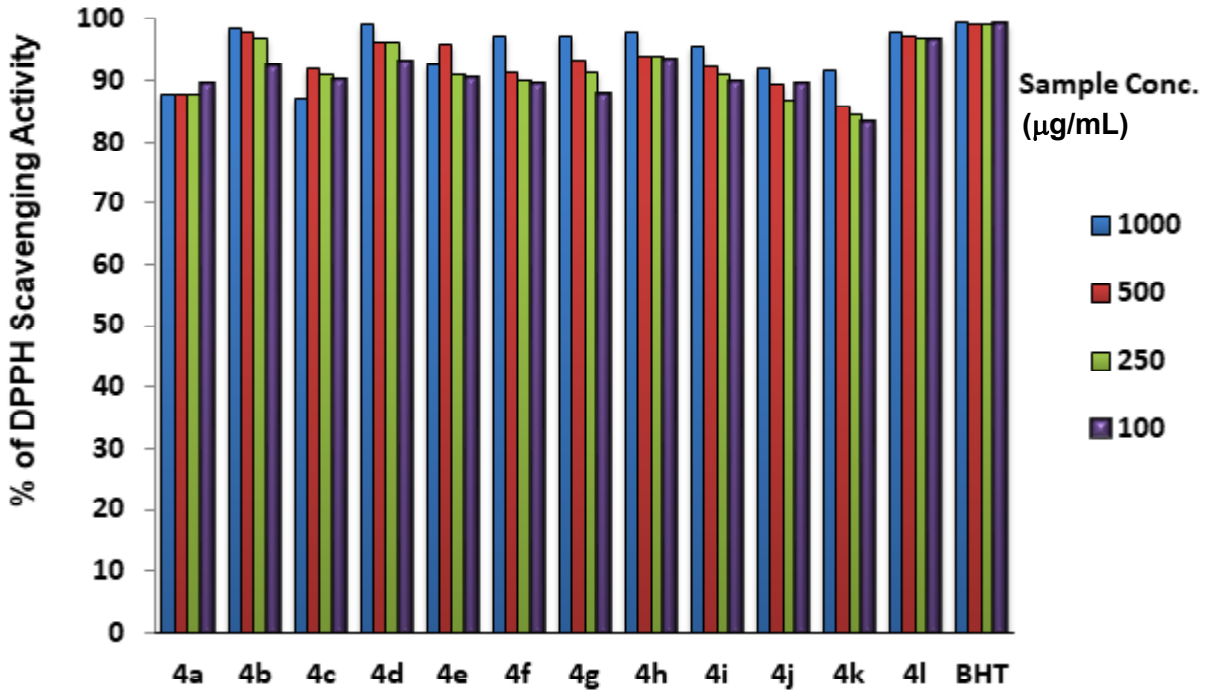

Graph 1: % inhibition of DPPH scavenging activity of 4a-4l

Amongst all the tested compounds **4l** and **4k** have shown remarkable antibacterial activity against all the five pathogens as compared to standard streptomycin. Other compounds which showed mild antibacterial activity are **4c, 4d, 4f, 4g, 4h, 4i** and **4j** as compared to standard drug (**Table 5**).

In the evaluation of antibacterial activity, the zone of inhibition (ZOI) for the most active compound **4k** and **4l** was between 20-29 and 16-28 respectively for *A. tumefaciens, E. chrysanthemi, X. phaseoli, E. coli and B. subtilis.* The compounds **4d, 4f, 4g** and **4j** exhibited good antibacterial activity against Gram –ve bacteria *E. chrysanthemi* with zone of inhibition as 26, 25, 25, and

25 respectively. However **4j** exhibited high activity against Gram +ve bacteria *B. subtilis* with ZOI as 27. The mild activity against Gram +ve bacteria *B. subtilis* was shown by compounds **4c, 4d, 4f** and **4i** with zone of inhibition as 21, 23, 20 and 20 respectively. Compound **4b** was found to be active against only one Gram –ve bacteria *E. chrysanthemi* with zone of inhibition as 24 while it has shown very poor activity against other pathogens tested.

As predicted by the SAR in general it is clear that value of zone of inhibitions was greater for compounds having electron withdrawing groups as compared to compounds having electron donating groups. Compounds **4k** and **4l** due to the presence of electron withdrawing groups i.e. the –OBz groups in **4k** and $–NO_2$ group in **4l** at phenyl ring had greater value of ZOI whereas compounds **4b, 4h** and **4i** have shown relatively less values of zone of inhibition due to the presence of methoxy groups (electron donating group) as compared to other analogs bearing electron withdrawing groups thus supporting the SAR prediction that electron withdrawing groups enhance the antibacterial activity.

The graphical representations of zone of inhibition of all the tested compounds are displayed in Graph 2.

Table 5: Antibacterial activity (ZOI)* of theobromine derivatives 4a-4l

S. No.	Samples	Gram negative bacteria				Gram Positive bacteria
		A. tumefaciens	*E. chrysanthemi*	*X. phaseoli*	*E. coli*	*B. subtilis*
1.	**4a**	10	9	5	7	12
2.	**4b**	14	**24**	12	11	16
3.	**4c**	**20**	17	**19**	14	**21**
4.	**4d**	17	**26**	14	10	**23**
5.	**4e**	13	12	10	13	16
6.	**4f**	19	**25**	10	**17**	**20**
7.	**4g**	**21**	**25**	15	**20**	14
8.	**4h**	15	**22**	14	13	**19**
9.	**4i**	13	15	**17**	15	**20**
10.	**4j**	17	**25**	15	**19**	**27**
11.	**4k**	**28**	**28**	**20**	**16**	**18**
12.	**4l**	**29**	**27**	**24**	**20**	**28**
17.	**[#]Std.**	**38.23**	**40.33**	**27.57**	**39.57**	**39.76**

[#]Std. Streptomycin (+control), All the compounds were screened at 200 µg/ml concentration

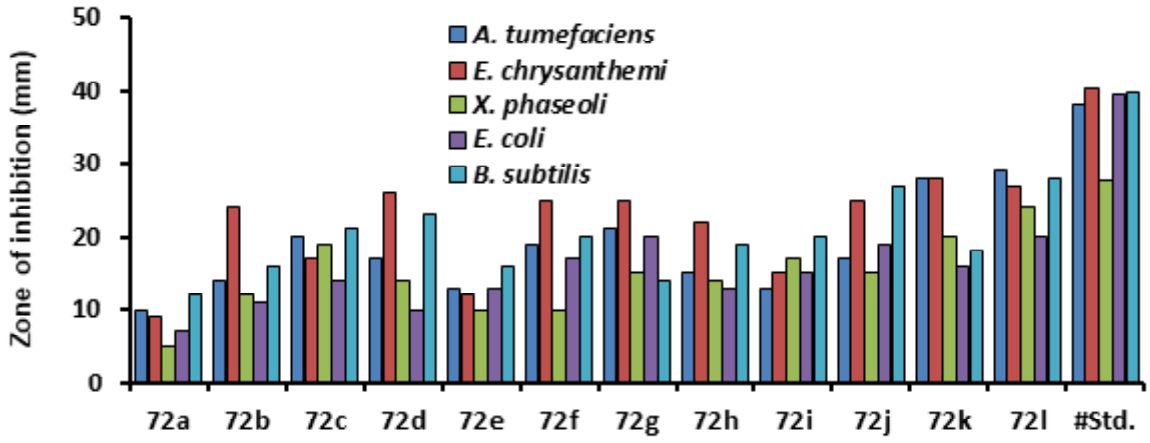

Graph 2: Zone of inhibitions (ZOI) of the theobromine analogs. #std streptomycin

Conclusions

We have synthesized a series of twelve new and novel theobromine analogs (**4a-4l)** by a three step reaction predicted by retrosynthetic analysis. All the synthesized analogs were screened for antioxidant (free radical scavenging activity) and antibacterial activity.

The biological studies revealed that out of all synthesized analogs only four analogs **4b** with 3,4-dimethoxybenzyl substituent**, 4d** with -OCH_2Ph substituent**, 4h** with 2-3-4-trimethoxybenzyl substituent and **4l** with 4-nitrobenzyl substituent showed free radical scavenging activity with % inhibition 98.55 %, 99.13 %, 97.91 % and 97.87 % as compared to standard BHT (99.35 %) at 1000 mg/ml concentration.

In the evaluation of antibacteraial activity it was found that amongst all the novel analogs (**4a-4l)**, only two compounds **4k** with -OBz and **4l** with 4-nitrobenzyl substituents were found to exhibit moderately active against all five bacterial strains.

Acknowledgement

The authors are thankful to the Department of Chemistry, University of Lucknow, Lucknow (U.P.) India for giving UV, IR and NMR spectroscopic and computational facilities. We are also thankful to SAIF Division, CSIR-Central Drug Research Institute, Lucknow, India for Mass spectral analysis.

References

1. Fischer E., 1899, *Ber. Dtsch. Chem. Ges*., **32**, 2550.
2. Wood H. G., Ragsdale S. W., Pezacka E., 1986,*Trends Biochem. Sci.*, **11**, 14.
3. Krger M., Salom G., Hoppe-Seyler Z., 1898, *Physiol. Chem,* **24**, 364.
4. Howell L. L., Coffin V. L., Spealman R. D., 1997, *Psychopharmacology,* **129**, 1–14.
5. Muller C. E., Jacobson K. A., 2011, *Biochim. Biophys. Acta,* **1808,** 1290–1308.
6. Muller C. E.,. Jacobson K. A, 2011, *Handb. Exp. Pharmacol.,* **200,** 151–199.
7. Hsu C. W., Wang C. S., Hsu T. H. C., 2010, *J. Biomed. Sci.,* **17,** 4.
8. Hollingsworth R.G., Armstrong J.W., Campbell E., 2002, *Nature*, **417**, 915–916.
9. Frischknecht P.M., Ulmer-Dufek J., Baumann T.W., **1986**, *Phytochemistry*, **25**, 613–616.
10. Monteiro J. P., Alves M. G., Oliveira P. F., Silva B. M., 2016, *Molecules*, **21,** 974.
11. Anaya A. L., Ortega R. C., Waller G. R., 2006, *Frontiers in Bioscience*, **11,** 2354-2370.
12. Clough B. H., Ylostalo J., Browder E., McNeill E. P., Bartosh T. J., Rawls H. R., Nakamoto T., Gregory C. A., 2017,*Calcified tissue international*, **100 (3)**, 298-310,
13. Khan N., Monagas M., Andres-Lacueva C., Casas R., Urpí-Sardà M., Lamuela-Raventós R. M., Estruch R., 2012, *Nutr. Metab. Cardiovasc. Dis.,* **22,** 1046–1053.
14. Etherton P. M. K., Derr J. A., Mustad V. A., Seligson F. H., 1994, *Am. J. Clin. Nutr.,* **60**, 1037S–1042S.
15. Mursu J., Voutilainen S., Nurmi T., Rissanen T. H., Virtanen J. K., Kaikkonen J., Nyyssönen K., Salonen J. T., 2004, *Biol. Med.,* **37,** 1351–1359.
16. Baba S., Osakabe N., Kato Y., Natsume M., Yasuda A., Kido T., Fukuda K., Muto Y., Kondo K., 2007, *Am. J. Clin. Nutr.,* **85,** 709–717.
17. Mellor D. D., Sathyapalan T., E. S. Kilpatrick, S. Beckett, S. L. Atkin, *Diabet.* 2010, *Med.,* **27,** 1318–1321.

18. Neufingerl N., Zebregs Y. E., Schuring E. A., Trautwein E. A., 2013, *Am. J. Clin. Nutr.*, **97,** 1201–1209.

19. Kumar N. S., Chandran T. B., Namratha S., Bharath B. R., Kumar H. P. C., Kishore V., 2013, *IRJP*, **4 (2),** 151-154

20. Timson J., 1975, *mutation research*, **32,** 169-178.

21. Barcz E., Sommer E., Janik P., Marianowski L., Rozewska E. S., 2000, *Oncol. Rep.,* **7**, 1285e1291.

22. Kakuyama A., Sadzuka Y., 2001, *Curr. Drug Metabol.*, **2,** 379e395.

23. Usmani O. S., Belvisi M. G., Patel H. J., Crispino N., Birrell M. A., Korbonits M., 2005, *Faseb. J.,* **19**, 231e233.

24. Lee I., Kamba A., Low D., Mizoguchi E., 2014, World J. Gastroenterol., **20,** 1127e1138.

25. Hasegawa T., Nadai M., Apichartpichean R., Muraoka I., Nabeshima T., Takagi K., 1991, *J. Pharm. Sci.,* **80,** 962e965.

26. Osswald H., Schnermann J., 2011, *Springer Berlin Heidelberg*, **34,** 391e412.

27. Katherine A., Belenichev I., Alexander S., Levich S., Yurchenko D., Buchtiyarova N., 2014, *Med. Sci.,* **3**, 187e194.

28. Vignoli J. A., Bassoli D. G., Benassi M. T., 2011, *Food Chem.*, **124**, 863e868.

29. Yashin A., Yashin Y., Wang J. Y., Nemzer B., 2013, Antioxidants, **2**, 230e245.

30. Schmidt D. T., Watson N., Dent G., Ruhlmann E., Branscheid D., Magnussen H., 2000, *Br. J. Pharmacol.,* **131**, 1607e1618.

31. Schroeder J. A., Ruta J. D., Gordon J. S., Rodrigues A. S., Foote C. C., 2012, *Behav. Pharmacol.*, **23,** 310e314.

32. Ogawa K., Takagi K., Satake T., 1989, *Br. J. Pharmacol.,* **97,** 542e.

33. Shibukaw N. S., okuda S. T., Kaneda T., 1967, *J. Jpn. Soc. Food Nutr.*, **19**, 373.

34. Berger J. M., *"Isolation, Characterization, and Synthesis of Bioactive Natural Products from Rainforest Flora",* Ph. D. Thesis, Virginia Polytechnic Instituteand State University, USA, 2001**.**

35. Cotterill A. S., Hartopp P., Jones G. B., Moody C. J., Norton C. L., O'Sullivan N., Swann E., 1994, *Tetrahedron,* **50,** 7857–7874.

36. Katoh T., Itoh E., Yoshino T., Terashima S., 1996, *Tetrahedron Lett.,* **37**, 3471–3474.

37. Krohn K., Loock U., Paavilainen K., Hausen B. M., Schmalle H. W., Kiesele H., 2001, *Arkivoc,* **i**, 88–130.

38. Lin C. F., Yang J. S., Chang C. Y., Kuo S. C., Lee M. R., Huang L. J., 2005, *Bioorg. Med. Chem.,* **13,** 1537–1544.

39. Iranpoor N., Firouzabadi H., Jamalian A., Kazemi F., 2005, *Tetrahedron,* **61,** 5699 - 5704.

RNI No. MAHENG/2017/74063
ISSN No. (Print) 2581-5911
ISI Impact Factor 1.724

Application of Nonlinear Least Squares Method for Better Depiction of Graph: In Phenol-Water Experiment

Shampa Bhattacharyya[1]*, Mrinal Kanti Dash[2], Mihir Baran Bera[2] and Gourisankar Roymahapatra[2]

[1] Department of Chemistry, Hansraj College, University of Delhi, Delhi 110 007, India

[2] Department of Applied Sciences, Haldia Institute of Technology, Haldia 721 657, India

*** Email: shampa@hrc.du.ac.in**

Abstract

The present paper discuss how students can use their programming skills in BASIC language to estimate the equation that describes the relationship between two variables in "Phenol-water" experiment. Usually, undergraduate students of Chemistry are familiar with the programs that deal with linear relationships. The program written in this paper will help the students with programming abilities to handle the nonlinear relations[1]. Furthermore, this will help in understanding how the program written in BASIC will derive the same results as obtained from machine learning.

Introduction

With the development of Machine learning (ML) methods, it is extremely useful to use ML to replace orthodox approaches to fitting data measured in Chemistry experiments, especially for students at undergraduate level. In our previous report[2] we have introduced ML and analyzed raw data collected from a Phenol-water experiment to arrive at the best fit curve. We have demonstrated how statistical machine learning technique can be used to fit data obtained from experiments performed in the lab. As an illustration, "Phenol-water" experiment was chosen. Based on feedback received, we have shown here how one can achieve similar results by using computer programming. In our research group, we are trying to incorporate basic computer application to study chemistry laboratory experiments.[3] In this case we have used BASIC programming[4,5] which is taught in the existing curriculum frame-work. This is a step up from free hand fitting, which is the normal method used by undergraduate science students.

Theory Phenol-water system is an example of partially miscible liquids. This experiment is performed to study the liquid-liquid phase equilibrium. When phenol is added to water at a given temperature (T) in small amounts slowly and successively, phenol will be dissolved completely until it reaches its solubility limit. A single phase homogeneous solution exists up to this point. With excess addition of phenol, it will split up into two layers. These two liquid layers are called conjugate solutions. Phenol being heavier than water, the lower layer contains phenol saturated with water and upper layer consists of water saturated with phenol. The same phenomenon of two conjugate solutions can be observed when water is

added to phenol slowly and successively. As a result the solution becomes turbid. The turbidity goes off on heating and reappears on cooling. The mutual solubility increases with the increase of temperature. Hence the mutual solubility temperature (Ts) will be different at different compositions. The highest miscible temperature above which both the liquids are soluble at all proportions is called upper critical solution temperature (CST). It is obtained from the graph between mutual solubility temperature (T_s) and mass % of phenol[6-8]. The graph generated from the experimental data form a curve which is often called umbrella curve.

Experimental Difficulty: During the experiment, the students face the following difficulties which lead to erroneous determination of temperatures which gets reflected in graph plotting.

a. Student finds difficulty to observe the turbidity appearing and disappearing in the solution for initial few compositions.
b. Sometimes there is a lot of difference between the two temperatures at which turbidity appears and disappears due to overheating of water bath.

Hence it makes an impact while drawing a free hand smooth curve from these experimental data points. As a result, students report wrong CST and its corresponding composition. One can use regression method to overcome this difficulty.

Method: The free hand plotting of the data shows that the curve depicting the relationship is nonlinear. A common nonlinear relationship is the quadratic relationship. Let us consider a quadratic equation of the form:

$$y = ax^2 + bx + c$$

The co-efficient 'a', 'b' and 'c' are to be estimated with the relations given below. Substituting the values of a, b and c in the above equation, the estimated values of y are obtained. Our estimated equation yields a value of $R^2 = 0.94$.

The computer program has been written to solve for three coefficients (a, b and c) and estimate y (mutual solubility temperature T_s). The program also plots the value of estimated y i.e. T_s against the value of x (mass% of phenol).

Table1: The formula for estimating a, b and c

$$a = \frac{\left(S_{x^2y}\, S_{xx}\right) - \left(S_{xy}\, S_{xx^2}\right)}{\left(S_{xx} S_{x^2x^2}\right) - \left(S_{xx^2}\right)^2}$$

$$b = \frac{\left(S_{xy} S_{x^2x^2}\right) - \left(S_{x^2y} S_{xx^2}\right)}{\left(S_{xx} S_{x^2x^2}\right) - \left(S_{xx^2}\right)^2}$$

$$c = Y_{mean} - aX^2_{mean} - bX_{mean}$$

$$Y_{mean} = \frac{\sum y_i}{n}\,;\, X_{mean} = \frac{\sum x_i}{n}\,;\, X^2_{mean} = \frac{\sum x_i^2}{n}$$

$$S_{x^2y} = \left[\left(\sum y_i x_i^2\right) - \left(nY_{mean} X^2_{mean}\right)\right] : S_{xx} = \left[\left(\sum x_i^2\right) - n\left(X_{mean}\right)^2\right]$$

$$S_{xy} = \left[\left(\sum x_i y_i\right) - \left(nX_{mean} Y_{mean}\right)\right] : S_{xx^2} = \left[\left(\sum x_i^3\right) - \left(nX_{mean} X^2_{mean}\right)\right]$$

$$S_{x^2x^2} = \left[\left(\sum x_i^4\right) - n\left(X^2_{mean}\right)^2\right]$$

Programme The programme (given in Appendix-I) has been written to help the students to find out the values of estimated y directly. The students have to input the no of observations (n) and data obtained from experiment (x_i,y_i) in the programme. The output of the program provides the best fit equation, plots the graph and indicates CST and the composition at CST.

Data source The experiment is performed the laboratory of Hansraj College, University of Delhi, India. The experimental data is shown in Table 2.

Table 2: Experimental values of mutual solubility temperature at various mass% of Phenol

Sl. No.	Mass (%) of Phenol	Mean temperature of disappearance and reappearance of turbidity / ^{0}C
1.	70	37.5
2.	67	44.8
3.	64.49	49.6
4.	59.85	56.8
5.	57.77	59.0
6.	55.83	62.1
7.	54.02	62.8
8.	46.47	65.1
9.	40.77	65.5
10.	36.32	66.0
11.	32.74	65.3
12.	27.36	64.8
13.	23.49	63.9
14.	18.32	61.0
15.	15.01	56.5
16.	12.71	51.3
17.	10.67	42.9

Results The estimated and experimental values of mutual solubility temperatures (Ts) are shown in Table-3. Output from the computer program is given in Fig 1.

Table 3: Comparison of mutual solubility temperatures (T_s) between experimental and estimated value

S. No.	Mass % of Phenol	Mean temperature of disappearance and reappearance of turbidity/ ^{0} C	
		Estimated	Experimental
1.	70.00	40.11	37.5
2.	67.00	45.17	44.8
3.	64.49	49.02	49.6
4.	59.85	55.21	56.8
5.	57.77	57.60	59.0
6.	55.83	59.61	62.1
7.	54.02	61.30	62.8
8.	46.47	66.38	65.1
9.	40.77	68.13	65.5
10.	36.32	68.24	66.0
11.	32.74	67.54	65.3
12.	27.36	65.14	64.8
13.	23.49	62.42	63.9
14.	18.32	57.50	61.0
15.	15.01	53.57	56.5
16.	12.71	50.48	51.3
17.	10.67	47.50	42.9

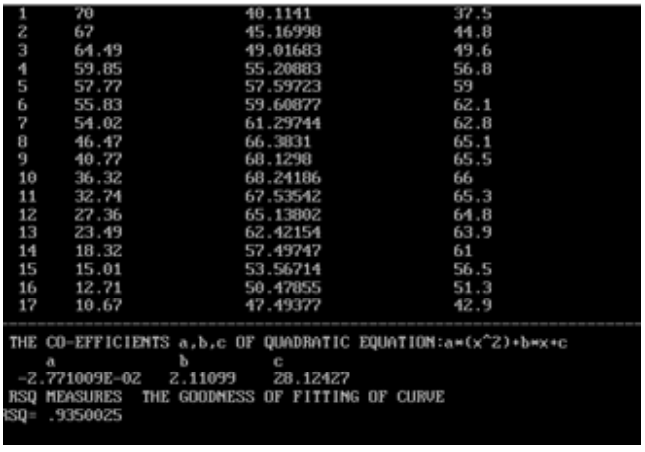

Fig. 1: Output from the computer programme

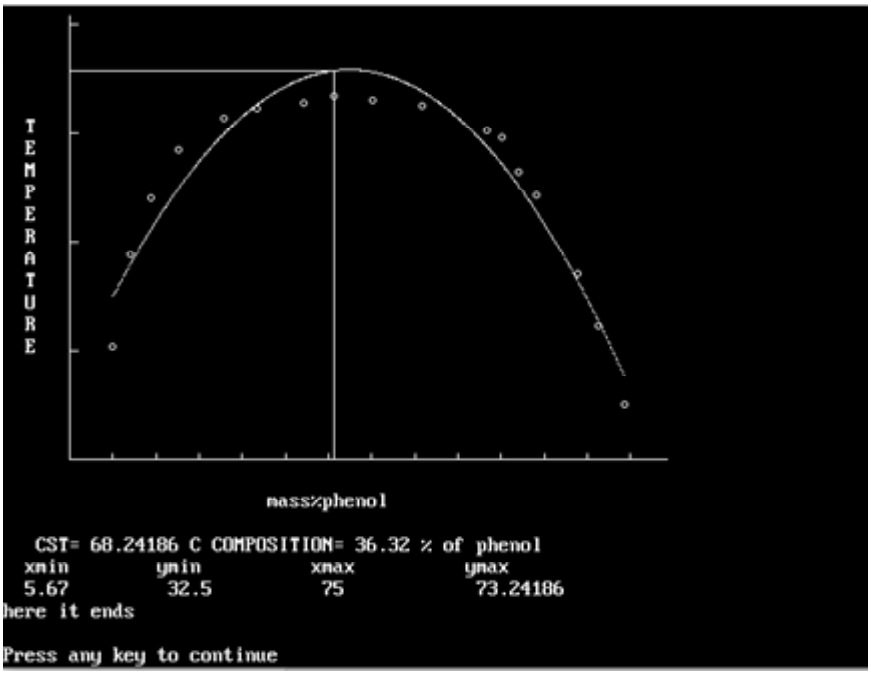

Fig. 2: The best fit line obtained from computer programme using the same experimental data.

A number of free hand curves passing through the experimental data points make it difficult to isolate the best fit one. The graph obtained from regression analysis gives the best fit. The free hand curves and the best fit line obtained from computer programme are displayed in Figure 1.

Conclusions

The paper presents a programme in BASIC for the students to use quadratic regression analysis to handle experimental data in Chemistry. Classroom experience shows a lack of knowledge among the undergraduate students of Chemistry beyond linear regression analysis. This paper seeks to address this gap.

In our earlier paper, we have demonstrated how machine learning (ML) can be applied in Chemistry experiments. The result obtained from the programme in BASIC matches with the values of coefficients obtained through the application of machine learning in our earlier paper. However, in ML the computer has been instructed to find out the degree of polynomial that yields the best fit. Our finding was that polynomial of degree two is the appropriate one. Accordingly, we have used a quadratic regression in BASIC. The basic programme would have required several programmings to be written to run the iteration for the desired degree of polynomial to be known. This is beyond the scope of the paper.

References

1. Polynomial Regression *https://en.wikipedia.org/wiki/Polynomial_regression*

2. Bhattacharyya S. and Roymahapatra, G., 2022, *Edu. Chem. Sci. Tech*., **2**, 97-109. DOI: 10.5281/zenodo.6813320

3. Bhattacharyya, S., Bag A. and Roymahapatra, G.,

2022, *G.P. Globalize Research Journal of Chemistry*, **6(2)**, 20-26.

4. Balagurusamy, E., 1984, Programming in BASIC, Tata McGraw-Hill, New Delhi

5. Gottfried, B. S., Programming with C, Tata McGraw-Hill, New Delhi, ISBN: 9780070145900, 0070145903

6. Castellan, G. W., 2004, Physical Chemistry. Narosa Publishing House, New Delhi.

7. Atkins P. and Paula, J. De., 2006, Physical Chemistry, Oxford University Press: New York.

8. Logan, S. R., 1998, The Behavior of a Pair of Partially Miscible Liquids, *J. Chem. Edu.*, **75**, 339.

9. R^2 (Coefficient of Determination) https://www.statisticshowto.com/probability-and-statistics/coefficient-of-determination-r-squared/

Appendix-I

```
CLS
REM n is the no of observations
Print " INPUT no of observations = n"
Input n
DIM x(n), y(n), y1(n)
REM x,y are experimental value and y1 is estimated value
REM INPUT THE VALUE OF x(I) & y(I)
FOR i = 1 TO n
  Input x(i), y(i)
NEXT i
FOR i = 1 TO n
  PRINT x(i), y(i)
NEXT I
REM to arrange mass % of Phenol in decreasing order for setting the
scale
FOR i = 1 TO n - 1
  FOR j = i + 1 TO n
    IF x(i) > x(j) GOTO 2
    temp = x(i)
    temp1 = y(i)
    x(i) = x(j)
    y(i) = y(j)
    x(j) = temp
    y(j) = temp1
  2 NEXT j
NEXT i
REM to calculate the coefficients a,b,c
FOR i = 1 TO n
  sumx = sumx + x(i)
  sumy = sumy + y(i)
  sumxsq = sumxsq + (x(i) ^ 2)
  sumxsqy = sumxsqy + ((x(i) ^ 2) * y(i))
  sumxy = sumxy + (x(i) * y(i))
  sumxcube = sumxcube + (x(i) ^ 3)
  sumxfour = sumxfour + (x(i) ^ 4)
NEXT i
avx = sumx / n
avy = sumy / n
avxsq = sumxsq / n
sxxy = (sumxsqy) - (n * (avy) * (avxsq))
sxx = (sumxsq) - (n * ((avx) ^ 2))
sxy = (sumxy) - (n * (avx) * (avy))
sxxsq = (sumxcube) - (n * (avx) * (avxsq))
sxsqxsq = (sumxfour) - (n * ((avxsq) ^ 2))
a = ((sxxy * sxx) - (sxy * sxxsq)) / ((sxx * sxsqxsq) - ((sxxsq) ^ 2))
b = ((sxy * sxsqxsq) - (sxxy * sxxsq)) / ((sxx * sxsqxsq) - ((sxxsq) ^ 2))
c = avy - (a * avxsq) - (b * avx)
'PRINT avx, avy, avxsq
REM ??????? =avy; ??????? =avx; ???????? =avxsq
REM ??? ?? =sxxy; ??? =sxx; ??? = sxy
REM ??? =sxxsq; ??? =sxsqxsq
REM storing of estimated value
FOR i = 1 TO n
  y1(i) = (a * (x(i) ^ 2)) + (b * x(i)) + c
NEXT i
'PRINT a, b, c
'FOR i = 1 TO n
FOR i = 1 TO n
y1(i) = (a * (x(i) ^ 2)) + (b * x(i)) + c
NEXT i
'PRINT a, b, c
FOR i = 1 TO n
  'PRINT i, x(i), y(i), y1(i)
NEXT i
REM determination of xmin,ymin,xmax,ymax
xmin = x(n) - 5
xmax = x(1) + 5
ymin = 1E+10
ymax = -1E-10
FOR i = 1 TO n
  IF y1(i) < ymin GOTO 10
  GOTO 11
  10 ymin = y1(i)
  p = i
11 NEXT i
'PRINT ymin
 FOR i = 1 TO n
  IF y(i) < ymin GOTO 12
  GOTO 13
  12 ymin = y(i)
13 NEXT i
'PRINT ymin
FOR i = 1 TO n
```

```
  IF y1(i) > ymax GOTO 14
  GOTO 15
  14 ymax = y1(i)
  p1 = i
15 NEXT i
FOR i = 1 TO n
  ssr = ssr + ((y1(i) - avy) ^ 2)
  sst = sst + ((y(i) - avy) ^ 2)
NEXT i
RSQ = (ssr) / (sst)
'PRINT "RSQ="; RSQ
'PRINT ymax
 FOR i = 1 TO n
  IF y(i) > ymax GOTO 16
  GOTO 17
  16 ymax = y(i)
17 NEXT i
'PRINT ymax
 PRINT
PRINT "------------------------------------------------------------------"
PRINT TAB(2); "S.N"; TAB(8); "mass % of phenol"; TAB(27);
"ESTIMATED TEMP/C"; TAB(48); "EXPERIMENTAL TEMP/C"
PRINT "------------------------------------------------------------------"
PRINT " THE CO-EFFICIENTS a,b,c OF QUADRATIC
EQUATION:a*(x^2)+b*x+c"
PRINT TAB(6); "a"; TAB(20); "b"; TAB(30); "c"
PRINT TAB(3); a; TAB(18); b; TAB(29); c
PRINT " RSQ MEASURES THE GOODNESS OF FITTING OF CURVE"
PRINT "RSQ="; RSQ
PRINT "do you want a graph also?"
PRINT "write down your answer either Y or N"
INPUT g$
IF g$ = "Y" GOTO 50
GOTO 70
 REM xmin is set to negative to label the yaxis
 50 SCREEN 12
WINDOW (-2, ymin - 20)-(100, ymax + 10)
FOR x3 = x(n) TO x(1) STEP 0.1
  y3 = (a * ((x3) ^ 2)) + (b * x3) + c
   PSET (x3, y3)
NEXT x3
FOR i = 1 TO n
  CIRCLE (x(i), y(i)), 0.3
NEXT i
```

```
REM “X-axis” to be drawn
LINE (x(n) - 5, ymin - 5)-(x(1) + 5, ymin - 5)
REM “Y-axis” to be drawn
LINE (x(n) - 5, ymin - 5)-(x(n) - 5, ymax + 5)
f1 = ymin - 5
f2 = ymax + 5
REM “calibration of X-axis”
FOR x = x(n) - 5 TO x(1) + 5 STEP 5
   LINE (x, ymin - 5)-(x, ymin - 4.5)
NEXT x
REM “calibration of Y-axis”
FOR y = ymin - 5 TO ymax + 5 STEP 10
   LINE (x(n) - 5, y)-(x(n) - 4.0, y)
```

```
NEXT y
LINE (x(n) - 5, y1(p1))-(x(p1), y1(p1))
LINE (x(p1), y1(p1))-(x(p1), ymin - 5)
LOCATE 25, 25
PRINT “mass%phenol”
‘LOCATE 24, 28
‘PRINT x(p1)
‘LOCATE 6, 1
‘PRINT y1(p1)
c$ = “TEMPERATURE”
L = LEN(c$)
c1 = 8
FOR i = 1 TO L
  LOCATE c1, 3
  d$ = MID$(c$, i, 1)
  PRINT d$
  LOCATE c1, 2
  c1 = c1 + 1
NEXT i
LOCATE 27, 4
PRINT “CST=”; y1(p1); “C”; “ COMPOSITION=”; x(p1); “% of phenol”
LOCATE 28, 3
PRINT “xmin”, “ymin”, “xmax”, “ymax”
LOCATE 29, 2
 PRINT xmin, f1, xmax, f2
70 PRINT “here it ends”
```

RNI No. MAHENG/2017/74063
ISSN No. (Print) 2581-5911
ISI Impact Factor 1.724

Synthesis and Characterization of Chalcone based Photochromic Fulgide

Arya Loke, Bharat K. Raut and Ravibabu A. Tayade*
Physical Chemistry Department, The Institute of Science,
Dr. Homi Bhabha State University,
15 Madam Cama Road, Mumbai-400032, Maharashtra, India
Email: ratayade121@gmail.com

Abstract
This paper reports the synthesis of Chalcone based Fulgide by step-wise Stobbe Condensation for it photochromic properties. Stobbe condensation is an important C=C bond forming reaction. The Stobbe condensation reaction of Benzaldehyde with Dimethyl succinate was carried out with solvent tert-butanol in the presence of potassium metal which gave 3-(methoxycarbonyl)-4-phenylbut-3-enoic acid which upon methylation underwent Stobbe condensation with 3,5-diiodo-4-hydroxy-3',4'-methylenedioxy Chalcone, which was synthesized using Friedel-Crafts acylation and gave the corresponding ester product 4-Benzo [1, 3] dioxol-5-yl-2-(benzylidene)-6-(3, 5-diiodo-4-methoxyphenyl)-3-(methoxycarbonyl) hexa-3, 5-dienoic acid which was further saponified to the corresponding dicarboxylic acid called 2-(-1-(benzo [1, 3] dioxol-5-yl)-3-(3, 5-diiodo-4-methoxyphenyl) allylidene)-3-(-benzylidene) succinic acid which further underwent dehydration to give an anhydride product Fulgide known as (Z)-3-((E)-1-(benzo[d][1,3]dioxol-5-yl)-3-(3,5-diiodo-4-methoxyphenyl)allylidene)-4-((Z)-benzylidene)dihydrofuran-2,5-dione. The product was confirmed using melting point, IR, UV and proton NMR. This fulgide was used to study photochromism. Photochromism is a change in colour, usually colourless to coloured, brought about by UV irradiation in an immersion well photochemical reactor.

Keywords: *Stobbe Condensation, Chalcone, Fulgide, Photochromism*

Introduction

Photochromism is defined as a reversible transformation in chemical species between two forms having different absorption spectra by photo irradiation[1]. This reversible physical phenomenon makes them applicable in the field of opto-electric materials and devices[2-5] for example light – density optical memory devices switches[6-7] etc. For this purpose, organic photochromic compounds are often incorporated in polymer, liquid crystalline materials or other materials.

Fulgides derived from Fulgenic acids are of great interest for their photochromic properties[8-10]. Santiago and Becker[11] have suggested that photochromism was observed only if one of the substituted group was an aromatic moiety. This makes Fulgide a substituted 1,2,5 – hexatriene in which an aromatic bond serves in place of one of the double bonds of the triene. This photochromism occurs in fulgides having either phenyl, substituted phenyl, furyl or styrl substituents[12,13]

Material and Methods

Materials

All the chemicals used were of analytical grade and with highest purity. The chemicals used were Dimethyl succinate, Benzaldehyde, Potassium metal, Butanol, 3-(benzo[d][1,3]dioxol-5-yl)acryloyl chloride, 2,6-diiodphenol,zinc oxide, dichloromethane, Acetone, Potassium carbonate , Dimethyl sulphate, 2M NaH, Benzene, Ethanol , 2M Sodium hydroxide , Ethyl acetate and chloroform, Rotary Evaporator, Column for chromatography setup, Immersion well Photochemical reactor (SAIC-model IQW-I), UV lamp (254nm), UV/VIS/NIR Spectrometer lambda -750 were used.

Methods

1. Synthesis of 3, 5-diiodo-4-methoxy-3', 4'-methylenedioxy Chalcone [3]

The straightforward route leading to the synthesis of Chalcone is Friedel-Crafts acylation of arenes with α,β-unsaturated aryl acid halides[14,15]. 3, 5-diiodo-4-hydroxy-3', 4'-methylenedioxy Chalcone was prepared by stirring a mixture of 3-(benzo[d][1,3]dioxol-5-yl)acryloyl chloride (3mmol), 2,6-diiodphenol (3mmol) and zinc oxide (1.5 mmol) which was stirred at room temperature (25-30°C). The process was monitored using TLC. The product was extracted with dichloromethane (3 x 5mL) and washed with aq. $NaHCO_3$. The organic layer was dried over anhydrous Na_2SO_4 and the removal of solvent under pressure furnished analytically pure product.[16]

A solution of Chalcone (1.761 g, 0.0035 M) in dry acetone (180 mL) containing anhydrous K_2CO_3 (1.37 g) was refluxed in dimethyl sulphate (0.66 mL) for 4 hours. After refluxing, the solution was filtered and the inorganic residue was washed with hot acetone. The acetone solution was distilled and the residue was treated with crushed ice, extracted in ether and dried using anhydrous sodium sulphate[17]. (Mol wt.: 534, Practical Yield: - 1.26g, % Yield: 70, NMR: δ 3.83 (3H,S), 6.06 (2H, S), 7.60 (1H, =CH), 8.08 (1H, =CH), 7.67 (2H, Ar). IR: 1675 cm-1 (C=O stretching, ketone) See Scheme 1.

2. Synthesis of (Z)-3-((E)-1-(benzo[*d*][1,3]dioxol-5-yl)-3-(3,5-diiodo-4-methoxyphenyl)allylidene)-4-((Z)-benzylidene)dihydrofuran-2,5-dione.

An equivalent mixture of dimethyl succinate (26.20g) and Benzaldehyde (19.02g) was added to a well-stirred solution of potassium tert-butanol prepared by dissolving potassium metal (7g) in 190 mL of butanol under dry anhydrous condition and stirred for about 1 hour. The reaction mixture, was acidified with ice-cold 3N HCl solution and tertiary butanol was removed under pressure using rotatory evaporator. After extraction with diethyl ether and washing with 10% solution of sodium bicarbonate under ice-cold conditions, acidification resulted in the isolation of **3-(methoxycarbonyl)-4-phenylbut-3-enoic acid** (1) as a semi-solid which was crystallized from alcohol-water as a yellow colored solid. Eq.wt (found): 284, M.P 143!, U.V λ_{max}: 291 (3.60); I.R: 1710 (C=O, ester), 1690 (C=O, acid), 1610 (C=C) and 1235 cm^{-1} (C-ostr); NMR: δ 3.76 (3H, s), 3.3 (2H, s), 7.17 (5H, Ar), 7.8 (1H, =CH).

3-(methoxycarbonyl)-4-phenylbut-3-enoic acid was refluxed for 8 hours with 8% alcoholic KOH solution and excess alcohol was distilled off. On acidification **2-benzylidenebutanedioic acid(2)** was obtained, which was crystallized from ether-pet ether (40:60) as a faint orange thick oil The dicarboxylic acid was then refluxed with EDC (250 mL) with methanol (75 mL) and a few drops of H_2SO_4 to give **Dimethyl-2-benzylidene succinate(2)**[12-14] **(**Eq.wt (found):135. Yield: 40%. IR 1839 and 1772 cm^{-1}(C=o, ester). Melting point: Chars at 218°C.)

A mixture of Dimethyl-2-benzylidene succinate (0.552 g) and 3, 5-diiodo-4-methoxy-3', 4'-methylenedioxy Chalcone 1.26 g was added drop-wise using a syringe for 3 hours to a solution containing Benzene and 2M

NaH 1.88g. A few drops of ethanol was then added to increase the entropy of the reaction. As the reaction proceeded, an orange layer started developing above the yellow solution and the solution was stirred for 48 hours. A red solution was obtained consisting of the desired product, half-ester and the unreacted chalcone. The solution was then added to crushed ice, resulting in the formation of two separate layers, which were separated using separating funnel and given washings using benzene. The product obtained was dark red. The product was added to NaOH and then extracted using ethyl acetate. The desired product was then separated by column chromatography by giving washing of Benzene 3 mL and Chloroform 3-4 drops. The reaction was monitored using TLC. After the separation of the product from silica where washing were given using acetone, faint red crystals **of 4-Benzo [1, 3] dioxol-5-yl-2-(benzylidene)-6-(3, 5-diiodo-4-methoxyphenyl)-3-(methoxycarbonyl) hexa-3, 5-dienoic acid** (**4**) could be seen.

IR: 1674cm^{-1} (C=O, acid), 1297cm-1 (C-O stretching, ester); NMR: δ: 3.83 (3H, S), 3.71(3H, S), 6.06 (2H, S), 15.12 (1H, S), 6.81(1H, = CH), 6.85 (1H = CH), 7.76 (2H, Ar); Eq.Wt (found): 483

4-Benzo [1, 3] dioxol-5-yl-2-(benzylidene)-6-(3, 5-diiodo-4-methoxyphenyl)-3-(methoxycarbonyl) hexa-3, 5-dienoic acid was refluxed for 8 hours with 8% alcoholic KOH. The excess of alcohol was distilled off. On acidification, the reaction mixture gave the dicarboxylic acid as a red sticky product. The dibasic product was then separated and removed from acetone and separated using column chromatography, where the washing was given using ethyl acetate and chloroform in 3:1 ratio. The reaction was monitored continuously using TLC and finally the solution was separated into three different beakers, each giving a single spot in TLC (using chloroform). The product **2-(-1-(benzo [1, 3] dioxol-5-yl)-3-(3, 5-diiodo-4-methoxyphenyl) allylidene)-3-(-benzylidene) succinic acid** (**5**) obtained had yellow crystals.

IR: 1674cm^{-1} (C=O, acid), 1611cm^{-1} (C=C); NMR: δ: 3.83 (3H,S), 6.06 (2H,S), 15.21 (1H,S) , 6.81 (1H, =CH), 6.85 (1H, =CH), 7.67 (2H, Ar) ; Eq wt. (found): 234.5. The dicarboxylic acid (**5**) was then refluxed with acetyl chloride for 2 hours on an oil-bath. Excess of acetyl chloride was removed under reduced pressure and triturated with diethyl ether giving brown crystals of Fulgide **(Z)-3-((E)-1-(benzo[*d*][1,3]dioxol-5-yl)-3-(3,5-diiodo-4-methoxy phenyl) allylidene)-4-((Z)-benzylidene)dihydrofuran-2,5-dione** (**6**)

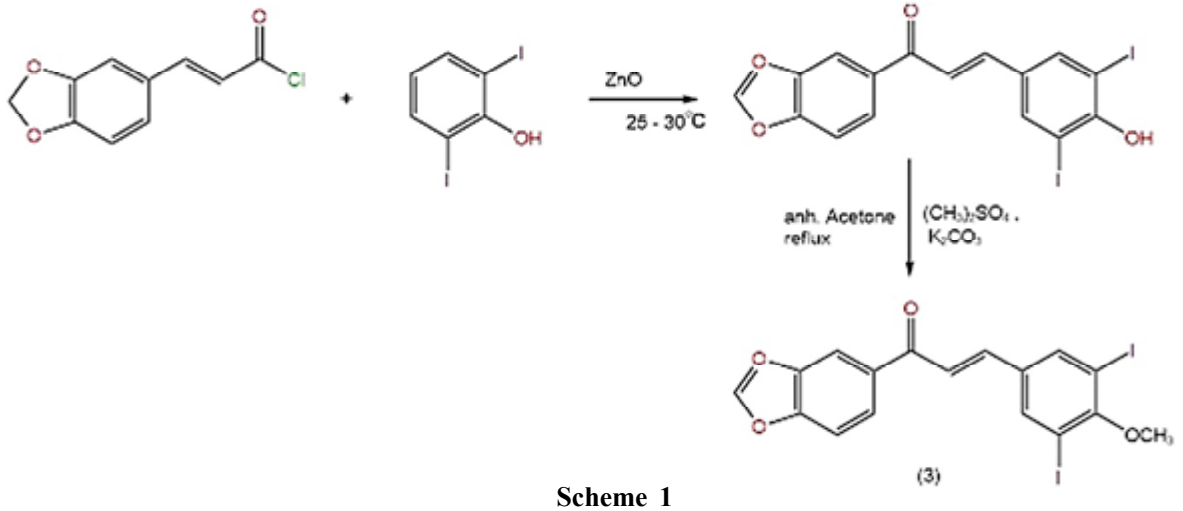

Scheme 1

Percent yield 80. IR: 1732 cm^{-1} (C=O, anhydride), 1611cm^{-1} (C=C); NMR: δ: 3.83 (3H, S), 6.06 (2H, S), 6.81 (1H, =CH), 0.85(1H, =CH), 7.67(2H, Ar). See Scheme (2)

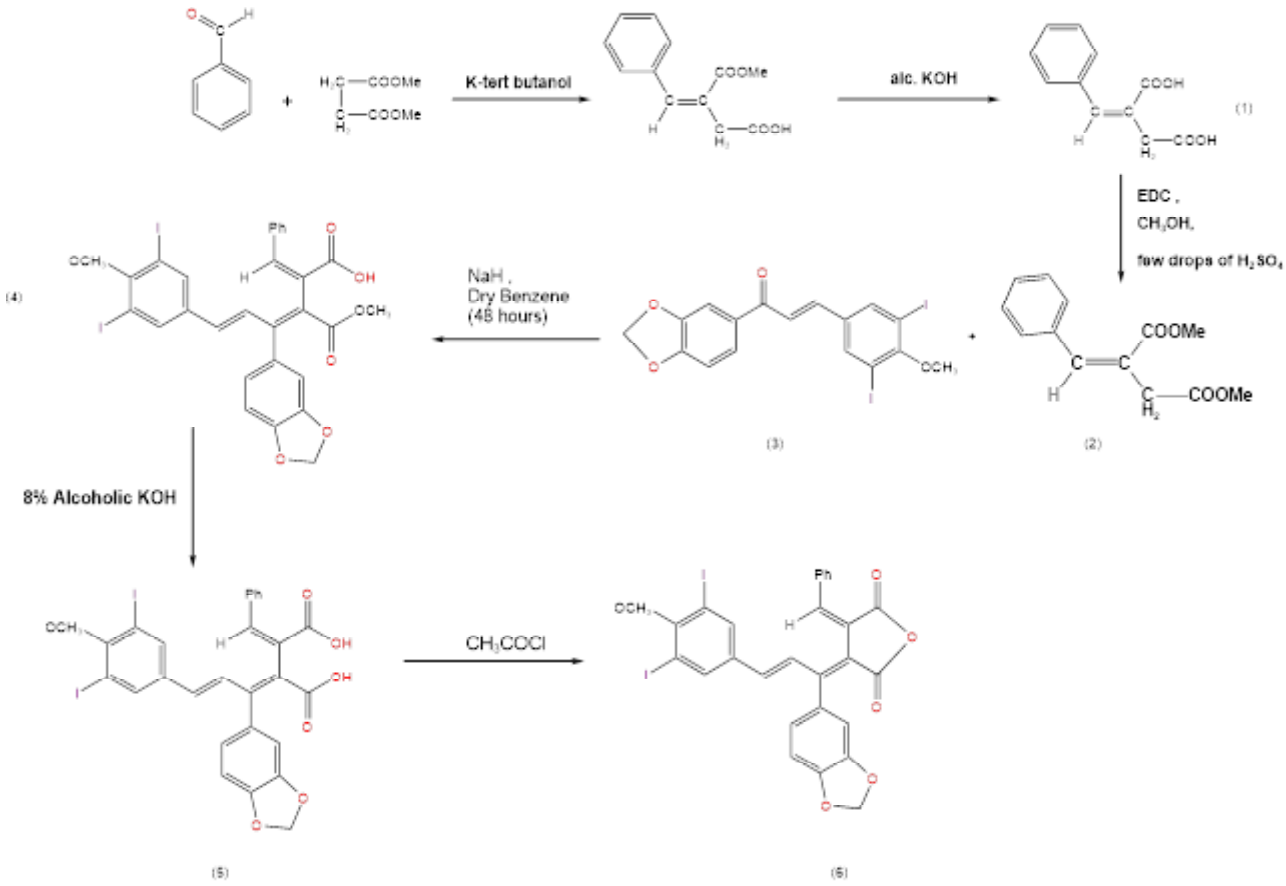

Scheme 2

Photochromism

To achieve the best conditions for photochromic studies a $1x10^{-5}$ mol dm^{-3} solution of compound **(6)** was taken and irradiated in a photochemical reactor at 254 nm for 5,10,20,25 and 30 minutes and structural changes were studied. It is usual to monitor the progress of the reaction by noting the disappearance of a characteristic absorption band in UV spectrum of the starting material.[22] The same technique has been applied here. When the compound was irradiated for 5, 10 and 15 minutes the main peak appeared at 287.80 nm whereas when exposed for 20,25 and 30 minutes, the main peak shifted from 287.80 nm to 346.50 nm (Table 1). Thus the UV irradiation at 254 nm in an inert atmosphere of compound 6 was done in an immersion well reactor (model IQW-1) for 20 minutes and the sample were scanned between 200-400nm by using instrument type; UV/VIS/NIR Spectrometer y = 750 nm. The observed shift was 38.70 nm. (Figure 1)

Table 1: Main peaks before and after irradiction

Time in Minutes	Main peaks before irradiation in nm	Main peaks after irradiation in nm
5	287.8	287.8
10	287.8	287.8
15	287.8	287.8
20	287.8	346.5
25	287.8	346.5
30	287.8	346.5

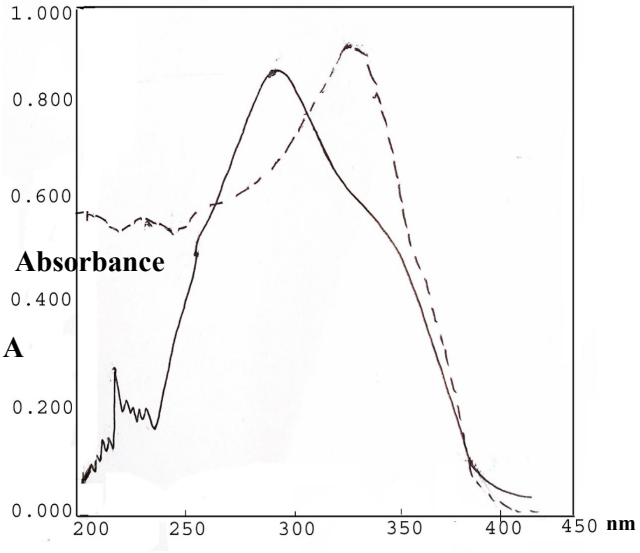

Fig. 1: μv spectrum of compound 6

Result and Discussion

The synthesis of 3, 5-diiodo-4-methoxy-3', 4'-methylenedioxy Chalcone was done by Friedel-Crafts acylation of arenes with α,β-unsaturated aryl acid halides with 70 percent yield. Photochromic Chalcone based Fulgide was synthesized by a multistep-reaction starting from dimethyl succinate and other chemical species with 5-diiodo-4-methoxy-3', 4'-methylenedioxy Chalcone. The reactions steps consist of the first Stobbe condensation, hydrolysis and esterification the second Stobbe condensation, hydrolysis and dehydration to yield photochromic chalcone based fulgide **(6)**.

When chalcone based fulgide were irradiated in an immersion well photochemical reactor for 20 minutes by UV 254 nm lamp, a shift in wavelength of 38.70 nm. was observed. Shift in wave length after irradiation shows that the compound has photochromic nature. The argument of Santiago and Becker that in 1, 3, 5-hexatriene an aromatic bond serves in place of one of the double bonds of triene holds good for anhydride.

Conclusions

The synthesized compound is photochromic and it validates the Santiago and Becker mechanism.

Acknowledgement

The authors are grateful to The Director, Institute of Science, Mumbai, India for providing necessary facilities.

References

1. Yasushi Yokoyama, Tohru Serizawa, Satoshi Suzuki, Yayoi Yokoyama, and Yukio Kurita, 1995, *Chem. Lett.,* **1**, 17-18.

2. Wittal, J., 1990, Photochromism, Molecules and system, Bouass-Laurent Elsevier, Amsterdam.

3. Yokoyama, Y., 2000, *Chem. Rev*., **100**, 1717-1739.

4. Irie. M., 2000, *Chem. Rev*., **100**, 1685-1716.

5. Yokoyama, Y. Kose, M.J., 2004, *Photoch. Photobio. A:Chem*., **166**, 9-8.

6. Yasushi Yokoyama and Taisuke Shiroyama, 1995, *Chem. Lett.,* **1**, 71-72.

7. Jitsuo Kiji, Tamon Okano, Hitoshi Kitamura, Yasushi Yokoyama, Shuji Kubota and Yukio Kurita, 1995, *Bull. Chem. Soc. Jpn.,* **68(2)**, 616-619.

8. Yasushi Yokoyama, Yuki Shimizu, Soichi Uchida and Yayoi Yokoyama, 1995, *J.Chem. Soc., Chem. Commun.,* **7**, 785-786.

9. Exelby and Grinter, 1965, *Chem. Rev.,* **65**, 247.

10. Brown, G.H., 1971, Techniques of Chemistry, Vol III. (John Wiley, New York), p.595.

11. Santiago A. and Becker, R.S., 1968, *J. Am. Chem. Soc*., **90**, 3654

12. Exelby and Grinter, 1965, *Chem. Rev*., **65**, 247

13. L. Chalkley, 1992, *Chem. Rev*., **6**, 217

14. Margarem and Miller, 1971, Techniques of Chemistry, Vol. III**.** John Wiley, New York, p.595.

15. N.O. Calloway, L.D. Green, 1937, *Journal of the American Chemical Society*, 809.

16. K. Johnston, M. Jones and F. Jones, 1969, *Journal of the Chemical Society C: Organic,* 814

17. Parmeshwar E. More, Babasaheb P. Bandgar and Vinod. T. Kamble, 2012, Zinc oxide as a regioselective and heterogeneous catalyst for the synthesis of chalcones at room temperature- Catalysis Communications, 27, - Elsevier

18. Ahluwalia, V.K., Pooja Bhagat, Ronn Aggarwal and Ramesh Chandra, Intermediates of Organic Synthesis–Stobbe and Collaborators, More than Fifty Publications **17**, 1893-1911

19. Banerjee, S., Tayade, R.A., and Sharma, B.D., 2013, Green synthesis of Acid Esters from Furfural via Stobbe Condensation., *Journal of Chemistry,* 1-5

20. Stobbe and Naoum, Ber., 1965, **37,** 2240.

21. Vogel's, Textbook of Practical Organic Chemistry, 2004, Pearson Education Singapore, p.106-114.

RNI No. MAHENG/2017/74063
ISSN No. (Print) 2581-5911
ISI Impact Factor 1.724

Moringa oleifera: Review on Herbal Healing Properties and Nutritional Values

Rakhi Das[1], Ranju Khatiwada[1], Rezina Pradhan[1], Rishav Das[2], Sarashwati Karn[1], Ravi Bhushan Sharma[1], Rojina Tandukar[4] and Roshan Kumar Yadav[4]*

[1] Central Department of Chemistry, Tribhuvan University, Kathmandu, Nepal
[2] Himalayan White House International College, Purbanchal University, Kathmandu, Nepal
[3] Department of Biotechnology, Kathmandu University, Dhulikhel, Nepal
*Correspondence: Roshan Kumar Yadav,
[4*] Nepal National Commission for UNESCO, Ministry of Education, Science and Technology, Government of Nepal, Kathmandu, Nepal.
Email: fsroshan@gmail.com (R.K.Y)
rakhidas021@gmail.com (R.D.); ranjukhatiwada98@gmail.com (R.K);
rezinapradhan01@gmail.com (R.P.); karnsarashwati@gmail.com (S.K.);
ravibhushansharma84@gmail.com (R.B.S)
rishavdas58@gmail.com (R.D.); rtandukar111@gmail.com

Abstract

Despite being indigenous to India, Nepal, and the highlands of the Himalayas, Moringa oleifera *flourishes in all tropical and subtropical regions of the world. Drumsticks or horseradish trees are frequently used words for this plant. Moringa plant is affordable, readily available, and extremely nutritious, and it is widely used for its therapeutic properties. The little softwood tree* Moringa oleifera *grows swiftly and adapts well to a dry, sandy environment. Moringa plants include substances that are anti-inflammatory, anti-cancer, anti-tumor, cardiovascular, and central nervous system support. The manufacturing of antifungal and antibacterial drugs, the production of biofuels and oils, and the treatment of wastewater are just a few of the many uses for which Moringa plants have been one of humanity's most significant suppliers. This review discusses the various medical applications of Moringa as well as its morphology, nutritional needs, notable pharmacological qualities, commercial uses, safety studies, and commercial viability.*

Keywords: Moringa oleifera*, Antidiabetic, Anticancer, Antimicrobial, safety studies.*

Introduction

Since plants fulfill the role of producers in the ecosystem, they are independent of other species in terms of food. There are many different types of plants on our planet. Plants are essential to life for a variety of reasons, including providing oxygen, conserving soil, producing food, and providing lumber. Plants have long been used as a treatment for a range of illnesses. The key benefit of using herbs as medicine and why they are preferred more is that they have fewer side effects, which boosts public trust in plant-based therapies. Various ailments can be treated using plant components such as roots, leaves, bark, and extracts[1]. The World Health

Organization (WHO) has stated that the finest sources of pharmaceuticals are medicinal herbs and plants. Human beings benefit considerably from therapeutic plants, especially those who are frail owing to poverty, unemployment, illness, and low-income sources. Hence it is important to treat them with easily available plant components with little cost and also boost public confidence in plant-based therapy. Again, WHO has said that herbs and plants with medicinal properties are the finest sources of medication. *Moringa oleifera* is the most common plant throughout various parts of the world, from Asia to Africa. The healing properties of this plant, also known as "Mother's best friend," "the miracle tree," "the horseradish tree," and "the drumstick tree," have made it a blessing to mankind. The Moringa plant is widely available, affordable, very nourishing, and well-known for its therapeutic properties[2,3]. Moringa leaves include a wide variety of macronutrients and micronutrients that are essential to both human beings and other living things. It contains many sources of proteins, vitamins, minerals, and carotenoids. Moringa is frequently referred to as the "Miracle plant" because of its beneficial therapeutic properties. Moringa oleifera is a little softwood tree that may grow quickly and bear fruit in a dry, sandy environment. One of the distinguishing features of the species is its long, drumstick-shaped pods, which contain seeds. In its first year of development, Moringa has shown the ability to grow up to 4 meters and bear fruit, both of which are shorter than average. The seeds, flowers, leaves, roots, and pods of the Moringa plant are all extremely valuable both commercially and medicinally.

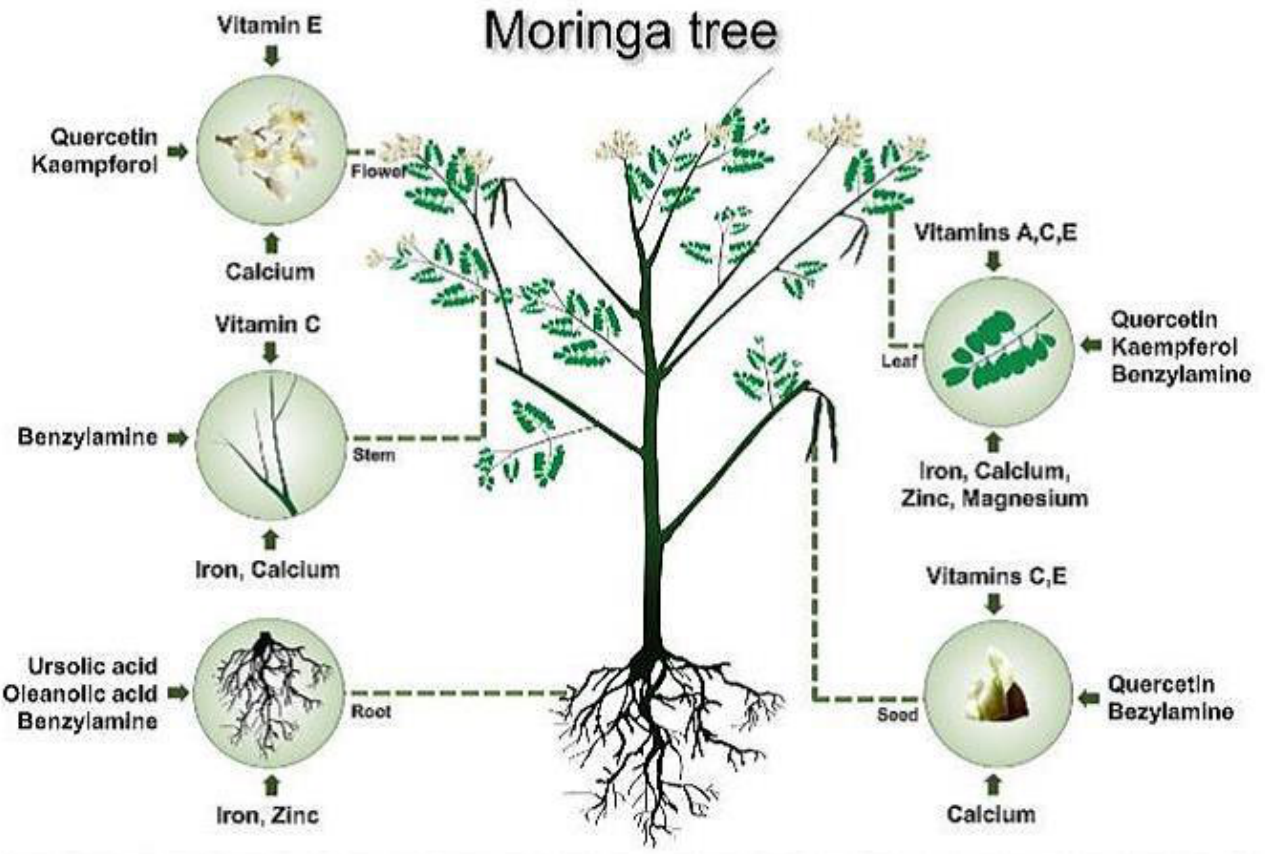

Fig. 1. *Moringa oleifera* plant parts and uses[4]

There are a few traditional and medicinal uses for Moringa. It has been used as a nutritional supplement for more than 20 years in Ghana and other countries. Hence, it has grown to be a well-known plant worldwide. Regardless of the nutraceutical value, the plant's diverse sections have unique pharmacological effects. Malnutrition is very well treated by the Moringa tree, especially in mothers and newborns. The entire plant, including leaf, flowers, root, bark, gum, seed, and seed oil, has been used for a variety of purposes in South Asian traditional medicine, including the treatment of infectious and inflammatory diseases as well as hematological, cardiovascular, gastrointestinal, and hepato-endocrine disorders[5,6,7]. The leaves of the Moringa plant contain a variety of chemicals, including flavonoids, ascorbic acid, phenolics, and carotenoids, which are good sources of natural antioxidants[8]. The juice from the leaves is used to treat eye infections. The leaf is exceptionally nutrient-dense and contains significant amounts of rough protein (20-29%), vitamins, and minerals[9,10]. Moringa seeds are said to have antibacterial properties. The roots and seeds have demonstrated antibacterial activity[11]. The antimicrobial action of the Moringa leaves is attributed to their ethanolic extract[12]. The plant is renowned for a variety of medicinal qualities, including the ability to treat tumors, prevent infertility, lower blood pressure, and have antibacterial effects[13,14]. Urinary stone formation is reduced and prevented by using the aqueous and alcoholic extracts of Moringa root wood[15]. The Moringa plant has been linked to a sizable number of primary and secondary metabolites as well as pharmacological actions.

Morphology

The slender, freely branching Moringa tree can grow incredibly quickly (Figure 1). Although it can grow taller than 10 meters, it is typically classified as a small to medium-sized tree, having green to dim green, fluffy, tripinnate numerous leaves 2cm long elliptical leaflets. The large finely fragmented blooms of the tree are carried on inflorescences 10 to 25 cm long and are typically white to cream in color, though they can occasionally be tinted with pink in some kinds. The tree is frequently mistaken for a legume because of its leaves. The fruit, which has a three-lobed shell, is frequently called a "pod". Light green, and in certain varieties, reddish, are the colors of immature pods. The fast-growing, drought-tolerant tree can withstand poor soil, a wide range of annual rainfall (28-300), and a pH range of 5.3-9.0. Dried seeds have a round or triangular shape when fully grown and a faintly forested capsule with three papery wings surrounding the kernel. It has been discovered that the composition of *Moringa oleifera*, includes a fatty acid profile, and that Moringa oleifera oil is high in oleic acid (>80%). *Moringa oleifera* seeds contain between 33 and 41% w/w of vegetable oil. The oil found in the seed, which is shown to be a source of biofuel makes up about 40 to 50 percent of the seed.

Different parts of Moringa plant

Stem: The stem is naturally lengthy but occasionally has an improper form. The tree is 1.8 to 3 meters tall and has a short, straight trunk[16].

Branch: The branches are formed in an irregular pattern, and the covering has the shape of an umbrella.

Leaves: Tripinnate complex leaves are fluffy and have 1-4 cm long, green, curving leaflets. Because of its leaves, the tree is frequently mistaken for a leguminous plant. In general, the branch tips are where the alternating twice or three times pinnate leaves appear (shown in Figure 2). They range in length from 20 to 70 cm, with a long petiole with 8 to 10 pairs of pinnae, each bearing two sets of inverted elliptic leaflets and one at the apex that is 1-2 cm long, and are greyish in color when young[17].
Flowers: Inflorescences 15-25 cm long bear prominent, delicately scented flowers that are 2.5 cm in diameter, primarily white to cream in color, and tinged pink in a few variations (shown in Figure 2). The 2.5 cm broad, agreeably scented flowers are delivered in abundance on supplementary, 10 to 25 cm long panicles. They have white dots at their bases. Straight lanceolate five-reflexed

sepals are seen. The five petals are speculatively thin. Except for the lowest, they consist of the five stamens and five staminodes and are reflexed.

Fruits: Fruits have three lobes and are frequently referred to as pods. Young pods are green and, in some varieties, have radish-like coloring. Pods are triangular, brown, and split longitudinally into three pieces when dried. They are between 35 and 130 cm long and 12.8 cm wide.

Seeds: The oval, tan, semi-permeable seeds have three papery wings and are arranged in an oval shape (Figure 2). The majority of seed arrangements are brown to dark brown, although they can sometimes be white if there are insufficiently viable sections. Within a week, viable seeds begin to grow. The body itself features three white wings that continuously beat at 130 seconds intervals from beginning to end.

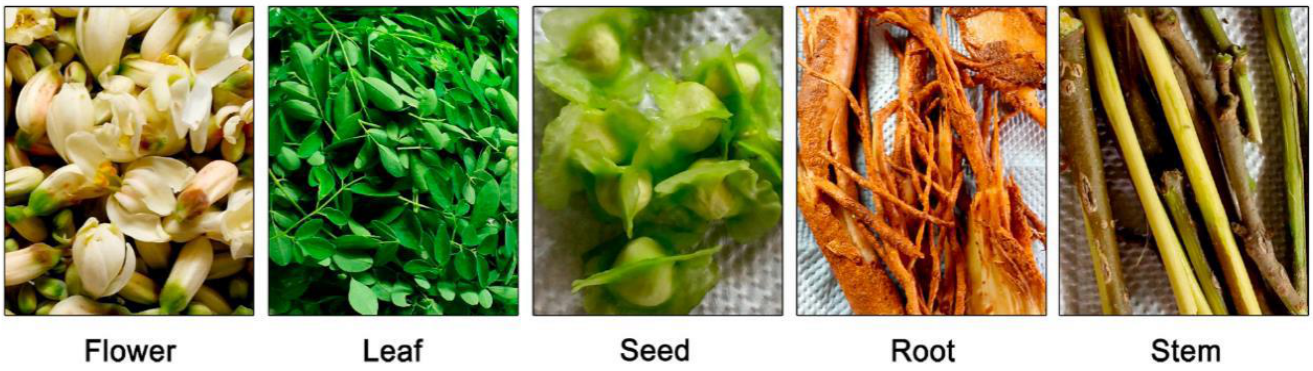

Fig. 2. Morphology of various tissues in *M. oleifera*[18].

Nutritional Properties

Every component of the Moringa oleifera plant contains valuable nutrients and antinutrients. Minerals like Calcium, Potassium, Zinc, Magnesium, Iron, and copper are abundant in Moringa oleifera leaves[19]. There are vitamins like Vitamin A's beta-carotene, Vitamin B's pyridoxine, nicotinic acid, and folic acid, as well as Vitamins C, D, and E[20]. Anti-cancerous substances such as glucosinolates, isothiocyanates, glycoside compounds, and glycerol-1-9-octadecanoic are present along with phytochemicals like tannins, sterols, terpenoids, flavonoids, saponins, anthraquinones, alkaloids, and reducing sugar[21]. Low in calories, Moringa leaves can be included in an obese person's diet. Fibrous pods are useful for treating digestive issues and preventing colon cancer[22,23]. A study reveals that immature pods have a protein level of about 20.66% and a fiber content of about 46.78%. Amino acid concentration is 30% in pods, 44% in leaves, and 31% in flowers. Similar quantities of palmitic, linolenic, linoleic, and oleic acids are found in the immature pods and flowers[24]. Among the several elements found in Moringa that are crucial for growth and development, Calcium is regarded as one of the key minerals for human growth. Moringa leaves can be consumed for 1000mg of Ca and Moringa powder can be consumed for more than 4000mg, compared to the 300-400mg found in 8 ounces of milk. In order to treat anemia, Moringa powder can be used in place of iron supplements. While Moringa leaf powder contains 28 mg of iron, beef has only 2 mg. According to some reports, Moringa has a higher iron content than spinach[25]. Zinc needs to be consumed in adequate amounts for DNA and RNA production as well as for healthy sperm cell development. The zinc content of Moringa oleifera leaves ranges from 25.5 to 31.03 mg/kg, which matches the recommended daily intake of zinc[26].

Linoleic, linolenic, and oleic acids are PUFAs that have the power to regulate cholesterol. According to research, Moringa seed oil has about 76% PUFA, which makes it a good alternative to olive oil[27]. The content of the nutrients varies depending on the place. The nutrient composition is affected by the seasons, according to Fuglie[25]. It has been demonstrated that whereas Vitamin C and iron were more prevalent in the cool-dry season, Vitamin A was more prevalent in the hot, wet season[28]. The variance in results can be related to the fact that the nutrient content of the tree is greatly influenced by the location, climate, and environmental factors[29]. Tables 1 and 2 provide a comprehensive list of the nutrients found in leaves, pods, and seeds along with their medicinal uses.

Table 1. The nutrient compositions of leaves, leaf powder, seeds, and pods[30, 31, 32].

Nutrients	Fresh Leaves	Dry Leaves	Leaf Powder	Seeds	Pods
Calories(cal)	92	329	205	-	26
Protein(g)	6.7	29.4	27.1	35.97±0.19	2.5
Fat(g)	1.7	5.2	2.3	38.67±0.03	0.1
Carbohydrate(g)	12.5	41.2	38.2	8.67±0.12	3.7
Fiber(g)	0.9	12.5	19.2	2.87±0.03	4.8
Vitamin B1(mg)	0.06	2.02	2.64	0.05	0.05
Vitamin B2(mg)	0.05	21.3	20.5	0.06	0.07
Vitamin B3(mg)	0.8	7.6	8.2	0.2	0.2
Vitamin C(mg)	220	15.8	17.3	4.5±0.17	120
Vitamin E(mg)	448	10.8	113	751.67±4.41	-
Calcium(mg)	440	2185	2003	45	30
Magnesium(mg)	42	448	368	635±8.66	24
Phosphorus(mg)	70	252	204	75	110
Potassium(mg)	259	1236	1324	-	259
Copper(mg)	0.07	0.49	0.57	5.20±0.15	3.1
Iron(mg)	0.85	25.6	28.2	-	5.3
Sulphur(mg)	-	-	870	0.05	137

Table 2. Nutritional compositions and medicinal uses of different parts of Moringa[32].

Part of tree	Medicinal Uses	Nutritive Properties	Suggestion
Leaves	Moringa leaves treat asthma, hyperglycemia, Dyslipidemia, flu, heartburn, syphilis, malaria, pneumonia, diarrhea, headaches, scurvy, Skin diseases, bronchitis, eye and ear infections. Also reduces, blood pressure and cholesterol and acts as an anticancer, antimicrobial, Antioxidant, antidiabetic and anti-atherosclerotic agents, neuroprotectant.	Moringa leaves contain fiber, fat proteins and minerals like Ca, Mg, P, K, Cu, Fe, and S. Vitamins like Vitamin-A (Beta-carotene), vitamin B-choline, vitamin B1-thiamine, riboflavin, nicotinic acid and Ascorbic acid is present. Various amino acids like Arg, His, Lys, Trp, Phe, Thr, Leu, Met, Ile, and Val are present. Phytochemicals like tannins, sterols, saponins, terpenoids, phenolics, alkaloids and flavonoids like quercetin, isoquercetin, kaemfericetin, isothiocyanates and glycoside compounds are present.	The presence of flavonoids give leaves the antidiabetic and antioxidant properties. The isothiocyanates are anticancer agents. Flavonoids like quercetin and others are known for anti-proliferative, anticancer agent. The presence of minerals and vitamins help in boosting the immune system and cure a myriad of diseases.

Part of tree	Medicinal Uses	Nutritive Properties	Suggestion
Seeds	Seeds of moringa help in treating hyperthyroidism, Chrohn's disease, anti herpes simplex virus arthritis, rheumatism, gout, cramp, epilepsy and sexually transmitted diseases can act as antimicrobial and anti-inflammatory agents.	Contains oleic acid (Ben oil), An antibiotic called pterygospermin, and fatty acids like Linoleic acid, linolenic acid, behenic acid, Phytochemicals like tannins, saponin, phenolics, phytate, flavonoids, terpenoids, and lectins. Apart from these, fats, fiber, proteins, minerals, vitamins like A, B, C, and amino acids.	The presence of flavonoids give anti-inflammatory property. The antibiotic pterygospermin is responsible for antimicrobial properties. The other phytochemicals help in treating various diseases
Root Bark	Root bark acts as a cardiac stimulant, anti-ulcer, and anti-inflammatory agent.	Alkaloids like morphine, moriginine, minerals like Calcium, Magnesium and Sodium.	The alkaloid helps the bark to be antiulcer, a cardiac stimulant and helps to relax the muscles.
Flower	Moringa flowers act as hypocholesterolemia, antiarthritic agents that can cure urinary problems and colds.	It contains calcium and potassium and amino acids. They also contain nectar.	The presence of nectar makes them viable for use by beekeepers.
Pods	Moringa pods treat diarrhea, liver and spleen problems, and joint pain.	Rich in fiber, lipids, non-structural carbohydrates, protein, and ash. Fatty acids like oleic acid, linoleic acid, palmitic acid, and linolenic acid are also present.	The presence of PUFA in the pods can be used in the diet of the obese.

Phytochemical Properties

Simple sugar, rhamnose, also known as glucosinolates, and isothiocyanates are among the substances found in *Moringa oleifera*[34,35]. Two alkaloids, Moringinine and Moringine, are present in the bark and stem of the Moringa plant[36]. Galactose, glucuronic acid, L-arabinose and L-rhamnose, xylose, mannose, and degraded-gum polysaccharide consisting of Glucuronic acid, L-mannose, and L-galactose have all been identified in purified gum exudate from *M. oleifera*. This information was obtained by mildly hydrolyzing the whole gum with acid[37]. From the stem of M. *oleifera,* isolation of substances such as sitosterol, -sitostenone, vanillin, 4-hydroxymellin, and octacosanoic acid has been done[38]. Nine amino acids, D-glucose, sucrose, quercetin, wax, traces of alkaloids, and kaempferol are all found in the Moringa flower; the ash is abundant in Calcium and Potassium[39]. In addition, alkaloids, kaempferitrin, kaempferol, rhamnetin, isoquercitin, and other flavonoid pigments are found. It has been discovered that the acetate phase of the ethanol extract of Moringa oleifera pods contains isothiocyanate and thiocarbamate glycosides[40]. The fruit has been reported to contain cytokinins[41]. Recently, research into extracting growth hormones and promoters from *M. oleifera* leaves has gained attention. Even if the nature of the active ingredient is unclear, it has been demonstrated that the application of an aqueous-ethanol extract of Moringa leaves increases black gram nodulation[42]. Because of the presence of numerous types of antioxidant components, including flavonoids, phenolics, ascorbic acid, and carotenoids, Moringa leaves serve as a good source of natural antioxidants[43, 44]. The leaves and pods of the Moringa plant have high concentrations of Calcium, Iron, Phosphorus, Copper, Vitamins A, B, and C, -tocopherol, folic acid, riboflavin, nicotinic acid, pyridoxine, beta-carotene, protein, ascorbic acid, oestrogenic substances, -sitosterol, and some

specific essential amino acids like tryptophan, methionine while stigmasterol, -sitosterol, campesterol, Claro sterol, and 5-avenasterol make up the majority of the sterols in Moringa seed oil, there are also trace levels of stigmasterol, 7-campesterol, 28-isoavenasterol, and 24-methlenecholesterol[45,46]. The sterol composition of major Moringa seed oil fractions differs significantly from that of traditional edible oils[47]. According to its fatty acid profile, M. oleifera seed oil decreases in the category of high-oleic oils (C18:1, 67.90%-76.00%). Essential components are the fatty acids C16:0 (6.04%-7.80%), C18:0 (4.14%-7.60%), and C20:0 (2.76%-4.00%). The concentration of certain tocopherols (alpha-, gamma-, and delta-) in Moringa oleifera is found to range from 96.72 to 124.45, 29.90 to 95.70, and 46.00 to 73.26 mg/kg, respectively.

Some of the important bioactive Phytocompounds from *Moringa oleifera*:

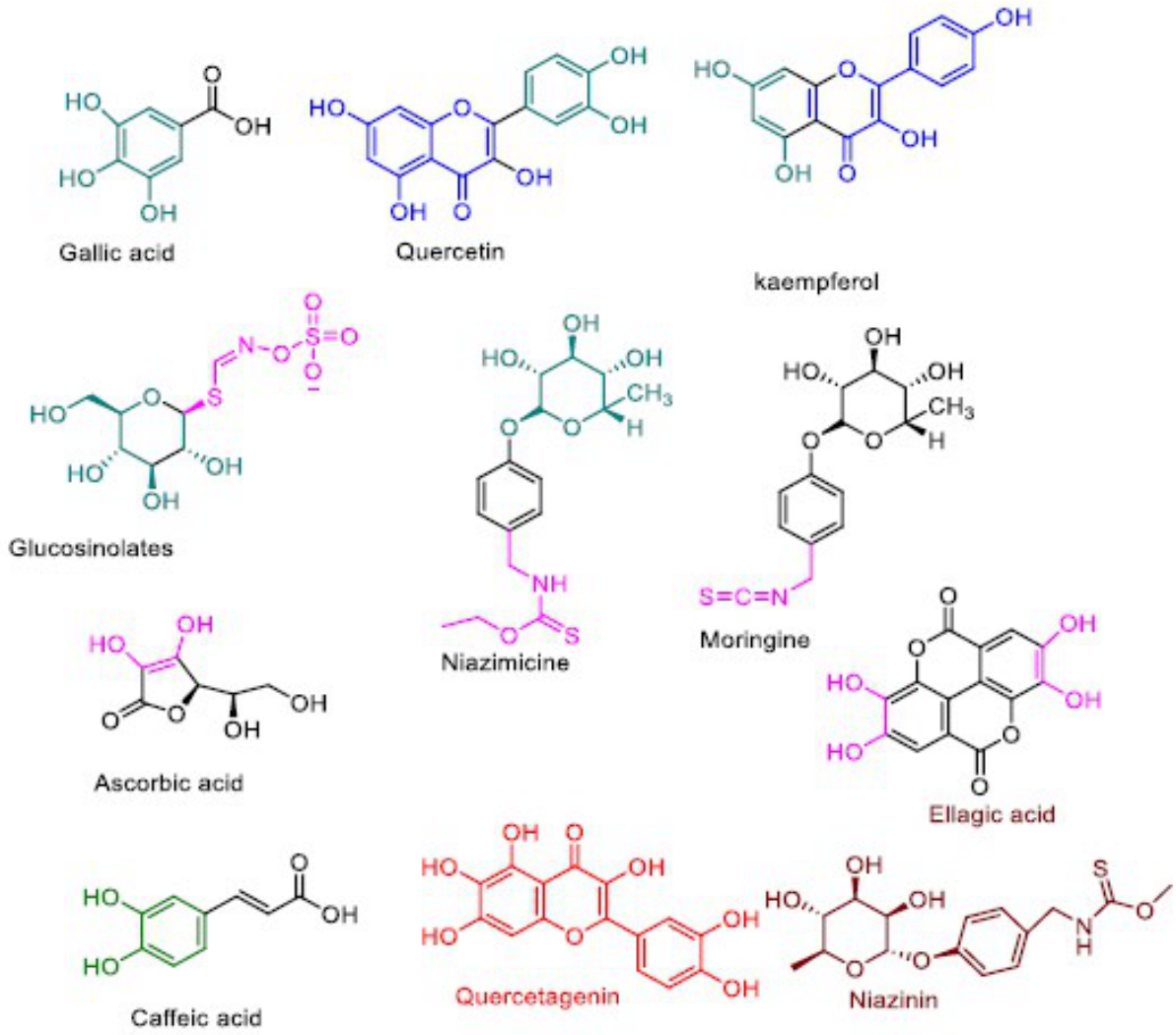

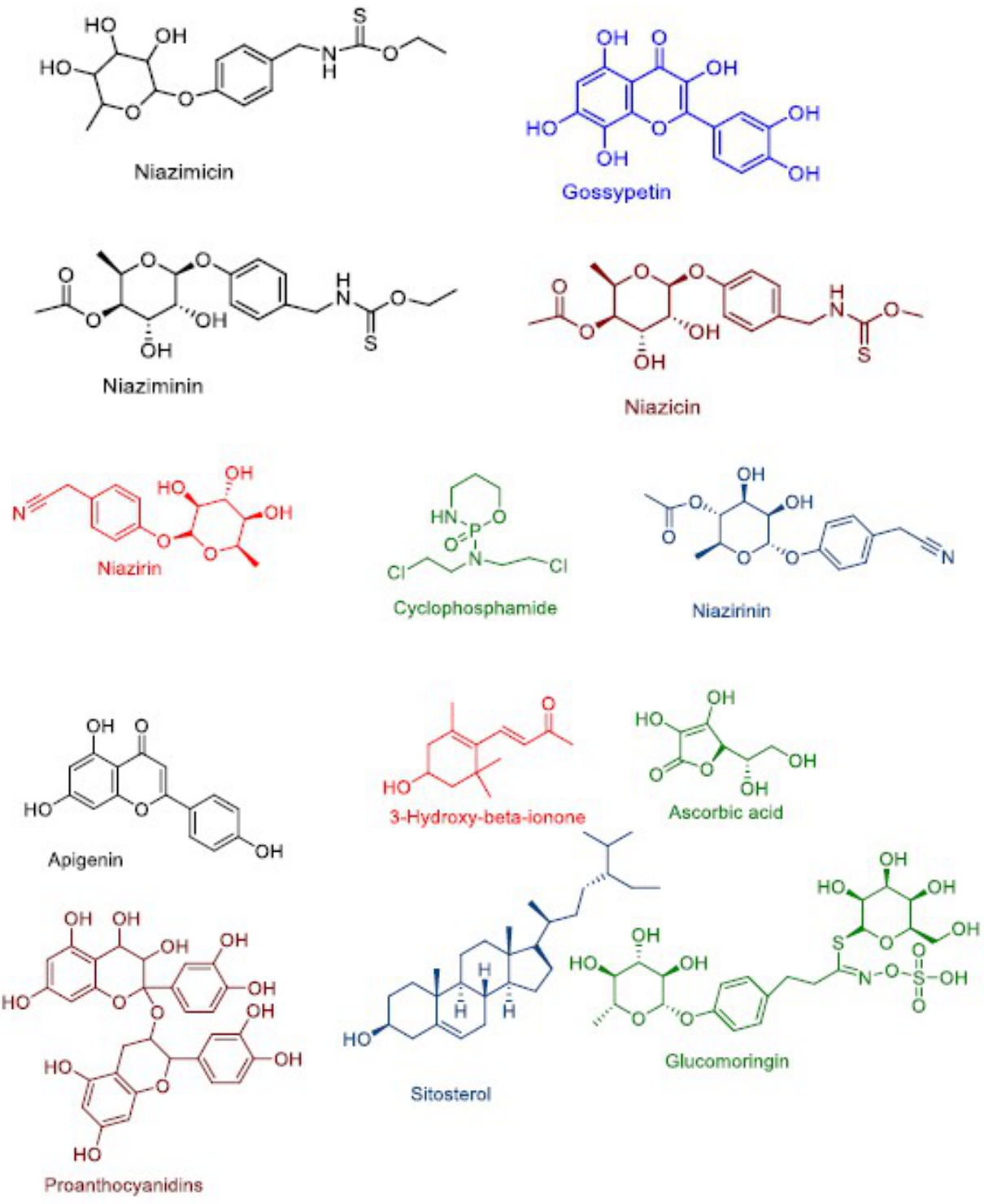

Fig. 3. Bioactive compounds are present in *Moringa oleifera*[48]

Medicinal Properties

More than 300 ailments can be cured by *Moringa oleifera*, which is frequently regarded as a panacea. Local populations in Asian nations have traditionally used Moringa as an herbal remedy. It works well as a medicinal agent because of the phytochemicals contained. The following list of its significant health advantages is provided.

Anti-Diabetic Properties

Type 1 and Type 2 diabetes have both been found to be cured by Moringa. Patients with type 1 diabetes do not produce insulin, a hormone that is necessary to keep blood glucose levels in the desired normal range. Insulin resistance is one that is connected to type 2 diabetes. Beta cell malfunction, which fails to detect glucose levels and lowers insulin signaling, as a result, may also contribute to type 2 diabetes and result in elevated blood sugar levels[49]. Research has demonstrated the anti-diabetic properties of Moringa. According to a study, aqueous extracts of *Moringa oleifera* aqueous extracts can treat rats with both insulin-resistant Type 2 diabetes and Type 1 diabetes caused by streptozotocin[50]. In a different study, researchers observed a decrease in fasting blood glucose levels after feeding Moringa seed powder to STZ-induced diabetes mice[51]. Additionally, the serum levels of antioxidant enzymes rose when the rats were given 500 mg of Moringa seed powder per kg of body weight. This demonstrates that the antioxidants in Moringa can reduce the ROS that STZ induction causes in the Beta-cells. In Beta cells, STZ induces ATP dephosphorylation processes that aid xanthine oxidase in producing superoxide and reactive oxygen species (ROS)[52]. Patients with hyperglycemia experience beta cell destruction. As a result, when there is excessive glucose inside the mitochondria, reactive oxygen species are released. Beta cells undergo apoptosis because they have a low level of antioxidants[53,54]. As a result, there will be less insulin secreted, which will cause hyperglycemia and eventually Type-2 diabetes. It has been suggested that flavonoids like quercetin and phenolics act as antioxidants by scavenging ROS. The flavonoids in Moringa are thought to scavenge the ROS generated from mitochondria, preserving the beta cells and, in turn, preventing hyperglycemia[55,51]. Diabetes can cause retinopathy, nephropathy, atherosclerosis, and other problems. Such illnesses can be prevented with Moringa. Blood glucose combines with proteins in hyperglycemia to produce advanced glycated end products (AGEs). RAGE, which is expressed on the surface of immune cells, is bound by these AGEs. Interleukin-6 and interferon transcription are both elevated as a result of this relationship. The surface endothelium of arteries expresses cell adhesion molecules concurrently[56]. This promotes trans-endothelial migration, which results in artery irritation and atherosclerosis. Atherosclerotic agents are treated with Moringa[57]. The antioxidant qualities of Moringa can be used to explain its antiatherogenic tendency.

Anticancer Properties

MO has the potential as an anticancer agent against several cancers[58]. MO leaf extract inhibited the cell viability of hepatocellular carcinoma, acute lymphoblastic, and myeloid leukemia[59]. The bioactive compounds responsible for the inhibition were attributed to niazimicin, β-sitosterol-3-O- β-D-glucopyranoside, and 4-(α-L-rhamnosyloxy) benzyl isothiocyanate. Berkovich et al., showed that MO leaves inhibited pancreatic cancer cell growth[60]. It targeted the cell cycle resulting in cell accumulation at the sub-G1 phase. In addition, MO leaves downregulated the IκBα pathway by decreasing the expression of IκBα, p- IκBα, and p65 proteins. It synergistically induced cytotoxicity with cisplatin in pancreatic cancer cells. It is also effective against breast cancer cells[58]. In rats, diethyl nitrosamine was used to develop liver cancer, and Sandek et al. demonstrated that MO leaves had the ability to prevent cancer[61]. The hot water MO leaf extract was studied by Madi et al.

because it had antiproliferative effects on A549 lung cancer cells[62]. The extract induced p53, caspases, and PARP-1 cleavage through increasing reactive oxygen species. The cancer cell line underwent apoptosis as a result of this. Additionally, it was demonstrated that both A549 lung cancer cells and SNO esophageal cancer cells were resistant to the proliferative effects of the hot water crude aqueous extract[63]. The extract caused DNA fragmentation and controlled oxidative stress. Additionally, the extract increased apoptotic signals, which caused cancer cells to die. In human melanoma A2058 cells, MO fruit extract boosted ROS generation, caspase 9, -3/7 activity, and MAPK activation to cause apoptosis via the mitochondria[64]. The MO's glucosinolate content prevents cancer[65]. It is able to trigger apoptosis. Anticancer medications are needed to target the high rate of proliferation of cancer cells. It is interesting to note that MO has been demonstrated to have a wide range of activities and can target a number of proteins and molecules to impede the growth of cancer cells[65]. As depicted in Figure 4, MO has the potential to be used in the creation of a brand new complementary and alternative therapeutic agent for the treatment of cancer. Effective anticancer compounds can be found in the leaves and bark[66]. It displayed antiproliferative effects in HCT-8 and MDA-MB-231 cancer cell lines. However, the seed extract was not effective. Apoptosis occurred with G2/M phase cell cycle arrest. The anticancer effect was attributed to bioactive compounds such as D-allose, hexadeconoic acid ethyl ester, eugenol and isopropyl isothiocyanate. This is particularly important as the bioactive compounds identified possessed a sugar moiety, aromatic rings and long chain hydrocarbons. Therefore, it can be seen that MO has potential in novel drug development.

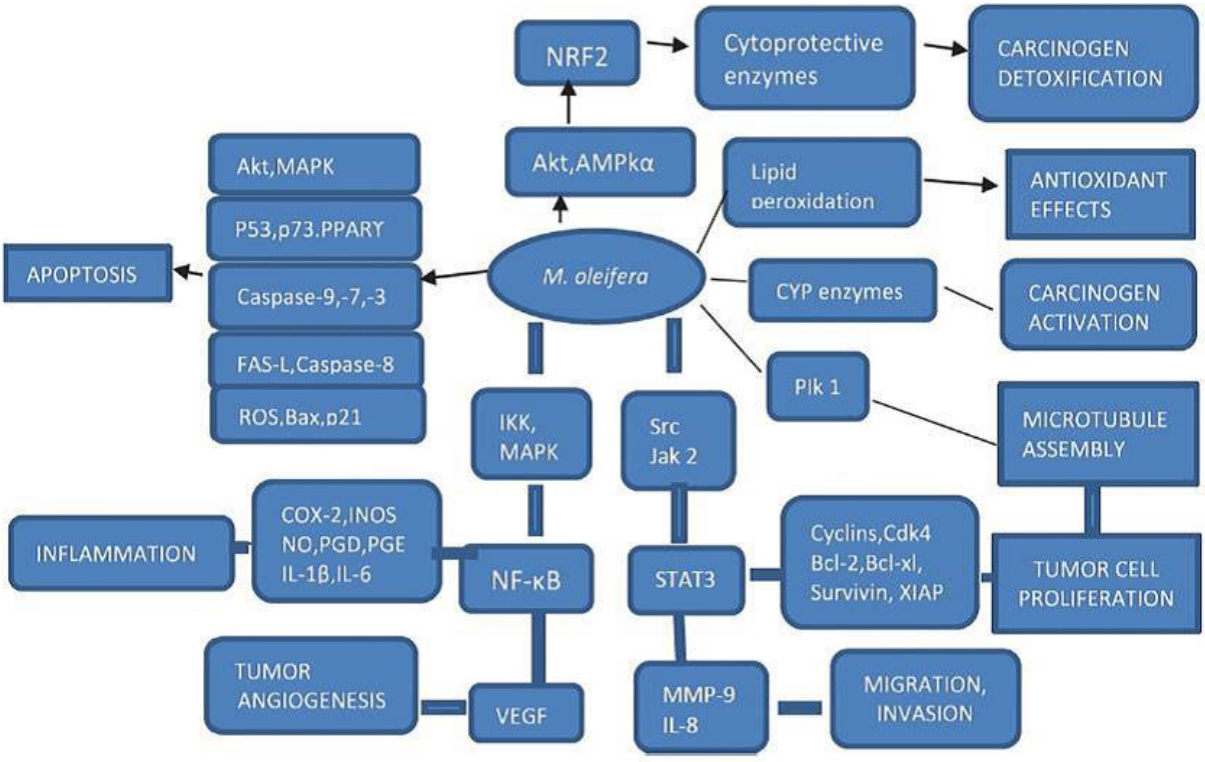

Fig. 4. The anticancer potential and molecular targets of *Moringa oleifera*[67]

Antioxidant Properties

By defeating the cell's antioxidant defense system, reactive oxygen species oxidize biological molecules, resulting in damage to DNA, proteins, and carbohydrates as well as cell membranes (Figure 4). This oxidative stress is brought on by a number of clinical conditions, including diabetes, heart failure, and hypertension[68]. Consumers always choose natural antioxidants over synthetic ones since they are superior to them[69]. Strong antioxidants discovered in *Moringa Oleifera* leaves include quercetin, kaempferol[70], ascorbic acid, β-carotene[71], isothiocyanates, polyphenols, and rutin[72]. Researchers have discovered that the extracts of leaves in a variety of organic solvents, including methanol, acetone, dichloromethane, water, diethyl ether, chloroform, and ethyl acetate, possess antioxidant capabilities[73,74]. The superoxide anion radical (O^{-}) can be more effectively neutralized by the ethyl acetate extract of *Moringa Oleifera,* which decreases tissue damage by preventing the interaction of free radicals with biological macromolecules. The linear association between phenolic chemicals and the leaves' greater antioxidant activity[74] aids in the development of products that increase the oxidative stability of food goods. Due to the presence of a greater polyphenolic content, the extract of *Moringa Oleifera* methanolic leaves demonstrated reasonable antioxidant activity (ICSO 49.86 g/mL) in comparison to ascorbic acid (ICSO 56.44 g/mL)[75]. Additionally, it has been claimed that leaves' antioxidant profile agrees with plants' ability to preserve themselves from freezing[76] and that its components are employed as a natural preservative for fat[77]. The antioxidant capacity of *Moringa Oleifera* tea (81% inhibition of DPPH radicals compared to Vitamin-C (0.1 mg/Ml) with 76.5% inhibition) may be useful in preventing chronic illnesses linked to stress[78]. In a recent study, Khalofah et al.[79] found that cadmium stress had a deleterious impact on Lepidium sativum but that *Moringa* leaf extract considerably lessened that impact. Intoxicated rats with aluminum phosphide experience an increase in antioxidant levels and a decrease in malondialdehyde after receiving a dose of 100 mg/kg body weight of *Moringa Oleifera* extract (MDA). As a result, it can be utilized as adjuvant therapy to treat cardiotoxicity brought on by aluminum phosphide (AlP)[80]. Alavrez Roman et al.[81] prepared topical formulations (nanoparticles and gel) from the hydroalcoholic fraction of *Moringa* leaves and identified the phytochemical profile's moisturizing and antioxidant potential. The viscosity, pH, and particle size of both formulations were good, indicating that they were suitable for use as a formulation. There were discovered to be seven distinct substances, including phenolic acids and flavonoids. Additionally, this formulation could be exploited as a new skin medication delivery system due to its increased antioxidant activity and positive skin biophysical evaluation results (higher stratum corneum water content and lower trans-epidermal water loss). Moringa leaves were substituted for alfalfa hay in a different trial to improve the milk and serum quality of goats[82]. Three diets containing alfalfa alone, 25% Moringa Oleifera leaves, and 25% Moringa peregrine in the diet of goat's fodder were all included in their analysis. Each experiment used ten goats and lasted two weeks to acclimate before collecting data for six weeks. In comparison to an alfalfa-only diet, goats fed with both types of *Moringa* leaves displayed higher fat content that was free from nitrogen extract and total phenols. Additionally, by increasing total antioxidant activity, Vitamin C, catalase activity, and lowering the quantity of thiobarbituric acid reactive substance (TBARS), goats fed *Moringa* have improved the oxidative status of serum and milk[82]. Saleem et al.[83] investigated the in vitro antioxidant activity of several extracts of *Moringa* leaves at doses ranging from 0.1563-5 mg/mL. They discovered that the greatest DPPH activity was present in the methanolic extract at all doses and that all the extracts had radical scavenging activity at a low dosage of 0.1563 mg/mL. Likewise, at a concentration of 1 mg/mL, the methanolic extract displayed the best H_2O_2 scavenging activity (70.56 ± 0.43%) and reducing power (925.48 ± 0.45%). The

methanolic extract has a higher total phenolic content (TPC) and total flavonoid (TFC) than other extracts, which accounts for its high antioxidant activity. Aju et al.[84] looked at the effects of a methanol extract from *Moringa* leaves on the heart of diabetic rats experiencing oxidative stress brought on by streptozotocin. For 60 days, rats were given *Moringa* leaves orally at a dosage of 300 mg/kg body weight. They were divided into six groups: normal control rats (group 1), normal rats treated with *Moringa* leaves (group 2), high-energy diet control rats (group 3), diabetic rats (groups 4 and 5), and diabetic rats treated with metformin and atorvastatin (group 6). According to the authors, rats from groups 3 and 4 had significantly lower activity levels of antioxidant enzymes like catalase (CAT), glutathione (GSH), glutathione peroxidase (GPx), and superoxide dismutase (SOD), whereas rats from group 2, 5 and 6 had significantly higher activity levels of antioxidant enzymes in their hearts. The antioxidant potential of *Moringa* leaves is due to a variety of antioxidant compounds, including hexadonic acid, DL-alpha-tocopherol, and other compounds.

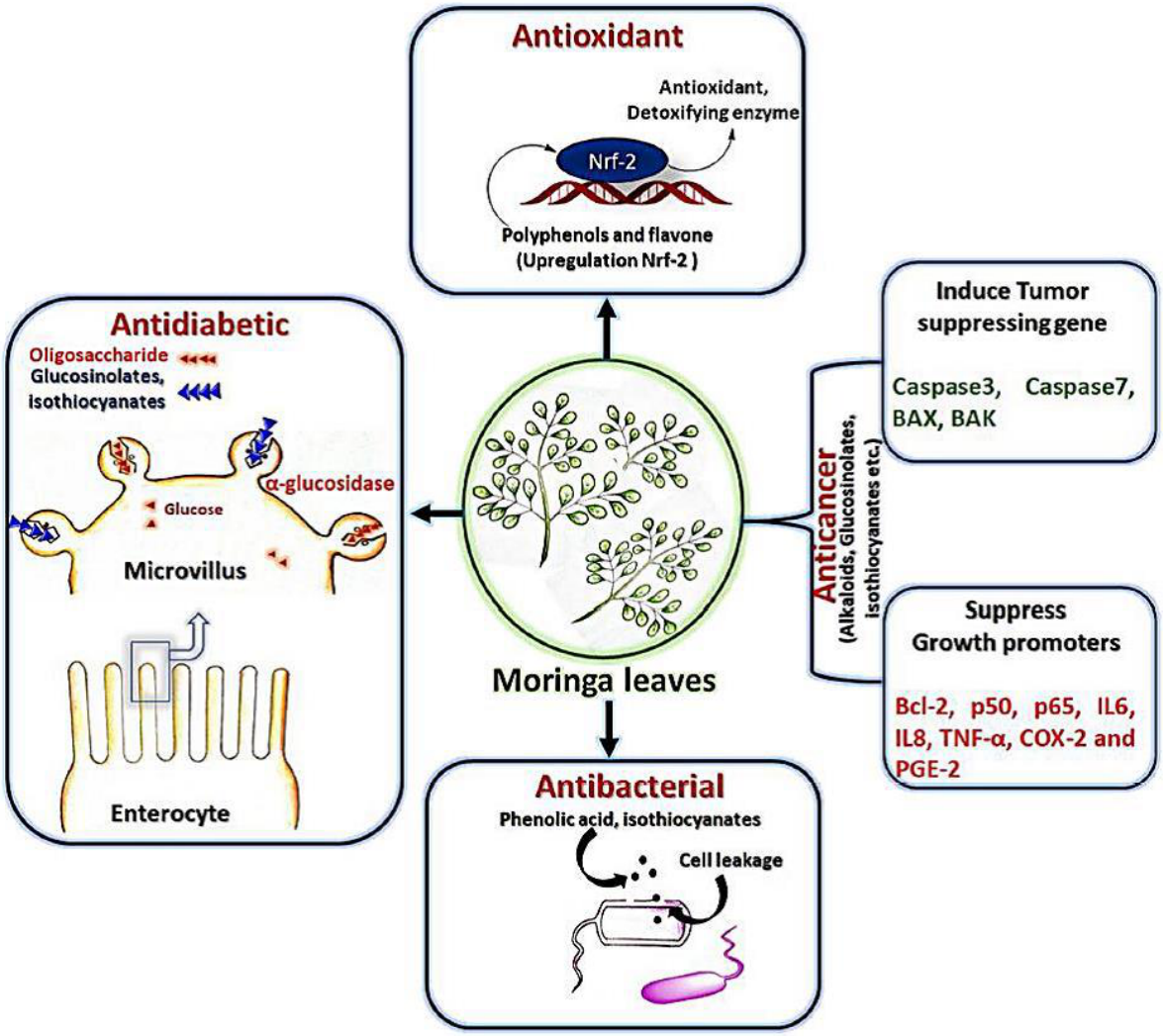

Fig. 5. Pharmacological activities of *Moringa* with the mechanism of action[48]

Antimicrobial Activity

The main issue of the modern era is antibiotic resistance. Due to the widespread use of antibiotics without caution, the majority of infectious organisms have developed a permanent resistance to both chemotherapeutic drugs and antibiotics. Finding novel antibacterial agents with diverse functions is necessary. *Moringa* leaves contain a variety of bioactive substances, and the antibacterial, antifungal, antiviral, and antiparasitic properties of its many preparations have been thoroughly established. However, some studies claim that chemical compounds found in *Moringa* leaves, such as pterygospermin, moringine, and benzyl isothiocyanate, were what caused the plant's antimicrobial effects. Important studies are available on crude extract[47]. Due to the enhanced activity of some apigenin derivatives, which have been found to be most effective against both Gram-positive and Gram-negative bacteria like *Bacillus subtilis, Escherichia coli, and Pseudomonas aeruginosa*, apigenin is thought to be a future green chemical to combat the problem of antibiotic resistance[85]. It was also mentioned as having possible antiviral properties against the HSV-1 and HSV-2 herpes simplex viruses, the hepatitis C virus, the influenza virus, the HFM virus, and the ASFV (African swine fever virus)[85]. There are numerous reports of catechin, epicatechin, Vallin phenols, vicinin-like anthocyanates, and glucosinolate present in *Moringa* leaves. These chemicals are all lipophilic in nature, which may be the cause of the antibacterial activity associated with the leaf extract that has been described in several investigations. The lipophilic nature of phenolic compounds favours their interaction with the cell membrane and other lipophilic cell components, which increases their antibacterial activity[86]. The contact leads to aggregates of cell components and long-lasting alterations to the cytoplasmic membrane, which impairs the function of channels and enzymes. According to reports, phenylpropanoid condensed cell content and tanning cause channels, membrane components, and crucial metabolic enzymes to become disrupted[87-89]. According to Borges et al.,[89] phenolic acids damage the integrity of the cytoplasmic membrane, which in turn causes the breakdown of the osmotic equilibrium and the integrity of the cell by leaking vital intracellular components. It was previously reported by Bouarab-Chibane et al.[90] that plant polyphenols have antibacterial potential against a variety of food pathogens, including *L. monocytogenes* ATCC19115, *B. subtilis* ATCC6633, and *S. aureus* CNRZ3, as well as three Gram-negative ones, *P. aeruginosa* ATCC2785, *S. enteritidis* E0220, and *E. coli* ATCC25. This inhibitory effect might be brought on by the capacity of the polyphenol's to change the outer membrane[91]. The growth of Gram-negative pathogenic bacteria like *S. dysenteriae, E. coli, Klebsiella pneumoniae, Enterobacter sp.,* and *Salmonella sp.* was arrested in several solvent extracts of *Moringa Oleifera,* (Rahaman et al.)[92] and comparable to tetracycline in terms of antistaphylococcal potential[92]. The ethanolic extract was reported to be effective against *Enterococcus faecalis, Vibrio parahaemolyticus*, and *Aeromonas caviae*. Additionally, these isothiocyanates were discovered in *Moringa* leaves[93], and their biological activities, such as antioxidant and antibacterial properties, are well known. *Moringa Oleifera's* glucomoringin and other metabolites have been shown to have anti-inflammatory, antioxidant, antibacterial, antifungal, and antiviral properties[94]. Numerous isothiocyanates demonstrated strong antibacterial activity through a variety of methods, including maintaining membrane integrity and preventing bacterial quorum sensing[95,96]. It has also been noted that the Iberian variety of *Moringa Oleifera* inhibits *S. aureus, P.aeruginosa*, and *E.coli*. The antibacterial potential of particular pure chemicals extracted from *Moringa* leaves needs to be determined. One of the reports indicate the antimicrobial activity of *Moringa* leaf extract in ethanol, water, and chloroform against *Staphylococcus aureus* and six Gram-negative bacteria (*Escherichia coli, Salmonella typhi, Enterobacter aerogenes, Salmonella typhimurium, Shigella spp.*), while no inhibition was seen at any tested concentration, Buker et al.[97] reported this finding. But against Mucor spp. and

Rhizopus spp., the *Moringa* leaf extract showed substantial antifungal ability. The ability of *Moringa* leaf extract to suppress *Candida tropicalis* and *Saccharomyces cerevisiae* at high concentrations was also demonstrated in both aqueous and ethanol forms. *Candida albicans* nevertheless displayed resistance to these extracts.

Aspergillus flavus, Aspergillus fumigates, Aspergillus niger, Cryptococcus neoformans, and *Candida albicans* all showed similar responses to *Moringa* leaf extract[98,99].

Wound Recovering Properties

In male Swiss albino mice, the aqueous extract of *Moringa Oleifera* has the ability to heal wounds. Significant improvements in skin-breaking strength, granuloma-breaking strength, wound healing rate, granuloma dry weight, hydroxyproline content, and scar area reduction were noted[100]. V.I. Hukkeri[101] revealed the antipyretic and wound-healing effects of the ethanolic and ethyl acetate extracts of *Moringa Oleifera* leaves. Ethyl acetate extract of dried leaves exhibits considerable wound healing activity (10% extracts in the form of ointment) on excision, incision, and dead space (granuloma) wound models in rats, whilst ethanolic and ethyl acetate extract of seeds show significant antipyretic action in rats.

Antifertility Activity

Moringa Oleifera root extract was tested for antifertility effects. Pre and post-implantation uterine histoarchitecture of rats has been examined in relation to the action of an aqueous extract[102]. In female reproductive organs of rats, the aqueous extract of *Moringa Oleifera* has an anti-implantation property, while the roots of the plant show antifertility activity. The moist weight of the uterus in rats with bilateral ovariectomies grew gradually after extract administration. This estrogenic activity was kept up by the histo-architecture of the uterus. When the extract was administered along with estradiol dipropionate (EDP), there was a consistent decrease in uterine weight as opposed to the growth with estradiol dipropionate alone[103]. Additionally, the histological configurations of the uterus were suppressed.

Hepato-protective movement

Alaaeldin A. Hamza[104] describes how the treatment of *Moringa Oleifera* seed extract decreased the $CC1_4$ induced rise of serum aminotransferase activity and level of globulin. Treatment with *Moringa Oleifera* also decreased the increases in myeloperoxidase activity and hepatic hydroxyproline levels. The oral treatment of 20% carbon tetrachloride ($CC1_4$) twice a week for six weeks promoted liver fibrosis. The findings of the histological and biochemical tests indicated that *Moringa Oleifera* decreased liver fibrosis and symptoms of liver damage. In the case of an overdose, it is thought that oxidative stress triggers the onset of acetaminophen toxicities[105], Aspartate aminotransferase (AST), alanine aminotransferase (ALT), and alkaline phosphate (ASP) levels, were significantly lower in the group treated with *Moringa Oleifera* than in the group treated with acetaminophen alone, according to histopathological examination. In animals treated with *Moringa Oleifera,* the amount of glutathione (GSH) was found to be recovered. Using male Wistar rats as a protective and curative model, Eshwar Kumar demonstrated the in vitro antioxidant and in-vivo hepatoprotective effects of crude ethanolic extracts of *Moringa Oleifera* seeds. *Moringa Oleifera's* capacity to scavenge superoxide, hydroxyl, and DPPH radicals was tested.

Antihypertensive, diuretic, and cholesterol-lowering properties

This plant is highly helpful in treating cardiovascular problems due to its potent mix of diuretic, lipid, and blood pressure-lowering components. Blood pressure can be stabilized by drinking *Moringa* leaf juice, which

contains thiocarbamate glycosides and mustard oil glycosides that have been isolated from *Moringa* leaves[106,107,108]. The majority of these compounds, which have carbamate, or nitrile groups, are fully acetylated glycosides, which are rare in nature. Four pure chemicals, niazimicin, niazinin A+B, niazinin A, and niazinin B, which exhibit lowering of blood pressure in rats through a calcium antagonist effect, were isolated through bioassay-guided fractionation of the ethanolic extract of *Moringa* leaves. Additional research on the pulp, coat, and seed of whole pods and their component parts-aqueous and ethanol extracts has found that the seed was more effective at lowering blood pressure, with similar outcomes in both water and ethanolic extracts demonstrating that activity is dispersed. Thiocarbamate and isothiocyanate glycosides were isolated from the ethanolic extract of *Moringa Oleifera* pods using activity-directed fractionation, and these compounds are known to be the active ingredients in hypotensive medications. Examined in the pods of *Moringa Oleifera,* methyl hydroxybenzoate and *β*-sitosterol also demonstrated encouraging hypotensive action. It has been discovered that the aqueous seed extract, flowers, leaves, roots, gum, and seeds of *Moringa* all have diuretic properties. These diuretic components may complement in lowering blood pressure. The presence of a bioactive phytoconstituent called *β*-sitosterol in the crude extract of *Moringa* leaves is likely to causes it to lower cholesterol in the serum of rats fed a high-fat diet[109]. In hypercholesteremic rabbits, *Moringa* fruit has been shown to lower serum cholesterol, low-density lipoprotein (LDL), phospholipids, triglycerides, very low-density lipoprotein (VLDL) cholesterol to phospholipid ratio, atherogenic index lipid, and affect the secretion of fecal cholesterol[110].

Moringa against Coronavirus Infections

Surprisingly, experts recommended employing a large dosage of bitter and cold herbs to clear heat and detoxify the infectivity in its early beginning, as well as middle and late stages[111] in the light of the novel universal and remarkable circumstances surrounding the coronavirus. The leaves of the *Moringa oleifera* plant have a sweet and bitter flavor as well as a cooling, ventilating, and dehumidifying effect. As a result, it makes for an excellent treatment option for the profound overall immunological abnormalities of diseases. It is possible to imagine a sufficient and supportive therapy for coronavirus infection when combined with conventional medicine. Some of the *Moringa oleifera* constituents that function include kaempferol, pterygospermin, morphine, quercetin, and apigenin. The most effective anti-SARS agent against MPro-Cov-2 is apigenin[112]. In contrast to the well-known SARS-CoV-2 MPro inhibitor baicalein, three flavonoids-isorhamnetin, kaempferol, and apigenin demonstrated good binding empathy stable protein-ligand complexes with high binding energy and similar binding poses[113]. Rutin and isorhamnetin-3-O-rutinoside from the *Moringa oleifera* plant are powerful inhibitors of the SARS-CoV-2 designated target major protease (MPro), according to a dynamic study that was confirmed by in vitro and in vivo research[114].

Safety Studies

All of the up-to-date human investigations, which will be covered in more detail later in the text, have not revealed any negative consequences. Additionally, a variety of formulations have been utilized as both foods and medicines all throughout the world without any negative side effects being reported. Specific assessments of the possible toxicity of various formulations of *Moringa oleifera* have been made in several animal experiments. The security of an oral administration of an aqueous leaf extract to rats at doses of 400, 800, 1600, and 2000 mg/kg body weight was investigated[115]. With the exception of the highest dose, the medication was either administered as an acute single dose or every day for 21 days. A number of factors were evaluated, including serum enzyme levels and blood cell counts. Scientists came to the conclusion that up to 2000 mg/kg of *Moringa oleifera* leaves might be safely consumed. Over the course of the study of 21 days, the body weights of the rats decreased in a dose-dependent manner. In

various experimental conditions, Asare et al.[116] investigated the possible toxicity of aqueous *Moringa oleifera* leaf extract. In one series of investigations, the cytotoxicity of the extract at various concentrations was tested on human peripheral blood mononuclear cells. Cytotoxicity was seen at a dosage of 20 mg/kg, which is insufficient for oral intake. In a further series of tests, rats received extract doses of 1000 and 3000 mg/kg and the animals underwent testing for as long as 14 days. Based on blood cell research, the *Moringa oleifera* leaf extract was proven to be genotoxic at a dose of 3000 mg/kg, which is still higher than most regularly used doses. Given to rats at a dose of 1000 mg/kg, which is still higher than most regularly used levels, it was determined to be safe and did not cause genotoxicity. Ambi et al.[117] fed 24 rats in four groups 25%, 50%, 75%, and control levels of *Moringa oleifera* powdered leaves along with regular livestock feed for 93 days. It is unknown how many *Moringa oleifera* leaves were ingested in total. After the experiment, the treated animals' organs had microscopic lesions that could be seen, while the 75% group exhibited necrosis of the liver cells, splenic blood vessels, and neural glial cells. In every organ inspected, the control animals lacked detectable microscopic abnormalities. No tissue photomicrographs were offered. Although the authors did not quantify the amounts of leaves consumed, they were far greater than the doses that would typically be used in either rats or humans. For instance, even at the modest dose of 25% of the chow, if the rats consumed an average of 15-20g of chow daily, the daily dose for an adult rat would be roughly 15-20g of leaves per kilogram, which is equivalent to 195-260g for an 80 kg human. Mice have also been used to test the toxicity of an aqueous extract of *Moringa oleifera* leaves[118]. Mice were given the extract in an acute trial at doses of up to 6400 mg/kg orally and 1500 mg/kg intraperitoneally. Mice were given oral doses of 250, 500, and 1500 mg/kg for 60 days in a subchronic study. The lethal dose of 50% LD50 was estimated to be 1585 mg/kg. No significant effects were observed with respect to hematological or biochemical parameters or sperm quality. A high degree of safety was observed during oral administration. The toxicological effects associated with the consumption of 50, 100, 200, or 400 mg/kg of methanol extract of *Moringa oleifera* for 8 weeks were performed in 30 rats[119]. The extract was a 30:1 concentration. All experimental animals that received *Moringa oleifera* had a significant increase in body weight in a dose-dependent manner, contrary to what is observed with an aqueous extract[115]. A substantial rise in serum levels of alanine aminotransferase, aspartate aminotransferase, blood urea nitrogen, and creatinine was observed in rats given *Moringa oleifera* at 200 and 400 mg/kg. It should be noted that methanol, not water, was used to create the extract. At a dose of 400 mg/kg, the 30:1 concentration of methanol extract would be equivalent to 12 g of leaves per kilogram, which is a very improbable dose. It is unclear how the composition of the methanol extract compares with that of commonly used aqueous extracts. According to Bakre et al.[120], mice required more than 6.4 g/kg of an oral ethanol extract of *Moringa oleifera* leaves to be fatal. Zvinorova et al.[121] studied the dietary benefits of *Moringa oleifera* leaves as a dietary supplement for liver function. The diets of normal rat feed fed at 20% and 14% of body mass or feed supplemented with *Moringa oleifera* fed at 20% and 14% of body mass were given to 32 weanling rats at random for 5 weeks. Supplementing with *Moringa oleifera* had no effect on the levels of blood metabolites, liver glycogen, or lipid storage. Rats were subjected to oral dosages of up to 1000mg /kg of an aqueous *Moringa oleifera* extract for 14 days and a single oral dose of 5000mg/kg of the extract, to determine any potential toxicological effects[122]. The authors reported that neither histological nor overt adverse effects were seen at these levels. Numerous liver enzymes showed small but statistically significant dose-dependent increases. A typical 400 mg dose of an aqueous extract in an 80 kg human is more than 30 times as powerful as a dose of 1000 mg/kg in rats. Three different assay techniques, including the Ames assay, were used to determine the

genotoxicity of an aqueous *Moringa oleifera* seed extract[123]. Without metabolic activity, the seed extract was not genotoxic and did not endanger human health. A hexane extract of *Moringa oleifera* leaves was tested for its impact on male rats' reproductive systems[124]. For 21 days, the extract was administered orally at dosages of 17,170 and 1700 mg/kg body weight. Without affecting plasma gonadotropin levels, a dose-dependent rise in testis and epididymis weights, seminiferous tubule diameter, and epididymal epithelium thickness was seen. The authors concluded that spermatogenesis had increased as a result of the alterations. Several investigations on *Moringa oleifera* seeds and roots can be presented for the sake of completeness, even if the findings cannot be directly compared to or equated with those of studies on leaves. Arajo et al. assessed the cytotoxicity of an aqueous extract of *Moringa oleifera* seeds[125]. After 14 days of extract administration to mice (at doses of 500 and 2000mg/kg), no symptoms of systemic toxicity were seen, and every animal survived. Between the treatment and control groups, there were no differences in organ indices. Erythrocytes, platelets, hemoglobin, and hematocrit all underwent minor but not appreciable modifications. Every value was within the acceptable range. Acute and subacute toxicity tests of rats were conducted using a methanol extract of *Moringa oleifera* seeds that had been phytochemically tested for chemical components[126]. Saponins, tannins, terpenes, flavonoids, carbohydrates, and cardiac glycosides were all found during the phytochemical screening, however, anthraquinones were not seen. Mortality was documented at a dose of 5000 mg/kg of the extract, even though indications of acute toxicity were visible at a dose of 4000 mg/kg. At dosages less than 3000 mg/kg, no unfavorable effects were noticed. The authors came to the conclusion that methanol extracts of *M. Oleifera* are suitable for use in food. Paul and Didia[127] looked into the outcome of methanol extract of *M. Oleifera* root on the liver and renal histoarchitecture of 24 guinea pigs. Daily intraperitoneal injections of the root extract at doses of 3.6, 4.6, and 7.0 mg/kg were used during the experiment, along with a control group, for three weeks. All treated groups' histological sections showed ballooning liver deterioration, which suggests time-dependent hepatotoxicity rather than a dose-dependent reaction. In the 4.6 mg/kg group, examination of the kidneys revealed little tubular damage and interstitial inflammation, whereas, in the 7.0 mg/kg group, the interstitium had been invaded by inflammatory cells and amorphous eosinophilic debris. Regarding the composition or level of concentration of the extract, nothing was reported. Studies using aqueous leaf extracts cannot be compared to or be comparable with the findings of this study. This study used an intraperitoneally administered, methanol-based root extract. In conclusion, numerous preparations of *M. Oleifera* have been shown to be effective in human, animal, and in vitro research, as well as the extrapolation of results from animal studies to humans. *M. Oleifera* leaves, including their aqueous extracts, seem to be incredibly safe at the dosages and quantities frequently used for thirty postmenopausal females. The results showed significant decreases in malondialdehyde (16.3%; lipid peroxidation), and increases in serum glutathione peroxidase (18.0%), superoxide dismutase (10.4%), and ascorbic acid (44.4%), markers of antioxidant capabilities. Additionally, it was shown that hemoglobin levels increased (17.5%), and fasting blood glucose levels decreased significantly (13.5%). There were no negative consequences noted. In conclusion, previous studies on humans have shown that whole-leaf powders of *M. Oleifera* administered orally have significant anti-hyperglycemic, anti-dyslipidemic, and antioxidant effects in human subjects without producing any negative effects. Leaf extracts weren't used in any of these studies.

Conclusions

A lot of work is currently being done to identify, classify and understand the activities of the proteins found in *Moringa oleifera.* The qualities of the plant *Moringa oleifera* are constantly being studied. *Moringa oleifera*

should therefore be thoroughly researched in order to better understand the action mechanisms. With a better understanding, *Moringa oleifera* can be used effectively in a variety of fortified nutraceutical and health-improving products. The use of *Moringa* as a natural complement to drugs may encourage the development of new drugs. By combining synthetic drug use with *Moringa*, the negative effects could be reduced. However, thorough risk assessment studies must be conducted to guarantee the security of the medications and items produced using *Moringa*. *Moringa oleifera* products' dietary consumption could be planned based on insightful analysis and some legal safety regulations.

References

1. Shawai S. and Singh, R., 2016, Phytochemical screening, antioxidant and antimicrobial activity of Moringa Oleifera leaf extract, **5**, 778–785.

2. Patel, P., Patel, N., Patel, D., Desai, S. and Meshram, D., 2014, Phytochemical analysis and antifungal activity of Moringa Oleifera, *Int. J. Pharm. Pharm. Sci.*, **6(5)**, 144–147.

3. Isitua, C. C., Ibeh, I. N. and Olayinka, J. N., 2016, Antibacterial Activity of Moringa oleifera Lam Leaves on Enteric Human Pathogens, *Indian J. Appl. Res.*, **6(8)**, 553–557.

4. https://news.ncbs.res.in/research/genomics-uncovers-mystery-magic-drumstick-tree-moringa-oleifera.

5. Singh K.K., Kumar K., 1999, Ethnotherapeutics of some medicinal plants used as antipyretic agent among the tribals of India. *Journal of Economic and Taxonomic Botany*, **23**, 135–141.

6. Morimitsu Y, Hayashi K, Nakagama Y, Horio F, Uchida K. and Osawa T., 2000, Antiplatelet and anticancer isothiocyanates in Japanese horseradish, wasabi BioFactors, **13**, 271-276.

7. Siddhuraju P. and Becker K., 2003, Antioxidant properties of various solvent extracts of total phenolic constituents from three different agroclimatic origins of drumstick tree (*Moringa oleifera* Lam). *Journal of Agriculture and Food Chemistry*, **15**, 2144-2155.

8. Dillard C.J. and German J.B., 2000, Phytochemicals: nutraceuticals and human health: A review. *Journal of the Science of Food and Agriculture*, **80**, 1744–1756.

9. Olugbemi T.S., Mutayoba S.K. and Lekule F.P., 2010, Effect of Moringa (*Moringa oleifera*) inclusion in Cassa based diets fed to broiler chickens. *International Journal of Poultry Science*, **9,** 363-367.

10. Abou-Elezz FMK, Sarmiento-Franco L, Santos-Ricalde R. and Solorio-Sanchez F., 2011, Healthful impacts of dietary consideration of Leucaena leucocephala and *Moringa oleifera* leaf meal on Rhode Island Red hens performance. Cuban *Journal of Agricultural Science*, **45**, 163-169.

11. Eilert U, Wolters B. and Nahrsted A., 1981, The antibiotic principle of seeds of *M. oleifera and M. stenopetala. Planta Medica*, **42B**, 55-61.

12. Buddy S.K., Mukherjee P.K. and Saha B.P., 1995, Contemplates on the antiulcer movement of *Moringa oleifera* leaf remove on gastric ulcer models in rats. *Phytother Res*., **9,** 463–465.

13. Biswas K. and Ghosh A., 1950, Bharatiya banousdhi (Bengali). Calcutta University, Kolkata, India. **1**.

14. Shukla S., Mathur R. and Prakash A.O., 1981, Effects of aqueous extract of *M. oleifera* Lam, on the periodicity of estrous cycle in adult intact rats. *Indian Journal of Pharmaceutical Science*, **49(6)**, 219-219.

15. Karadi R.V., Gadgeb N.B., Alagawadi K.R. and Savadi R.V., 2006, Effect of *Moringa oleifera* Lam. root-wood on ethylene glycol induced urolithiasis in rats. *Journal of Ethnopharmacology*, **105**, 306–311.

16. Foidl N., Makkar HPS. and Becker K., 2001, The Potential of *Moringa oleifera* for Agricultural and industrial uses. What development potential for Moringa products.

17. Morton J.F., 1991, The horseradish tree, *Moringa pterygosperma* (Moringaceae): A boon to arid lands? *Economics Botany*, **45**, 318-333.

18. Shaik Naseer Pasha, et al., Genomics, https://doi.org/10.1016/j.ygeno.2019.04.014

19. Kasolo, J.N., Bimenya, G.S., Ojok, L., Ochieng, J. and Ogwal-okeng, J.W., 2010, Phytochemicals and uses of *Moringa oleifera* leaves in Ugandan rural communities, *J. Med. Plants Res.* **4**, 753–757.

20. Mbikay, M., 2012, Therapeutic potential of *Moringa oleifera* leaves in chronic hyperglycemia and dyslipidemia: A review, *Front. Pharmacol*. **3**, 1–12.

21. Berkovich, L., Earon, G., Ron, I., Rimmon, A., Vexler, A. and S. Lev-Ari, 2013, *Moringa Oleifera* aqueous leaf extract down-regulates nuclear factor-kappaB and increases cytotoxic effect of chemotherapy in pancreatic cancer cells., BMC Complement. *Altern. Med.,* **13**, 212-219.

22. Oduro, I., Ellis, W.O. and Owusu, D., 2008, Nutritional potential of two leafy vegetables: *Moringa oleifera* and *Ipomoea batatas* leaves, *Sci. Res. Essay*., **3,** 57–60.

23. Oduro, I., Ellis, W.O. and Owusu, D., 2008, Nutritional potential of two leafy vegetables: *Moringa oleifera* and *Ipomoea batatas* leaves. *Sci. Res. Essays*., **3**, 57-60.

24. Sánchez-Machado, D.I., Núñez-Gastélum, J.A., Reyes-Moreno, C., Ramírez-Wong, B., 2010, J. López-Cervantes, Nutritional quality of edible parts of *Moringa oleifera*, *Food Anal. Methods*., **3**, 175–180.

25. Fuglie, L.J., 2005, THE MORINGA TREE A local solution to malnutrition Church World Service in Senegal.

26. Barminas, J.T., Charles, M. and Emmanuel, D., 1998, Mineral composition of non-conventional leafy vegetables, *Plant Foods Hum. Nutr.,* **53**, 29–36.

27. Lalas, S. and Tsaknis, J., 2002, Characterization of *Moringa oleifera* seed oil variety Periyakulam- 1, *J. Food Compos. Anal*., **15**, 65–77.

28. Yang, R., Chang, L., Hsu, J., Weng, B.B.C., Palada, C., Chadha, M.L. and V. Levasseur, 2006, Nutritional and functional properties of moringa leaves from germplasm, to Plant, to food, to health, American Chemical Society, p.1-17.

29. Moyo, B., Masika, P., Hugo, A. and Muchenje, V., 2011, Nutritional characterization of Moringa (*Moringa oleifera* Lam.) leaves, *African J. Biotechnol*. **10**, 12925–12933.

30. Fuglie, L.J., 2005, THE MORINGA TREE A local solution to malnutrition Church World Service in Senegal.

31. Olagbemide, P.T. and Alikwe P.C., 2014, Proximate Analysis and Chemical Composition of Raw and Defatted *Moringa oleifera* Kernel, *Advances in Life Science and Technology*., **24**, 92-99.

32. Moringa Leaf Powder: A nutritional analysis of leaf powder. http://www..co.za/analysis.html moringaleafpowder

33. Gopalakrishnan, L., Doriya, K., Kumar, D.S., 2016, Moringa Oleifera: A Review on Nutritive Importance and its Medicinal Application, *Food Science and Human Wellness*, http://dx.doi.org/10.1016/j.fshw.2016.04.001

34. Fahey J.W., Zalcmann A.T. and Talalay P., 2001, The Chemical diversity and distribution of

glucosinolates and isothiocyanates among plants. *Phytochemistry*, **56**, 5–51.

35. Bennett, R.N., Mellon F.A. and Foidl, N., 2003, Profiling glucosinolates and phenolics in vegetative and reproductive tissues of the multi-purpose trees *Moringa oleifera* L. (Horseradish tree) and Moringa stenopetala L. *J. Agric Food Chem*, **51**, 3546–3553.

36. Kerharo P.J., 1969, Un remede populaire Sengalais: Le „Nebreday (*Moringa oleifera* lam.) employs therapeutiques en milieu Africain chimie et pharmacologie. *Plantes Med Phytother*, **3**, 14–219.

37. Bhattacharya S.B., Das A.K. and Banerji N., 1982, Chemical investigations on the gum exudates from Sonja (*Moringa oleifera*). *Carbohydras Res*., **102**, 253–262.

38. Faizi S, Siddiqui B, Saleem R, Saddiqui S. and Aftab K., 1994, Isolation and structure elucidation of new nitrile and mustard oil glycosides from *Moringa oleifera* and their effect on blood pressure. *J Nat Prod*, **57**, 1256–1261.

39. Ruckmani, K., Kavimani, S., Anandan, R. and Jaykar, B., 1998, Effect of *Moringa oleifera* Lam on paracetamol-induced hepatoxicity. *Indian J. Pharm. Sci*., **60**, 33–35.

40. Faizi S, Siddiqui B.S., Saleem R, Aftab K, Shaheen F. and Gilani A.H., 1998, Hypotensive constituents from the pods of *Moringa oleifera*. *Planta Med*., **64**, 225–228.

41. Nagar P.K., Iyer R.I. and Sircar P.K., 1992, Cytokinins in developing fruits of *Moringa pterigosperma* Gaertn. *Physiol Plant*, **55**, 45–50.

42. Bose B., 1980, Enhancement of nodulation of Vigna mungo by ethanolic extract of Moringa leaves – a new report. *Nat Acad Sci Lett.*, **3**, 103–104.

43. Anwar F., Ashraf M, and Bhanger M.I., 2005, Interprovenance variation in the composition of *Moringa oleifera* oilseeds from Pakistan. *J. Am Oil Chem. Soc*., **82**, 45–51.

44. Makkar HPS. and Becker K., 1996, Nutritional value and antinutritional components of whole and ethanol extracted *Moringa oleifera* leaves. *Anim Feed Sci. Technol*., **63**, 211–228.

45. Tsaknis J., Lalas S., Gergis V., Dourtoglou V. and Spiliotis V., 1999, Characterization of *Moringa oleifera* variety Mbololo seed oil of Kenya. *J. Agric Food Chem.,* **47**, 4495–4499.

46. Anwar F. and Bhanger M.I., 2003, Analytical charactarization of *Moringa oleifera* seed oil developed in temperate region of Pakistan. *J. Agric Nourishment Chem.,* **51**, 6558–6563.

47. Rossell J.B., 1991, Vegetable oil and fats. In Analysis of Oilseeds, Fats and Fatty Foods, Rossell JB, Pritchard JLR (eds). Elsevier Applied Science: New York, p.261–319.

48. Patil V., Satish, Mohite.V. Bhavana, Marathe. R. and Kiran et. al., 2022, Moringa Tree, Gift of Nature: a Review on Nutritional and Industrial Potential. *Current Pharmacology Reports*, **8**, 262–280.

49. Cerf, M.E., 2013, Beta cell dysfunction and insulin resistance, *Front. Endocrino*., **4**, 1–12.

50. Divi, S.M., Bellamkonda, R. and Dasireddy, S.K., 2012, Evaluation of antidiabetic and antihyperlipedemic potential of aqueous extract of *Moringa oleifera* in fructose fed insulin resistant and STZ induced diabetic wistar rats: A comparative study, *Asian J. Pharm. Clin. Res.* **5**, 67–72.

51. Al-Malki, A.L. and El Rabey, H.A., 2015, The Antidiabetic Effect of Low Doses of *Moringa oleifera* Lam. seeds on streptozotocin induced diabetes and diabetic nephropathy in male rats, *BioMed Res Int*., **2015**, 1-13.

52. Wright, E., Scism-Bacon, J.L. and Glass, L.C., 2006, Oxidative stress in type 2 diabetes: the role of fasting and postprandial glycaemia, *Int. J. Clin. Pract*., **60**, 308–314.

53. Kaneto, H., Kajimoto, Y., Miyagawa, J., Matsuoka, T., Fujitani, Y., Umayahara, Y., Hanafusa, T., Matsuzawa, Y., Yamasaki Y. and Hori, M., 1999, Beneficial Effects of Antioxidants in Diabetes: possible protection of pancreatic â-cells against glucose toxicity, *Diabetes.*, **48,** 2398-2406.

54. Prentki, M. and Nolan, C.J., 2006, Islet â cell failure in type 2 diabetes, *J. Clin. Invest*., **116**, 1802–1812.

55. Kamalakkannan, N. and Prince, P.S.M., 2006, Antihyperglycaemic and antioxidant effect of rutin, a polyphenolic flavonoid, in streptozotocin-induced diabetic wistar rats, *Basic Clin. Pharmacol. Toxicol*., **98,** 97–103.

56. Aronson, D. and Rayfield, E.J. 2002, How hyperglycemia promotes atherosclerosis: molecular mechanisms, *Cardiovasc. Diabetol*., **1**, 1.

57. Chumark, P., Khunawat, P., Sanvarinda, Y., Phornchirasilp, S., Morales, N.P., Phivthong-ngam, L., Ratanchamnong, P., Srisawat, S. and Pongrapeeporn, K.U., 2008, The *in vitro* and *ex vivo* antioxidant properties, hypolipidaemic and antiatherosclerotic activities of water extract of *Moringa oleifera* Lam. leaves, *J. Ethnopharmacol.* **116,** 439–446.

58. Vergara-Jimenez, M., Almatrafi, M.M. and Fernandez, M.L., 2017, Bioactive components in Moringa oleifera leaves protect against chronic disease, *Antioxidants,* **6**, 1–13.

59. Khalafalla, M.M., Abdellatef, E., Dafalla, H.M., Nassrallah, A., Aboul-Enein, K.M., Lightfoot, D.A., El-Deeb, F.E. and El-Shemyet, H.A., 2010, Active principle from Moringa oleifera Lam leaves effective against two leukemias and a hepatocarcinoma, Afr. *J. Biotechnol*. **9**, 8467–8471.

60. Berkovich, L., Earon, G., Ron, I., Rimmon, A., Vexler, A. and Lev-Ari, S., 2013, Moringa oleifera aqueous leaf extract down-regulates nuclear factor-kB and increases cytotoxic effect of chemotherapy in pancreatic cancer cells, *BMC Complement. Altern. Med*., **13**, 1–7.

61. Sadek, K.M., Abouzed, T.K., Abouelkhair, R. and Nasr, S., 2017, The chemo-prophylactic efficacy of an ethanol Moringa oleifera leaf extract against hepatocellular carcinoma in rats, *Pharm. Biol.,* **55,** 1458–1466.

62. Madi, N., Dany, M., Abdoun, S. and Usta, J., 2016, Moringa oleifera's nutritious aqueous leaf extract has anticancerous effects by compromising mitochondrial viability in an ROS-dependent manner, *J. Am. Coll. Nutr.,* **35**, 604–613.

63. Tiloke, C., Phulukdaree, A. and Chuturgoon, A.A., 2016, The antiproliferative effect of Moringa oleifera crude aqueous leaf extract on human esophageal cancer cells, *J. Med. Food*. **19**, 398–403.

64. Guon, T.E. and Chung, H.S., 2017, Moringa oleifera fruit induce apoptosis via reactive oxygen species-dependent activation of mitogen-activated protein kinases in human melanoma A2058 cells, *Oncol. Lett*., **14**, 1703–1710.

65. Karim, N.A.A., Ibrahim, M.D., Kntayya, S.B., Rukayadi, Y., Hamid, H.A., Razis and A.F.A., 2016, Moringa oleifera Lam: targeting chemoprevention, *Asian Pac. J. Cancer Prev.* **17**, 3675–3686.

66. Al-Asmari, A.K., Albalawi, S.M., Athar, M.T., Khan, A.Q., Al-Shahrani, H. and Islam, M., 2015, Moringa oleifera as an anti-cancer agent against breast and colorectal cancer cell lines, *PLoS One*, **10**, 1–14.

67. Charlette, T., Krishnan, A., Robert, G.M. and Anil,

C.A., 2018, Moringa oleifera and their phytonanoparticles: Potential antiproliferative agents against cancer. *Biomedicine & Pharmacotherapy*, **108**, 457–466.

68. Gönenç, A., Hacý¸ sevki, A., Tavil, Y., Çengel, A., Torun, M., 2013, Oxidative Stress in Patients with Essential Hypertension: A Comparison of Dippers and Non-Dippers. *Eur. J. Intern. Med*., **24**, 139–144. [CrossRef] [PubMed]

69. Kashyap, P., Anand, S. and Thakur, A., 2017, Evaluation of Antioxidant and Antimicrobial Activity of Rhododendron Arboreum Flowers Extract. *Int. J. Food Ferment. Technol*. **7**, 123–128. [CrossRef]

70. Wang, Y., Gao, Y., Ding, H., Liu, S., Han, X., Gui, J. and Liu, D., 2017, Subcritical Ethanol Extraction of Flavonoids from Moringa oleifera Leaf and Evaluation of Antioxidant Activity. *Food Chem*., **218**, 152–158. [CrossRef]

71. Mahajan, S.G. and Mehta, A.A., 2007, Inhibitory Action of Ethanolic Extract of Seeds of Moringa oleifera Lam. on Systemic and Local Anaphylaxis. *J. Immunotoxicol*., **4**, 287–294. [CrossRef] [PubMed]

72. Bajpai, M., Pande, A., Tewari, S.K. and Prakash, D., 2005, Phenolic Contents and Antioxidant Activity of Some Food and Medicinal Plants. *Int. J. Food Sci. Nutr.,* 5**6**, 287–291. [CrossRef] [PubMed]

73. Atawodi, S.E., Atawodi, J.C., Idakwo, G.A., Pfundstein, B., Haubner, R., Wurtele, G., Bartsch, H. and Owen, R.W., 2010, Evaluation of the Polyphenol Content and Antioxidant Properties of Methanol Extracts of the Leaves, Stem, and Root Barks of Moringa oleifera Lam. *J. Med. Food.,* **13**, 710–716. [CrossRef] [PubMed]

74. Charoensin, S., 2014, Antioxidant and Anticancer Activities of Moringa oleifera Leaves. *J. Med. Plants Res.,* **8,** 318–325.

75. Rakesh, S. and Singh, V.J., 2011, Anti-Inflammatory Activity of Moringa oleifera Leaf and Pod Extracts against Carrageenan Induced Paw Edema in Albino Mice. *J. Pharm. Sci. Innov*., **1**, 22–24.

76. Sreelatha, S. and Padma, P.R., 2011, Modulatory Effects of Moringa oleifera Extracts against Hydrogen Peroxide-Induced Cytotoxicity and Oxidative Damage, *Hum. Exp. Toxicol*., **30**, 1359–1368. [CrossRef]

77. Patel, S., Thakur, A.S., Chandy, A. and Manigauha, A., 2010, Moringa Leifera: A Review of the Medicinal and Economic Importance to the Health and Nation, *Drug Invent Today*, **2**, 339–342.

78. Fombang, E.N., Saa, W.R., 2016, Production of a Functional Tea from Moringa oleifera LAM Leaf Powder: Optimization of Phenolic Extraction Using Response Surface Methodology. *J. Nutr. Food Sci*., **6**, 556.

79. Khalofah, A., Bokhari, N.A., Migdadi, H.M. and Alwahibi, M.S., 2020, Antioxidant Responses and the Role of Moringa oleifera Leaf Extract for Mitigation of Cadmium Stressed Lepidium sativum L. S. *Afr. J. Bot*., **129**, 341–346.

80. Gouda, A.S., El-Nabarawy, N.A. and Ibrahim, S.F., 2018, Moringa oleifera Extract (Lam) Attenuates Aluminium Phosphide-Induced Acute Cardiac Toxicity in Rats. *Toxicol. Rep*., **5,** 209–212. [CrossRef] [PubMed]

81. Álvarez-Román, R., Silva-Flores, P.G., Galindo-Rodríguez, S.A., Huerta-Heredia, A.A., Vilegas, W., Paniagua-Vega, 2020, D. Moisturizing and Antioxidant Evaluation of Moringa oleifera Leaf Extract in Topical Formulations by Biophysical Techniques. *S. Afr. J. Bot.,* **129**, 404–411. [CrossRef]

82. Al-Juhaimi, F.Y., Alsawmahi, O.N., Abdoun, K.A., Ghafoor, K. and Babiker, E.E., 2020, Antioxidant Potential of Moringa Leaves for Improvement of

Milk and Serum Quality of Aardi Goats. *S. Afr. J. Bot*., **129**, 134–137. [CrossRef]

83. Saleem, A., Saleem, M. and Akhtar, M.F., 2020, Antioxidant, Anti-Inflammatory and Antiarthritic Potential of Moringa oleifera Lam: An Ethnomedicinal Plant of Moringaceae Family. *S. Afr. J. Bot*., **128**, 246–256. [CrossRef]

84. Aju, B.Y., Rajalakshmi, R. and Mini, S., 2019, Protective Role of Moringa oleifera Leaf Extract on Cardiac Antioxidant Status and Lipid Peroxidation in Streptozotocin Induced Diabetic Rats. *Heliyon*, **5**, e02935. [CrossRef] [PubMed]

85. Liu R., Zhang H., Yuan M., Zhou J., Tu Q., Liu J.J. and Wang J., 2013, Synthesis and biological evaluation of apigenin derivatives as antibacterial and antiproliferative agents. *Molecules*., 2013, **18(9)**, 11496–511.

86. Sikkema J. and de Bont J.A., 1995, Poolman B. Mechanisms of membrane toxicity of hydrocarbons. *Microbiol Rev*., **59(2)**, 201–22.

87. Ya C, Gaffney SH, Lilley TH and Haslam E., 1988, Carbohydrate polyphenol complexation. in Chemistry and Significance of Condensed Tannins, eds Hemingway RW, Karchesy JJ. New York, NY: Plenum Press, p.553.

88. Chung KT, Lu Z. and Chou MW, 1998, Mechanism of inhibition of tannic acid and related compounds on the growth of intestinal bacteria. *Food Chem. Toxicol.,* **36(12)**, 1053–60.

89. Borges A., Ferreira C., Saavedra MJ. and Simoes M., 2013, Antibacterial activity and mode of action of ferulic and gallic acids against pathogenic bacteria. *Microb Drug Resist*., **19(4)**, 256–65.

90. Bouarab-Chibane L, Forquet V, Lanteri P, Clement Y, Leonard- Akkari L, Oulahal N, Degraeve P, and Bordes C., 2019, Antibacterial properties of polyphenols: characterization and QSAR (Quantitative structure–activity relationship) models. *Front Microbial*., **18(10)**, 829.

91. La Storia A, Ercolini D, Marinello F, Di Pasqua R, Villani F. and Mauriello G., 2011, Atomic force microscopy analysis shows surface structure changes in carvacrol-treated bacterial cells. *Res. Microbiol*., **162(2)**, 164–72.

92. Rahman, M. and Mashiar, et al., 2009, Antibacterial activity of leaf juice and extracts of Moringa oleifera Lam. against some humanpathogenic bacteria. *CMU J. Nat. Sci*., **8(2)**, 219.

93. Tripoli E., La Guardia M., Giammanco S., Di Majo D. and Giammanco M., 2007, Citrus flavonoids: Molecular structure, biological activity and nutritional properties: a review. *Food Chem*., **104(2),** 466–79.

94. Giacoppo S., Rajan T.S., Iori R., Rollin P., Bramanti P. and Mazzon E., 2017, The á-cyclodextrin complex of the Moringa isothiocyanate suppresses lipopolysaccharide-induced inflammation in RAW 2647 macrophage cells through Akt and p38 inhibition. *Inflamm Res*. **66(6)**, 487–503.

95. Ganin H., Rayo J., Amara N., Levy N., Krief P. and Meijler MM., 2013, Sulforaphane and erucin, natural isothiocyanates from broccoli, inhibit bacterial quorum sensing. *Med Chem. Comm*., **4(1)**, 175–9.

96. Dias C., Aires A., Bennett R.N., Rosa EAS. and Saavedra M.J., 2012, First study on antimicriobial activity and synergy between isothiocyanates and antibiotics against selected Gram-negative and Grampositive pathogenic bacteria from clinical and animal source. *Med Chem*., **8(3)**, 474 80.

97. Bukar A,, Uba A. and Oyeyi T., 2010, Antimicrobial profile of *Moringa oleifera* Lam. extracts against some food–borne microorganisms. bayero *J. Pure Appl Sci.,* **3(1)**.

98. Isitua C.C., Ibeh I.N. and Olayinka J.N., 2016, In vitro Antifungal Activity of *Moringa oleifera* Lam Leaf on some selected clinical fungal strains. *Indian J. Appl. Res*., **6(8)**.

99. Patel P., Patel N., Patel D., Desai S., Meshram D., Phytochemical analysis and antifungal activity of *Moringa oleifera*., *Int. J. Pharm. Pharm Sci*., **6(5)**, 144–7.

100. Rathi B.S., Bodhankar S.L. and Baheti AM., 2006, *Indian Journal of Experimental Biology*, **44**, 898-901.

101. Hukkeri V.I., Nagathan C.V., Karadi R.V. and Patil B.S., 2006, *Indian J Pharm Sci*., **68**, 124-126.

102. Prakash A.O., Pathak S., Shukla S. and Mathur R., 1987, *Acta Eur Fertil*., **18(2)**, 129-135.

103. Shukla S., Mathur R. and Prakash A.O., 1998, *Acta Eur Fertil*, **19(4)**, 225-232.

104. Hamza Alaaeldin., 2010, Ameliorative effects of *Moringa oleifera* Lam seed extract on liver fibrosis in rats, *Food and Chemical Technology*, **48**, 345-355.

105. Fakurazi SI Hairuszah and Nanthini U., 2008, *Moringa oleifera* Lam prevents acetaminophen induced liver injury through restoration of glutathione level. *Food Chem. Toxicol*, **46**, 2611-2615.

106. Dahot M.U., 1998, Vitamin contents of flowers and seeds of *Moringa oleifera*. Pak J. *Biochem*., **21**, 1–24.

107. Faizi S., Siddiqui B., Saleem R., Siddiqui S., Aftab K., Gilani A., 1994, Novel hypotensive agents, niazimin A, niazimin B, niazicin A and niazicin B from *Moringa oleifera*; Isolation of first naturally occurring carbamates. *J. Chem. Soc. Perkin Trans. I*., 3035–3640.

108. Faizi S., Siddiqui B.S., Saleem R., Siddiqui S., Aftab K., Gilani A.H., 1995, Fully acetylated carbamate and hypotensive thiocarbamate glycosides from *Moringa oleifera*. *Phytochemistry*, **38**, 957–963.

109. Ghasi S., Nwobodo E., Ofili J.O., 2000, Hypocholesterolemic effects of crude extract of leaf of *Moringa oleifera* Lam in high-fat diet fed Wistar rats. *J. Ethnopharmacol*, **69,** 21– 25.

110. Mehta L.K., Balaraman R., Amin A.H., Bafna P.A. and Gulati O.D., 2003, Effect of fruits of *Moringa oleifera* on the lipid profile of normal and hyper cholesterolaemic rabbits. *J. Ethnopharmacol*, **86**, 191–195.

111. Yang, J., 2022, Online academic conference of integrated TCM and western medicine on prevention and treatment of COVID-19. https:// hd. guahao. com/n/ 26881. Accessed 5 Feb 2022

112. Fajri M., 2021, The potential of *Moringa oleifera* as immune booster against COVID 19. In IOP Conference Series: Environ. Earth Sci., 807(2), 022008.

113. Sen D., Bhaumik S., Debnath P. and Debnath S., 2021, Potentiality of *Moringa oleifera* against SARS-CoV-2: identified by a rational computer aided drug design method. *J. Biomol. Struct. Dyn*., 1–18.

114. Sivani B.M., Venkatesh P., Murthy T.K., Kumar S.B., 2021, In silico screening of antiviral compounds from *Moringa oleifera* for inhibition of SARS-CoV-2 main protease. CRGSC. **4**, 100202.

115. Adedapo A.A., Mogbojuri O.M. and Emikpe B.O., 2009, Safety evaluations of the aqueous extract of the leaves of Moringa oleifera in rats. *J Med Plant* **3,** 586–591.

116. Asare G.A., Gyan B. and Bugyei K., et al. 2012, Toxicity potentials of the nutraceutical Moringa

oleifera at supra-supplementation levels. *J. Ethnopharmacol,* **139**, 265–272.

117. Ambi A.A., Abdurahman E.M., Katsayal U.A., et al., 2011, Toxicity evaluation of Moringa oleifera leaves. *Int J Pharmaceut Res Innovat*, **4**, 22–24.

118. Awodele O., Oreagbe I.A., Odoma S., et al., 2012, Toxicological evaluation of the aqueous leaf extract of Moringa oleifera Lam. (Moringaceae). *J. Ethnopharmacol,* **139**, 300–306.

119. Oyagbemi A.A., Omobowale T.O., Azeez I.O., et. al., 2013, Toxicological evaluations of methanolic extract of Moringa oleifera leaves in liver and kidney of male Wistar rats. *J. Basic Clin Physiol Pharm.* **24**, 307–312.

120. Bakre A.G., Aderibigbe A.O., Ademowo O.G., 2013, Studies on neuropharmacological profile of ethanol extract of Moringa oleifera leaves in mice. *J. Ethnopharmacol,* **149**, 783–789.

121. Zvinorova P.I., Lekhanya L., Erlwanger K. and Chivandi E., 2014, Dietary effects of Moringa oleifera leaf powder on growth, gastrointestinal morphometry and blood and liver metabolites in Sprague Dawley rats. *J Anim Physiol Anim Nutr*. DOI:10.1111/jpn.12182.

122. Asiedu-Gyekye I.J., Frimpong-Manso S., Awortwe C., et al., 2014, Micro- and macroelemental composition and safety evaluation of the nutraceutical Moringa oleifera leaves. *J. Toxicol*. DOI:10.1155/2014/786979.

123. Rolim L.A., Macedo M.F., Sisenando H.A., et al., 2011, Genotoxicity evaluation of Moringa oleifera seed extract and lecithin. *J. Food Sci.* **76**, T53–T58.

124. Cajuday L.A., Pocsidio G.L., 2010, Effects of Moringa oleifera Lam (Moringaceae) on the reproduction in male mice (Mus musculus). *J. Med. Plant Res.,* **4**, 1115–1121.

125. Araújo LCC., Aguiar J.S., Napoleão T.H., et al., 2013, Evaluation of cytotoxic and anti-inflammatory activities of extracts and lectins from Moringa oleifera seeds. PLoS One **8**, e81973.

126. Ajibade T.O., Arowolo R., Olayemi F.O., 2013, Phytochemical screening and toxicity studies on the methanol extract of the seeds of Moringa oleifera. *J. Complement Integr Med.* **10**, 11–16.

127. Paul C.W., Didia B.C., 2012, The effects of methanolic extract of Moringa oleifera Lam roots on the histology of kidney and liver in guinea pigs. *Asian J. Med. Sci*., **4**, 55–60.

RNI No. MAHENG/2017/74063
ISSN No. (Print) 2581-5911
ISI Impact Factor 1.724

Oxidation of some Vicinal and Non-Vicinal Diols by Diethylammonium Chlorochromate: A Kinetic and Mechanistic Study

Devendra Kumar[1], Manju Baghmar[2] and Anurag Choudhary*[1]
[1]Chemical Kinetics Lab., Department of Chemistry,
J.N.V. University, Jodhpur (Rajasthan)
[2]Department of Chemistry, SS Jain, Subodh PG Mahila Mahavidyalaya,
Jaipur (Rajasthan)
Email: drpkvs27@yahoo.com

Abstract
The kinetics of oxidation of four vicinal, four non vicinal diols and two of their monoethers by diethylammonium chlorochromate (DEACC) has been studied in dimethylsulphoxide (DMSO). The main product of oxidation is the corresponding hydroxycarbonyl compound. The reaction is first order in DEACC. Michaelies-Menten type of kinetics was observed with respect to the diols. The reaction was catalysed by hydrogen ions. The hydrogen ion dependence has the form: $k_{obs} = a + b[H^+]$. The oxidation of [1,1,2,2 $^2H_4$] ethanediol exhibits a substantial primary kinetic isotope effect (k_H/k_D = 5.75 at 298 K). The reaction has been studied in nineteen different organic solvents and the solvent effect has been analysed using Taft's and Swain's multiparametric equations. The temperature dependence of the kinetic isotope effect indicates the presence of a symmetrical transition state in the rate determining step. A suitable mechanism has been proposed.

Keywords: *Correlation analysis, diols, halochromate, kinetics, mechanism, oxidation*

Introduction

Inorganic salts of Cr(VI) are well known oxidants for the organic compounds. However, these salts are rather drastic and non-selective oxidants. Further, they are insoluble in most organic solvents. Thus miscibility is a problem. To overcome these limitations, a large number of organic derivatives of Cr(VI) have been prepared and used in organic synthesis as mild and selective oxidants in non-aqueous solvents[1-4]. One of such compounds is diethylammonium chlorochromate (DEACC), prepared by reported method.[5] We have been interested in the kinetic and mechanistic aspects of the oxidation by complex salts of Cr(VI) and several reports on halochromates have already been reported from our laboratory[6-9]. There seems to be no report on the oxidation aspects of diols using diethylammonium chlorochromate (DEACC). Therefore, it was of interest to investigate the kinetics of the oxidation of some vicinal and non-vicinal diols by DEACC in DMSO. A suitable mechanism has also been postulated.

Materials and Methods

Materials: The diols (BDH or Fluka) were distilled under reduced pressure before use. DEACC was prepared by

the reported method[5]. [1,1,2,2 $^2H_4$]Ethanediol (DED) was prepared by reducing diethyl oxalate with lithium aluminium deuteride[10]. Its isotopic purity, determined by its NMR spectrum, was 95±4%. Due to the non aqueous nature of the medium, toluene p sulphonic acid (TsOH) was used as a source of hydrogen ions. TsOH is a strong acid and in a polar solvent like DMSO, it is likely to be completely ionized.

Product analysis: Product analysis was carried out under kinetic conditions. In a typical experiment, ethanediol (0.1 mol) and DEACC (0.01 mol) were taken in DMSO (100 mL) and the mixture was allowed to stand in the dark for ca. 10 h to ensure completion of the reaction. Most of the solvent was removed under reduced pressure and residue treated overnight with an excess (250 ml) of a saturated solution of 2,4 dinitrophenylhydrazine in 2 mol dm^3 HCl. The precipitated 2,4 dinitrophenylhydrazone(DNP) was filtered off, dried, recrystallized from ethanol and weighed. The product was found to be identical (m.p. and mixed m.p.) with an authentic sample of DNP of hydroxyethanal. The oxidation state of chromium in completely reduced reaction mixture determined by an iodometric method is 3.95±0.15.

Kinetic measurements: The reactions were followed under pseudo first order conditions keeping a large excess (x 15 or greater) of the diols over DEACC. The temperature was kept constant to ±0.1K. The solvent was DMSO, unless specified otherwise. The reactions were followed by monitoring the decrease in the concentration of DEACC spectrophotometrically at 380 nm for up to 80% of the reaction. No other reactant or product has any significant absorption at this wave length. The pseudo first order rate constants, k_{obs}, were evaluated from the linear (r = 0.995 0.999) plots of log [DEACC] against time. Duplicate kinetic runs showed that the rate constants were reproducible to within ±4%. All experiments, other than those for studying the effect of hydrogen ions, were carried out in the absence of TsOH.

Results and Discussion

Stoichiometry: The homogeneity of the DNP derivatives indicated the formation of only one product in each case. Under our reaction conditions, therefore, there is no observable oxidation of the second hydroxy group. This may be due to the presence of a large excess of the diol over DEACC. The overall reaction may, therefore, be written as Equation 1.

$$HOCH_2\text{-}CH_2OH + O_2CrClO^-N^+H_2Et_2 \longrightarrow HOCH_2\text{-}CHO + H_2O + OCrClO^-N^+H_2Et_2 \quad (1)$$

DEACC undergoes a two electron change. This is in accord with the earlier observations with structurally similar halochromates. It has already been proved earlier also that both pyridinium fluorochromate (PFC)[11] and pyridinium chlorochromate (PCC)[12] act as two electron oxidants and are reduced to chromium (IV) species, by determining the oxidation state of chromium by magnetic succeptibility, ESR and IR studies.

Kinetic Dependence: The reactions are of first order with respect to DEACC. Further, the pseudo-first order rate constant, k_{obs} is independent of the initial concentration of DEACC. Figure 1 depicts a typical kinetic run.The reaction rate increases with increase in the concentration of the diols but not linearly (Table 1). A plot of $1/k_{obs}$ against 1/[Diol] is linear ($r > 0.995$) with an intercept on the rate ordinate (Figure 2). Thus, Michaelis Menten type kinetics are observed with respect to the diol. This leads to the postulation of following overall mechanism (2) and (3) and rate law (4).

$$\text{Diol} + \text{DEACC} \underset{k_2}{\overset{K}{\rightleftarrows}} [\text{complex}] \quad (2)$$

$$[\text{Complex}] \xrightarrow{k_2} \text{Products} \quad (3)$$

$$\text{Rate} = k_2 K [\text{Diol}] [\text{DEACC}] / (1+k [\text{diol}]) \quad (4)$$

Table 1. Rate constants for the oxidation of propan-1,2-diol by DEACC at 298 K

10^3 [DEACC] (mol dm^{-3})	[Diol] (mol dm^{-3})	10^4 k_{obs} (mol dm^{-3})
1.0	0.10	4.47
1.0	0.20	6.82
1.0	0.40	9.27
1.0	0.60	10.8
1.0	0.80	11.3
1.0	1.00	11.8
1.0	1.50	12.6
1.0	3.00	13.5
2.0	0.40	6.66
4.0	0.40	6.75
6.0	0.40	6.92
8.0	0.40	6.84
1.0	0.20	9.36*

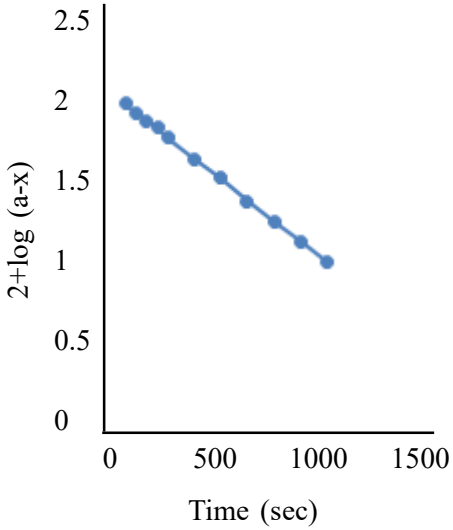

Fig. 1. Oxidation of Propane-1,2-diol by DEACC: A typical Kinetic Run

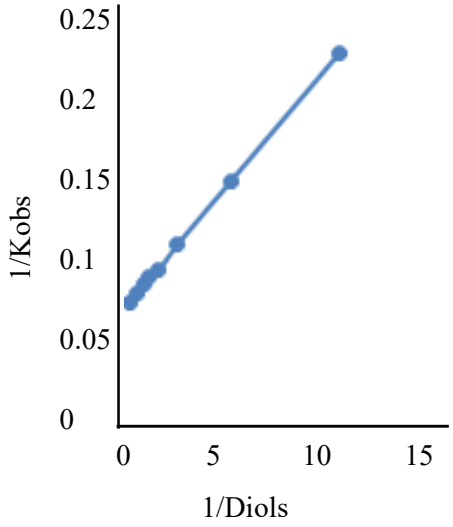

Fig. 2. Oxidation of Propane-1,2-diol by DEACC: A double reciprocal plot

The dependence of reaction rate on the reductant concentration was studied at different temperatures and the values of K and k_2 were evaluated from the double reciprocal plots. The thermodynamic parameters of the complex formation and activation parameters of the decomposition of the complexes were calculated from the values of K and k_2 respectively at different temperatures (Tables 2 and 3).

Table 2. Rate constants for the decomposition of DEACC-Diol complexes and activation parameters

$10^4\ k_2$ / ($dm^3\ mol^{-1}\ s^{-1}$)					ΔH^*	$-\Delta S^*$	ΔG^*
Diols	288 K	298 K	308 K	318 K	(kJ mol^{-1})	(J $mol^{-1}K^{-1}$)	(kJ mol^{-1})
Ethane-1,2	2.33	5.90	14.4	34.2	66.6±0.6	86±2	91.4±0.4
Propan-1,2	9.55	21.6	50.4	107	59.4±0.5	97±2	88.2±0.2
Butane-2,3	38.7	82.8	170	350	52.2±0.5	108±2	84.8±0.3
Butane-1,2	12.8	83.9	63.9	135	58.5±0.9	99±3	87.5±0.4
Propan-1,3	17.9	26.9	89.1	198	58.5±0.7	96±2	86.6±0.1
Butane-1,3	22.3	40.1	98.1	206	53.1±0.8	109±3	86.2±0.7
Butane-1,4	25.9	45.9	126	269	56.7±0.7	97±2	85.8±0.5
Pentane-1,5	35.1	55.8	153	322	53.0±0.8	108±2	85.1±0.7
DED	0.37	1.03	2.61	6.10	70.2±0.7	88±2	95.4±0.9
k_H/k_D	6.29	5.75	5.52	5.10			

Table 3. Formation constants for the decomposition of DEACC-Diols complexes and thermodynamic parameters

K ($dm^3\ mol^{-1}$)					$-\Delta H^*$	$-\Delta S^*$	$-\Delta G^*$
Diols	288 K	298 K	308 K	318 K	(kJ mol^{-1})	(J $mol^{-1}K^{-1}$)	(kJ mol^{-1})
Ethane-1,2	5.76	5.13	4.50	3.96	12.1±0.3	19±1	6.53±0.2
Propan-1,2	6.94	6.39	5.69	5.04	10.7±0.4	13±1	7.09±0.3
Butane-2,3	5,14	4.51	3.87	3.24	14.2±0.4	28±1	6.18±0.3
Butane-1,2	6.90	6.30	5.72	5.08	10.3±0.3	12±1	7.04±0.2
Propan-1,3	6.48	5.94	5.25	4.60	11.2±0.4	15±1	6.86±0.3
Butane-1,3	5.49	6.21	4.27	3.63	13.0±0.5	23±1	6.39±0.4
Butane-1,4	6.84	5.22	5.65	4.95	10.6±0.3	13±1	7.02±0.3
Pentane-1,5	5.83	6.03	5.50	3.92	12.7±0.5	21±2	6.56±0.4
DED	6.67	5.90	5.35	4.68	10.9±0.4	14±1	6.84±0.3

Test for free radicals: The oxidation of diols, by DEACC, in an atmosphere of nitrogen failed to induce the polymerisation of acrylonitrile. Further, addition of acrylonitrile had no effect on the rate (Table 1). To further confirm the absence of free radicals in the reaction pathway, the reaction was carried out in the presence of 0.05 mol dm^{-3} of 2,6-di-t-butyl-4-methylphenol (butylated hydroxytoluene or BHT). It was observed that BHT was recovered unchanged, almost quantitatively.

Effect of hydrogen ions: The reaction is catalyzed by hydrogen ions (Table 4). The hydrogen ion dependence has the form: $k_{obs} = a + b\ [H^+]$. The values of a and b for ethanediol are $4.49\pm0.23 \times 10^{-4}\ s^{-1}$ and $8.40\pm0.38 \times 10^{-4}\ mol^{-1}\ dm^3\ s^{-1}$ respectively ($r^2 = 0.9920$).

Table 4. Dependence of the reaction rate on hydrogen-ion concentration

[IDC] = 0.001 mol dm^{-3};	[Ethane Diol] = 1.0 mol dm^{-3};			Temp. = 298 K		
$[H^+]$/mol dm^{-3}	0.10	0.20	0.40	0.60	0.80	1.00
10^4 k_{obs}/s^{-1}	5.30	6.21	7.75	9.54	11.7	12.6

Kinetic isotope effect: To ascertain the importance of the cleavage of the α C-H bond in the rate determining step, the oxidation of DED was studied. The results (Tables 2 and 3) showed that the formation constants, K, of the intermediate complex of the deuteriated and protiated diols do not differ much, however, the rate of disproportionation of the intermediate exhibited the presence of a substantial primary kinetic isotope (k_H/k_D = 5.75 at 298 K).

Reactive oxidizing species: The observed hydrogen ion dependence suggests that the reaction follows two mechanistic pathways, one is acid independent and the other is acid-dependent. The acid catalysis may well be attributed to a protonation of DEACC to yield a protonated Cr(VI) species which is a stronger oxidant and electrophile (Eq.5).

$$[O_2CrClO^-N^+H_2Et_2] + H^+ \underset{\leftarrow}{\overset{+}{\rightleftarrows}} [HOCrOClO^-N^+H_2Et_2] \quad (5)$$

Formation of a protonated Cr(VI) species has earlier been postulated in the reactions of structurally similar halochromates.

Effect of organic solvents: The oxidation of ethanediol was studied in 19 different organic solvents. The choice of solvents was limited due to the solubility of DEACC and its reaction with primary and secondary alcohols. There was no reaction with the solvents chosen. The values of formation constants K and decomposition constants of the complex, k_2 are recorded in Table 5.

Table 5. Effect of solvents on the oxidation of Propan-1,2-diol by DEACC at 308 K

Solvents	K (dm^{-3} mol^{-1})	10^5 k_{obs} (s^{-1})	Solvents	K (dm^{-3} mol^{-1})	10^5 k_{obs} (s^{-1})
Chloroform	5.67	41.7	Toluene	4.86	18.2
1,2-Dichloroethane	5.58	51.3	Acetophenone	5.88	77.6
Dichloromethane	6.30	49.0	THF	4.90	31.6
DMSO	4.50	144	t-Butylalcohol	5.45	19.9
Acetone	6.12	57.5	1,4-Dioxane	5.60	27.5
DMF	5.40	95.4	1,2-Dimethoxyethane	5.49	14.8
Butanone	5.94	34.7	CS_2	6.01	9.77
Nitrobenzene	5.85	63.1	Acetic Acid	5.75	8.32
Benzene	5.67	22.4	Ethyl Acetate	5.80	24.5
Cyclohexane	6.03	2.81			

A satisfactory linear correlation (r^2 = 0.9064) between the values of activation enthalpies and entropies of oxidation of diols indicated the operation of compensation effect in this reaction[13]. The reaction also exhibited an excellent isokinetic effect, as determined by Exner's criterion[14]. An Exner's plot between log k_2 at 288K and at 318K was

linear (r^2 = 0.9984) (Figure 3). The value of isokinetic temperature is 788±108 K. The linear isokinetic correlation implies that all the diols are oxidized by the same mechanism and the changes in rate are governed by the changes in both the enthalpy and entropy of the activation.

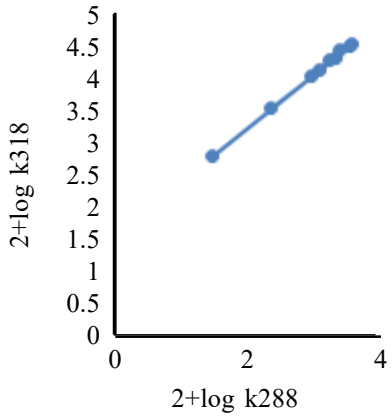

Fig. 3. Exner's Isokinetic Relationship in the oxidation of Diols by DEACC

Solvent effect: The rate constants, k_2, for the oxidation of ethanediol in 18 organic solvents (CS_2 was not considered, as the complete range of solvent parameters was not available) did not exhibit any significant correlation in terms of the linear solvation energy relationship (Eq. 5) of Kamlet et al[15].

$$\log k_2 = A_0 + p\Pi^* + b\beta + a\alpha \qquad (5)$$

In this equation, Π^* represents the solvent polarity, β the hydrogen bond acceptor basicities and α is the hydrogen bond donor acidity. A_0 is the intercept term. It may be mentioned here that out of the 18 solvents, 13 have a value of zero for α. The results of correlation analyses in terms of Equation 5, a biparametric equation involving Π^* and β, and separately with Π^* and β are given below Equations 6-9.

$$\log k_2 = -4.54 + (1.40 \pm 0.18)\,\pi^* + (0.22 \pm 0.15)\,\beta - (0.26 \pm 0.14)\,\alpha \qquad (6)$$
R^2 = 0.8659; sd = 0.16; n = 18; Ψ = 0.40

$$\log k_2 = -4.47 + (1.49 \pm 0.18)\,\pi^* + (0.14 \pm 0.15)\,\beta \qquad (7)$$
R^2 = 0.8327; sd = 0.17; n = 18; Ψ = 0.43

$$\log k_2 = -4.50 + (1.53 \pm 0.18)\,\pi^* \qquad (8)$$
r^2 = 0.8236; sd = 0.17; n = 18; Ψ = 0.43

$$\log k_2 = -3.66 + (0.40 \pm 0.33)\,\beta \qquad (9)$$
r^2 = 0.0848; sd = 0.40; n = 18; Ψ = 0.98

Here n is the number of data points and y is the Exner's statistical parameter[16].

Kamlet's[15] triparametric equation explains *ca.* 86% of the effect of solvent on the oxidation. However, by Exner's criterion[16] the correlation is not even satisfactory (*cf.* Equation 6). The major contribution is of solvent polarity. It alone accounted for *ca.* 82% of the data. Both β and α play relatively minor roles.

The data on the solvent effect were analysed in terms of Swain's[17] Equation 10 of cation and anion solvating concept of the solvents also.

$$\log k_2 = aA + bB + C \quad (10)$$

Here A represents the anion solvating power of the solvent and B the cation solvating power. C is the intercept term. (A + B) is postulated to represent the solvent polarity. The rates in different solvents were analysed in terms of Equation 11, separately with A and B and with (A + B).

$$\log k_2 = (0.37 \pm 0.05)\,A + (1.57 \pm 0.03)\,B - 3.65 \quad (11)$$
$R^2 = 0.9930$; sd = 0.04; $n = 19$; $\Psi = 0.09$

$$\log k_2 = 0.15(\pm 0.52)\,A - 2.57 \quad (12)$$
$r^2 = 0.0048$; sd = 0.42; $n = 19$; $\Psi = 1.02$

$$\log k_2 = 1.54(\pm 0.07)\,B - 3.53 \quad (13)$$
$r^2 = 0.9633$; sd = 0.08; $n = 19$; $\Psi = 0.20$

$$\log k_2 = 1.17 \pm 0.16\,(A + B) - 3.61 \quad (14)$$
$r^2 = 0.7698$; sd = 0.20; $n = 19$; $\Psi = 0.49$

The rates of oxidation of ethanediol in different solvents showed an excellent correlation in Swain's equation (cf. Equation 11) with the cation solvating power playing the major role. In fact, the cation solvation alone account for *ca.* 96% of the data. The correlation with the anion solvating power was very poor. The solvent polarity, represented by (A + B), also accounted for *ca.* 77% of the data. In view of the fact that solvent polarity is able to account for *ca.* 77% of the data, an attempt was made to correlate the rate with the relative permittivity of the solvent. However, a plot of $\log k_2$ against the inverse of the relative permittivity is not linear (r^2 = 0.5345; sd = 0.29; ψ = 0.70).

Correlation analysis of reactivity: The rates of oxidation of the four vicinal diols in DMSO showed the excellent correlation with Taft's σ^* values[18] with negative reaction constants (Table 6), this indicates the presence of an electron-deficient rate-determining step. Here $\Sigma\sigma^*$ represents the sum of the substituent constants for the substituents present on the two alcoholic carbons of the vicinal diols. The fact that σ^* values alone account for 99% of the data showed that steric factors do not play any significant role in the reaction. The magnitude of the reaction constants decreases with an increase in the temperature, indicating that selectivity decreases with an increase in the reactivity.

Table 6. Reaction constants of the oxidation of vicinal diols by DEACC

Temp./ K	$-\rho^*$	r^2	Sd	ψ
288	1.26±0.09	0.9890	0.06	0.12
298	1.17±0.07	0.9933	0.05	0.09
308	1.09±0.09	0.9865	0.06	0.13
318	1.01±0.07	0.9909	0.05	0.11

Mechanism

The presence of a substantial primary kinetic isotope effect confirms the cleavage of an a C H bond in the rate

determining step. The negative values of the polar reaction constant together with substantial deuterium isotope effect indicate that the transition state has an electron-deficient carbon centre. Hence the transfer of a hydride ion from diol to the oxidant is suggested. The hydride transfer mechanism is also supported by the major role of cation solvating power of solvents.

The hydride ion transfer may take place either by a cyclic process via an ester intermediate or by an acyclic one-step bimolecular process. Kwart and Nickle[19] have shown that a study of the dependence of the kinetic isotope effect on temperature can be gainfully employed to resolve this problem. The data for protio and deuterio ethandiols, fitted to the familiar expression $k_H/k_D = A_H/A_D \exp(E_a/RT)$[20,21] show a direct correspondence with the properties of a symmetrical transition state in which the activation energy difference (DE_a) for k_H/k_D is equal to the zero point energy difference for the respective C H and C D bonds (≈ 4.5 kJ/mol) and the frequency factors and the entropies of activation of the respective reactions are nearly equal. Bordwell[22] has documented a very cogent evidence against the occurrence of concerted one step bimolecular processes by hydrogen transfer and it is evident that in the present studies also the hydrogen transfer does not occur by an acyclic bimolecular process. It is well established that intrinsically concerted sigmatropic reactions, characterized by transfer of hydrogen in a cyclic transition state, are the only truly symmetrical processes involving a linear hydrogen transfer[23]. Littler[24] has also shown that a cyclic hydride transfer, in the oxidation of alcohols by Cr(VI), involves six electrons and, being a Huckel type system, is an allowed process. Thus the overall mechanism is proposed to involve the formation of a chromate ester in a fast pre equilibrium step and then a disproportionation of the ester in a subsequent slow step via a cyclic concerted symmetrical transition state leading to the product (Scheme 1). The observed hydrogen ion dependence can be explained by assuming a rapid reversible protonation of the chromate ester (A) with the protonated ester decomposing at a rate faster than (A) (Scheme 2).

It is of interest to recall that pinacol is oxidized by chromic acid but not by DEACC. Chatterjee and Mukherji[25] reported an abrupt change from butane 2,3 diol to pinacol, the latter reacting very fast. As pointed out by Littler[24], a cyclic ester mechanism is forbidden in the diol Cr(VI) reaction. Chromic acid oxidation of pinacol may therefore involve two one electron steps. Chromic acid oxidations are known to induce polymerization of acrylamide under certain conditions[26]. No such observation has yet been recorded with DEACC. Thus the capability of chromic acid and the inability of DEACC to act as a one electron oxidant may explain the different behaviour of pinacol towards these two oxidants.

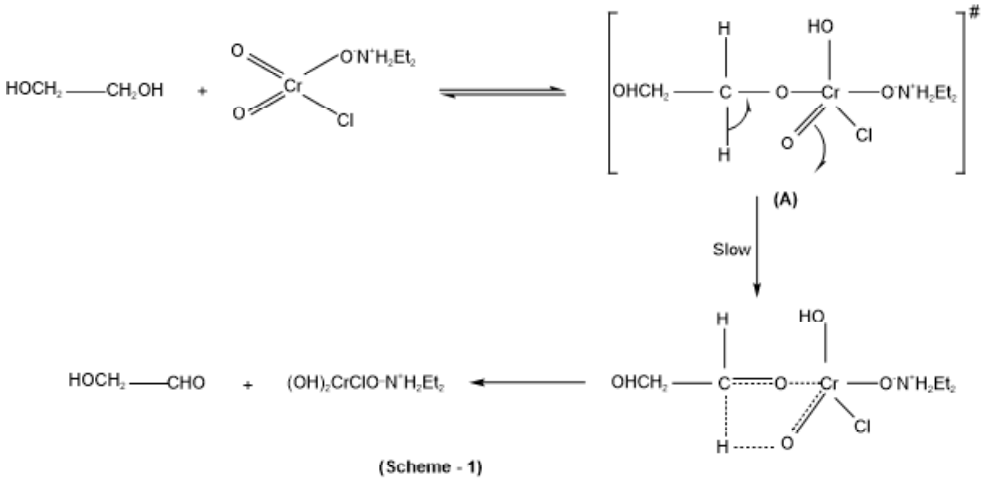

(Scheme - 1)

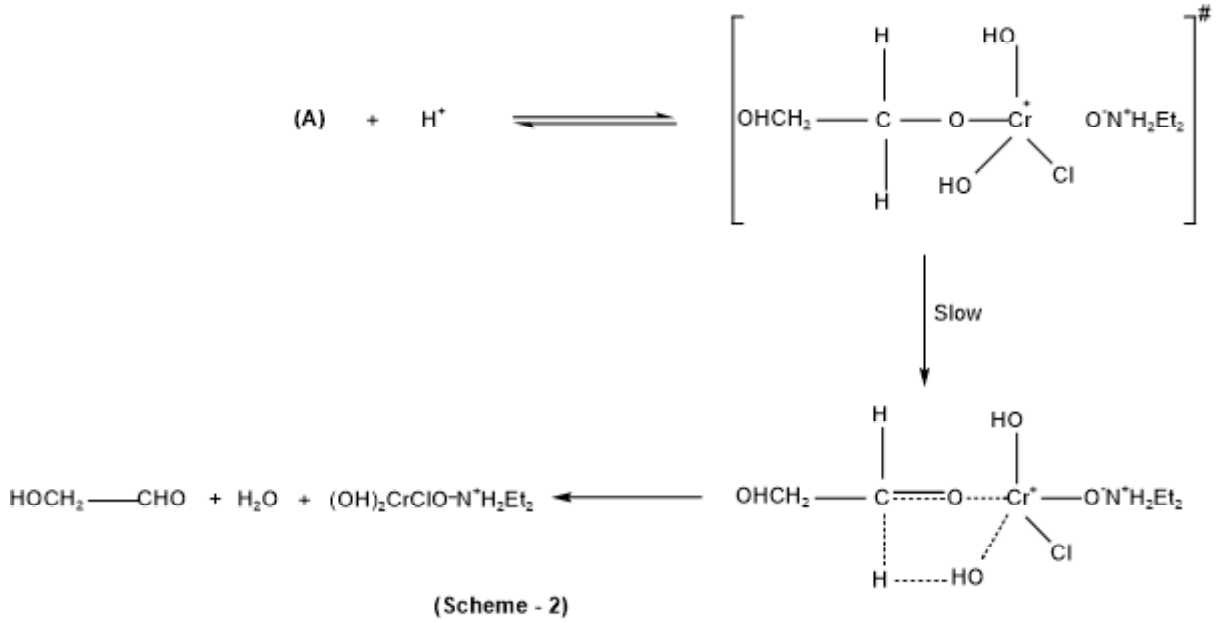

(Scheme - 2)

Conclusions

Oxidation of these diols indicated the involvement of the formation of a chromate ester in fast pre-equilibrium and then a disproportionation of the ester in a subsequent slow step via a cyclic concerted symmetrical transition state leading to the product, carbonyl compound.

Acknowledgement

Thanks are due to the UGC, New Delhi, India for financial support in the form of UGC-BSR, One time grant to AC and UGC-NET-JRF to DK, and to Department of Chemistry, JNV University, Jodhpur for lab facilities.

References

1. Balasubramanian K. and Prathiba V., 1986, *Indian J. Chem*., **25B**, 326.
2. Corey E.J. and Suggs W.J., 1975, *Tetrahedron Lett*., **16(31)**, 2647.
3. Guziec F.S. and Luzio F.A., 1980, *Synthesis*, **5**, 691.
4. Pandurangan A., Murugesan V. and Palamichamy P., 1995, *J. Indian Chem. Soc.*, **72**, 479.
5. V. Sinhg, S. Mahajan, V.S. Jasrotia, M. Sharma, H.N. Sheihk and B.L. Kalsotra,2009, *J. Indian Chem. Soc.*, **84**, 528.
6. Vyas N., Daiya A., Choudhary A., Sharma M. and Sharma V., 2013, *Eur. Chem. Bull.*, **2(11)** 859.
7. Mathur L., Choudhary A., Prakash O. and Sharma P.K., 2014, *Asian J. Chem.,* **26(9)** 2597.
8. Kalla R., Kumar D., Choudhary A. and Sharma V., 2021, *Rasayan J. Chem.*, **14(4)** 2436.
9. Chandora D., Kumar D., Choudhary A. Sharma V., 2021, *J. Adv. Sci. Res.*, **12(3)** 155.
10. T.J. Kemp and W.A. Waters, *Proc Roy Soc Ser A*, 1963, **274**, 480.
11. Bhattacharjee M.N., Choudhuri M.K. and Purakayastha S., 1987, *Tetrahedron*, **43**, 5389.

12. Brown H.C., Rao G.C. and Kulkarni S.U., 1979, *J. Org. Chem.*, **44**, 2809.

13. Liu L. and Guo W.E., 2001, *Chem. Review*, **101**, 673.

14. Exner O., 1966, *Collect Chem. Czech. Commun.*, **31**, 3222.

15. Kamlet M.J., Abboud J L M., Abraham M.H. and Taft R.W., 1983, *J. Org. Chem.*, **48**, 2877.

16. Exner O., 1977, *Collect Chem. Czech. Commun.*, **38**, 411.

17. Swain C.G., Swain M.S., Pqwel A.L. and Alunni S., 1983, *J. Am. Chem. Soc.*, **105**, 502.

18. Wiberg K.B., 1964, *Physical Organic Chemistry*, Wiley, New York.

19. Kwart H. and Nickel J.H., 1953, *J. Am. Chem. Soc*., **95**, 3394.

20. Kwart H. and Latimer M.C., 1971, *J. Am. Chem. Soc.*, **93**, 3770.

21. Kwart H. and Slutsky J., 1972, *J. Chem. Soc. Chem. Commun.*, **21**, 1182.

22. Bordwell F.G., 1974, *Acc. Chem. Res.*, **5**, 374.

23. Woodward R.W. and Hoffmann R., 1969, *Angew. Chem. Int. Ed. Eng.*, **8**, 781.

24. Littler J.S., 1971, *Tetrahedron*, **27**, 81.

25. Chatterjee A.C. and Mukherji S.K., 1957, *Z. Phys. Chem.*, **207**, 372.

26. Rahman M. and Rocek J., 1971, *J. Am. Chem. Soc.*, **93**, 5462.

RNI No. MAHENG/2017/74063
ISSN No. (Print) 2581-5911
ISI Impact Factor 1.724

Kinetics and Mechanism of the Oxidation of Formic and Oxalic acids by Tributylammonium Chlorochromate

Heena Kansara, Pooja Tak, Pramila Naga, Yashsvi Inaniyan and Priyanka Purohit*
Chemical Kinetics Laboratories, Department of Chemistry,
J.N.V. University, Jodhpur - India
Email: drpkvs27@yahoo.com

Abstract
Kinetics and mechanism of oxidation of formic and oxalic acids by tributylammonium chlorochromate (TBACC) have been studied in dimethylsulphoxide. The main product of oxidation is carbon dioxide. The reaction is first order with respect to TBACC. Michaelis-Menten type kinetics was observed with respect to organic acids. The reaction is acid catalysed and the acid dependence has the form $k_{obs} = a + b[H^+]$. The oxidation of a deuterioformic acid exhibits a substantial primary kinetic isotope effect (k_H/k_D = 5. 30 at 298 K). The reaction has been studied in nineteen different organic solvents and the solvent effect has been analysed using Taft's and Swain's multiparametric equations. The temperature dependence of the kinetic isotope effect indicates the presence of a symmetrical cyclic transition state in the rate determining step. Suitable mechanisms have been proposed.

Keywords: *Acids, halochromate, kinetics, mechanism, oxidation*

Introduction

For the selective oxidation of organic compounds, halochromates have long been used as mild and selective oxidizing reagents in synthetic organic chemistry[1-4]. Tributylammonium chlorochromate (TBACC) is also one such compound used for the oxidation of alcohols and hydrocarbons[5]. We have also been interested in the kinetic and mechanistic aspects of oxidation by complexed Cr(VI) species and several reports on mechanistic aspects of organic functions have already been published from our laboratory[6-9]. There seems to be no report on the kinetics and mechanism of oxidation by tributylammonium chlorochromate (TBACC). Therefore, we report in this article the kinetics of oxidation of Oxalic and Formic acids by TBACC in dimethylsulphoxide (DMSO) as solvent. The mechanistic aspects are discussed. A suitable mechanism has also been proposed.

Materials and Methods

Materials: TBACC and a deuterioformic acid (DCO_2H or DFA) were prepared by the reported methods[5,10]. Due to the non aqueous nature of the medium, toluene p sulphonic acid (TsOH) was used as a source of hydrogen ions. TsOH is a strong acid and in a polar solvent like DMSO it is likely to be completely ionised. Solvents were purified by the usual methods[11].

Stoichiometry: To determine the stoichiometry, an excess

of TBACC (× 5 or greater) was reacted with the organic acid in DMSO (100 mL) and the amount of residual TBACC after the completion of reaction was measured spectrophotometrically at 346 nm. The results indicated 1:1 stoichiometry. No quantitative determination of carbon dioxide formed was carried out. The oxidation state of chromium in completely reduced reaction mixtures, determined by an iodometric method, was 3.90 ± 0.10.

Kinetic measurements: The reactions were followed under pseudo first order conditions by keeping a large excess (×15 or greater) of the organic acid over TBACC. The temperature was kept constant to ±0.1°K. The solvent was DMSO, unless specified otherwise. The reactions were followed by monitoring the decrease in the concentration of TBACC spectrophotometrically at 346 nm for up to 80% of the reaction. No other reactant or product had any significant absorption at this wavelength. The pseudo first order rate constants, k_{obs}, were evaluated from the linear (r = 0.995 0.999) plots of log [TBACC] against time. Duplicate kinetic runs showed that the rate constants were reproducible to within ±3%.

Results and Discussion

The oxidation of organic acids leads to the formation of carbon dioxide. The stoichiometric determination indicated the following overall reactions:

$$(COOH)_2 + O_2CrClO^-NH^+(C_4H_9)_3 \longrightarrow 2CO_2 + H_2O + OCrClO^-NH^+(C_4H_9)_3 \quad (1)$$

$$HCOOH + O_2CrClO^-NH^+(C_4H_9)_3 \longrightarrow CO_2 + H_2O + OCrClO^-NH^+(C_4H_9)_3 \quad (2)$$

TBACC undergoes a two-electron change. This is in accordance with the earlier observations with structurally similar PCC[12] and PFC[13]. It has already been shown that both PCC[12] and PFC[13] act as two electron oxidants and are reduced to chromium (IV) species by determining the oxidation state of chromium by magnetic susceptibility, ESR and IR studies.

Rate Laws: The reactions are of first order with respect to TBACC (Figure 1). Further, the pseudo-first order rate constant, k_{obs} is independent of the initial concentration of TBACC. The reaction rate increases with increase in the concentration of the organic acid but not linearly (Table 1). A plot of $1/k_{obs}$ against 1/[FA] is linear (r > 0.995) with an intercept on the rate ordinate (Figure 2). Thus, Michaelis Menten type kinetics is observed with respect to the acids. This leads to the postulation of following overall mechanism (3) and (4) and rate law (5).

$$\text{Organic Acid} + \text{TBACC} \underset{}{\overset{K}{\leftrightarrows}} [\text{complex}] \quad (3)$$

$$[\text{Complex}] \xrightarrow{k_2} \text{Products} \quad (4)$$

$$\text{Rate} = k_2 K [\text{Organic Acid}] [\text{TBACC}] / (1 + K [\text{Organic Acid}]) \quad (5)$$

The dependence of reaction rate on the reductant concentration was studied at different temperatures and the values of K and k_2 were evaluated from the double reciprocal plots. The thermodynamic parameters of the complex formation and activation parameters of the decomposition of the complexes were calculated from the values of K and k_2 respectively at different temperatures (Tables 2 and 3).

Table 1. Rate constants for the oxidation of oxalic and formic acids by TBACC at 298 K

10^3 [TBACC]	[Acid]	10^4 k_{obs} s^{-1}	
mol dm^{-3}	mol dm^{-3}	(OA)	(FA)
1.00	0.10	21.9	2.90
1.00	0.20	27.8	4.55
1.00	0.40	32.1	6.35
1.00	0.60	33.9	7.31
1.00	0.80	35.0	7.91
1.00	1.00	35.5	8.32
1.00	1.50	36.3	8.94
1.00	3.00	37.2	9.66
2.00	0.20	26.1	4.41
4.00	0.20	28.8	4.68
6.00	0.20	27.0	4,14
8.00	0.20	27.9	4.59
1.00	0.40	33.3*	6.48*
[a] contained 0.001 M acrylonitrile			

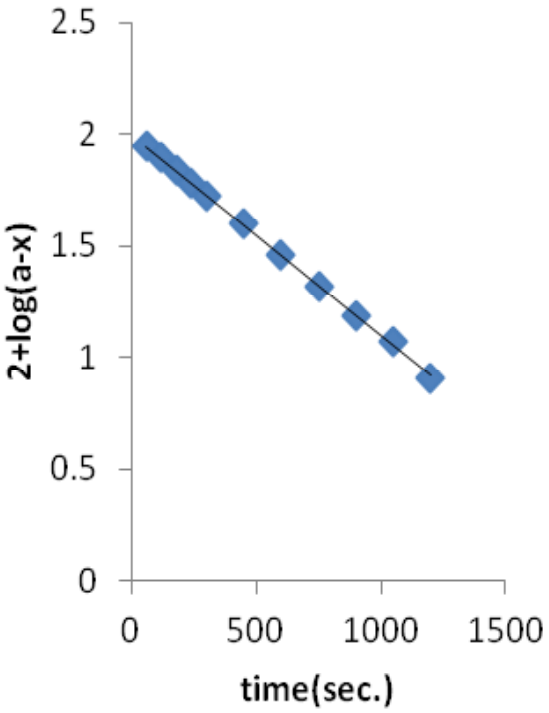

Fig. 1 Oxidation of Formic Acid: A typical kinetic run

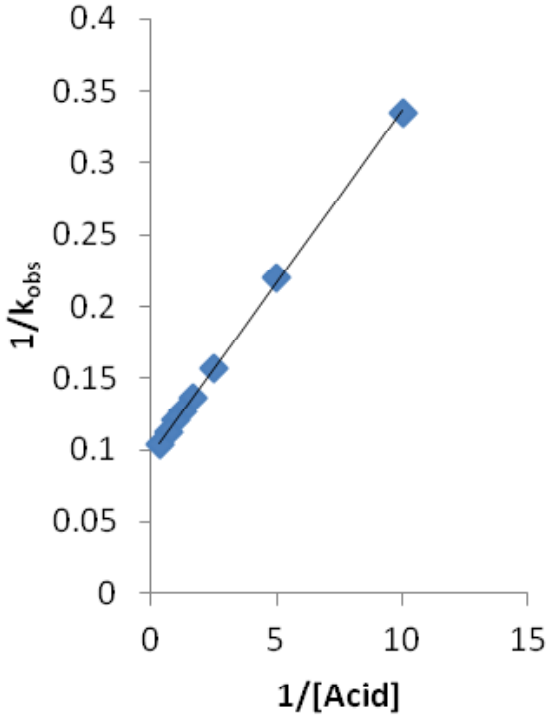

Fig. 2 Oxidation of Formic Acid: A Double Rec\iprocal Plot

Test for free radicals / induced polymerization of acrylonitrile: The oxidation of organic acids by TBACC, in an atmosphere of nitrogen, failed to induce the polymerization of acrylonitrile. In blank experiments, with organic acid absent, no noticeable consumption of TBACC was observed. Further, the addition of acrylonitrile had no effect on the rate (Table 1). Thus a one-electron oxidation giving rise to free radials is unlikely. To further confirm the absence of the free radicals in the reaction pathways, the reaction was carried out in the presence of 0.05 mol dm^{-3} of 2,6-di-t-butyl-4-methylphenol (butylated hydroxytoluene or BHT). It was observed that BHT was recovered unchanged, almost quantitatively.

Table 3. Rate constants for the decomposition of TBACC-Organic acid complexes and activation parameters

$10^4 k_2$ / (dm^3 mol^{-1} s^{-1})					ΔH^*	$-\Delta S^*$	ΔG^*
Acids	288 K	298 K	308 K	318 K	(kJ mol^{-1})	(J $mol^{-1}K^{-1}$)	(kJ mol^{-1})
OA	18.4	38.1	75.7	153	511+0.6	120±1	86.8±0.5
FA	5.31	10.5	21.7	44.1	51.9±0.9	128±2	90.0±0.8
DFA	0.93	1.98	4.06	8.73	54.1±0.9	135±3	94.1±0.7
k_H/k_D	5.52	5.30	5.19	5.05			

Table 4. Formation constants for the decomposition of TBACC-Organic acids complexes and thermodynamic parameters

	K (dm^3 mol^{-1})				$-\Delta H^*$	$-\Delta S^*$	$-\Delta G^*$
Acids	288 K	298 K	308 K	318 K	(kJ mol^{-1})	(J $mol^{-1}K^{-1}$)	(kJ mol^{-1})
OA	28.8	13,5	6.15	3.30	58.0±0.6	165±2	8.91±0.6
FA	4.95	3.82	2.91	2.28	22.3±0.2	56±1	5.67±0.2
DFA	5.52	4.35	3.46	2.58	21.6±0.7	52±2	6.12±0.6

Effect of acidity / Hydrogen ion effect: The reaction is catalysed by hydrogen ions. The hydrogen ion dependence has the following form (Table 4). $k_{obs} = a + b\ [H^+]$ (6)

The values of a and b, for oxalic acid, are 4.96±0.17 x 10^{-3} s^{-1} and 8.77±0.27 x 10^{-3} mol^{-1} dm^3 s^{-1} respectively (r^2 = 0.9959). The corresponding values for the oxidation of formic acid are 1.32±0.06 x 10^{-3} and 2.39±0.10 x 10^{-3} mol^{-1} dm^3 s^{-1} (r^2 = 0.9928).

Table 5. Dependence of the reaction rate on hydrogen-ion concentration

[TBACC] = 0.001 mol dm^{-3}			[Acid] = 1.0 mol dm^{-3}			Temp. = 298 K
$[H^+]$/mol dm^{-3}	0.10	0.20	0.40	0.60	0.80	1.00
OA -10^4 k_{obs}/s^{-1}	29.1	36.3	52.2	71.1	84.6	101
FA -10^4 k_{obs}/s^{-1}	3.87	4.95	6.93	9.36	11.2	13.5

Kinetic isotope effect: To ascertain The importance of the cleavage of the a C H bond in the rate determining step, the oxidation of α-deuterio formic acid (DFA) was studied. The results recorded in Table 2, exhibited a substantial primary kinetic isotope effect (k_H/k_D = 5.30 at 298 K).

Effect of solvents: The oxidation of formic acid was studied in 19 different organic solvents. The choice of solvents was limited due to the solubility of TBACC and its reaction with primary and secondary alcohols. There was no reaction with the solvents chosen. The kinetics were similar in all the solvents. The values of K and k_2 are recorded in Table 5.

Table 6. Effect of solvents on the oxidation of formic acid by TBACC at 298 K

Solvents	K (dm^{-3} mol^{-1})	10^5 k_{obs} (s^{-1})	Solvents	K (dm^{-3} mol^{-1})	10^5 k_{obs} (s^{-1})
Chloroform	4.27	36.3	Toluene	3.214.66	7.08
1,2-Dichloroethane	4.58	34.6	Acetophenone	3.3.5467	37.2
Dichloromethane	4.14	33.1	THF	3.49	13.5
DMSO	3.82	105	t-Butylalcohol	4.55	16.2
Acetone	3.76	28.8	1,4-Dioxane	4.23	12.3
DMF	4.06	50.1	1,2-Dimethoxyethane	3.88	7.59
Butanone	4.88	21.4	CS_2	4.58	3.24
Nitrobenzene	3.95	35.5	Acetic Acid		14.8
Benzene	3.96	8.91	Ethyl Acetate		10.2
Cyclohexane	4.25	0.72			

Reactive oxidizing species: The observed hydrogen ion dependence suggests that the reaction follows two mechanistic pathways, one is acid independent and the other is acid dependent. The acid catalysis may well be attributed to a protonation of TBACC to yield a protonated Cr(VI) species which is a stronger oxidant and electrophile (Eq. 7).

$$[O_2CrClO^-NH^+(C_4H_9)_3] + H^+ \text{ -⇆ } [HOCrOClO^-NH^+(C_4H_9)_3]^+ \quad (7)$$

Formation of a protonated Cr(VI) species has earlier been postulated in the reactions of structurally similar halochromates like QFC[14] and DEACC[15].

Solvent effect: The rate constants, k_2, in eighteen solvents (CS_2 was not considered, as the complete range of solvent parameters was not available) were correlated in terms of the linear solvation energy relationship (Eq. 8) of Kamlet et al[16].

$$\log k_2 = A_0 + p\pi^* + b\beta + a\alpha \quad (8)$$

In this equation, π* represents the solvent polarity, α the hydrogen bond acceptor basicities and β is the hydrogen bond donor acidity. A_0 is the intercept term. It may be mentioned here that out of the 18 solvents, 12 have a value of zero for α.

The results of correlation analyses in terms of Eq. 8, a biparametric equation involving π* and β, and separately with π* and β are given below as Equation 9-12.

$\log k_2 = -4.13 + 1.72(\pm0.19)\pi^* + 0.14(\pm0.15)\beta + 0.27(0.15)\alpha$ (9)
$R^2 = 0.8783$; sd = 0.17; n = 18; $\psi = 0.38$

$\log k_2 = -4.20 + 1.62\ (\pm0.19)\ \pi^* + 0.24\ (\pm0.16)\beta$ (10)
$R^2 = 0.8484$; sd = 0.18; n = 18; $\psi = 0.41$

$\log k_2 = -4.25 + 1.69\ (\pm0.19)\ \pi^*$ (11)
$r^2 = 0.8256$; sd = 0.25; n = 18; $\psi = 0.43$

$\log k_2 = -5.15 + 0.53\ (\pm0.36)\beta$ (12)
$r^2 = 0.1197$; sd = 0.12; n = 18; $\psi = 0.97$

Here n is the number of data points and y is the Exner's statistical parameter.[17]

Kamlet's[16] triparametric equation explains ca. 88% of the effect of solvent on the oxidation. However, by Exner's[17] criterion the correlation is not even satisfactory. (cf. Eq. 9). The major contribution is of solvent polarity. It alone accounts for 82% of the data. Both β and α play relatively minor roles.

The data on solvent effect were also analyzed in terms of Swain's equation[18] of cation and anion solvating concept of the solvents also (13).

$\log k_2 = aA + bB + C$ (13)

Here A represents the anion solvating power of the solvent and B the cation solvating power. C is the intercept term. (A + B) is postulated to represent the solvent polarity. The rates in different solvents were analysed in terms of equation (12), separately with A and B and with (A + B).

$\log k_2 = 1.23(\pm0.03)\ A + 1.62\ (\pm0.02)\ B - 3.92$ (14)
$R^2 = 0.9976$; sd = 0.02; n = 19; $\psi = 0.01$

$\log k_2 = 1.01\ (\pm0.53)\ A - 2.97$ (15)
$r^2 = 0.1710$; sd = 0.43; n = 19; $\psi = 0.94$

$\log k_2 = 1.53\ (\pm0.22)B - 3.68$ (16)
$r^2 = 0.7414$; sd = 0.24; n = 19; $\psi = 0.52$

$\log k_2 = 1.49\pm0.05\ (A + B) - 3.93$ (17)
$r^2 = 0.9792$; sd = 0.07; n = 19; $\psi = 0.15$

The rates of decomposition of the complex in different solvents showed an excellent correlation in Swain's equation [cf. Eq.14] with the cation solvating power playing the major role. In fact, the cation solvation alone account for ca. 74% of the data. The correlation with the anion solvating power was very poor. The solvent polarity, represented by (A + B), also accounted for ca. 98% of the data. In view of the fact that solvent polarity is able to account for ca.98% of the data, an attempt was made to correlate the rate with the relative permittivity of the solvent. However, a plot of log (rate) against the inverse of the relative permittivity is not linear

(r^2 = 0.4557; sd = 0.32; ψ = 0.76).

Mechanism:

In view of the absence of any effect of acrylonitrile on the rate of the reaction and failure to induce the polymerization of acrylonitrile, it is unlikely that a one-electron oxidation, giving rise to free radicals, is operative in this reaction. The presence of a substantial kinetic isotopic effect confirmed that a a C H bond is cleaved in the rate determining step. The observed solvent effect also indicated that the transition state of the reaction is more polar than the reactants.

For the formic acid oxidation, the cation solvating power of the solvents plays a relatively more important role, supporting the preposition that an electron-deficient carbon center is formed in the transition state. Thus the transfer of a hydride-ion from the acid to the oxidant is indicated.

This hydride ion transfer may take place either via an anhydride or by an acyclic process. The involvement of a concerted cyclic process is supported by a study of the temperature dependence of the kinetic isotope effect[19]. The data for protio and deuterio formic acids when fitted in the familiar expression $k_H/k_D = A_H/A_D \exp(-\Delta H^*/RT)$ show a direct correspondence with the properties of a symmetrically transition state in which the differences in the activation energies for the protio and deuterio compounds are equal to the differences in the zero point energies of the corresponding C H and C D bonds (ca. 4.5 kJ mol^{-1}) and the entropies of the activation of the respective reactions are almost equal.[20,21] Similar phenomena were observed earlier in the oxidation of benzhydrol by PCC[22] and of diols by BPCC[23]. Bordwell[24] has documented a very cogent evidence against the occurrence of concerted one step bimolecular processes by hydrogen transfer and it is evident that in the present studies also the hydrogen transfer does not occur by an acyclic biomolecular process. It is well established that intrinsically concerted sigmatropic reactions, characterised by transfer of hydrogen in a cyclic transition state, are the only truly symmetrical processes involving a linear hydrogen transfer[25]. Littler[26] has also shown that a cyclic hydride transfer, in the oxidation of alcohols by Cr(VI), involves six electrons and, being a Huckel type system, is an allowed process. Thus, a transition state having a planar, cyclic and symmetrical structure can be envisaged for the decomposition of the ester intermediate. Hence, the overall mechanism is proposed to involve the formation of a chromate ester in a fast pre equilibrium step and then a decomposition of the ester in a subsequent slow step via a cyclic concerted symmetrical transition state leading to the product (Schemes 1 and 2).

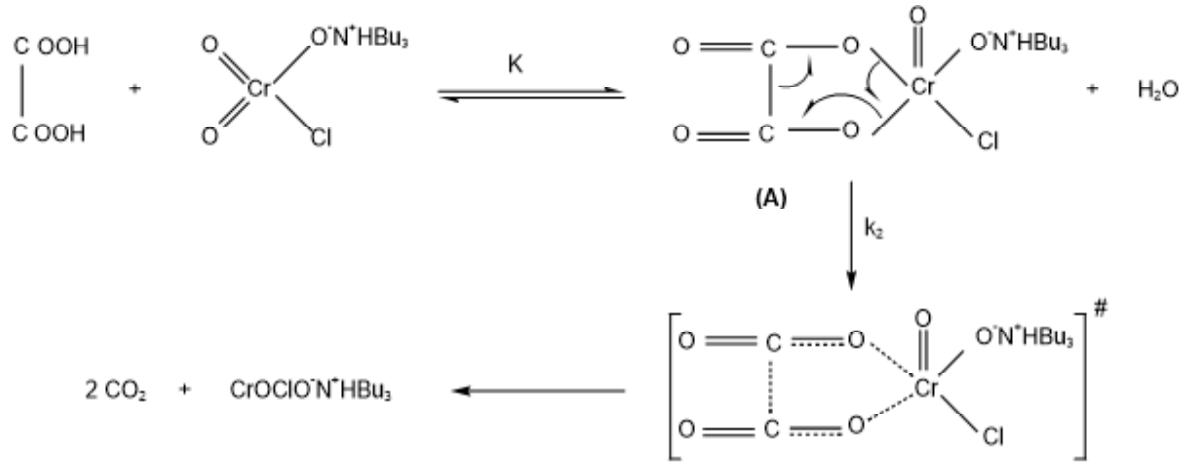

Scheme - 1 - Acid Independent Path

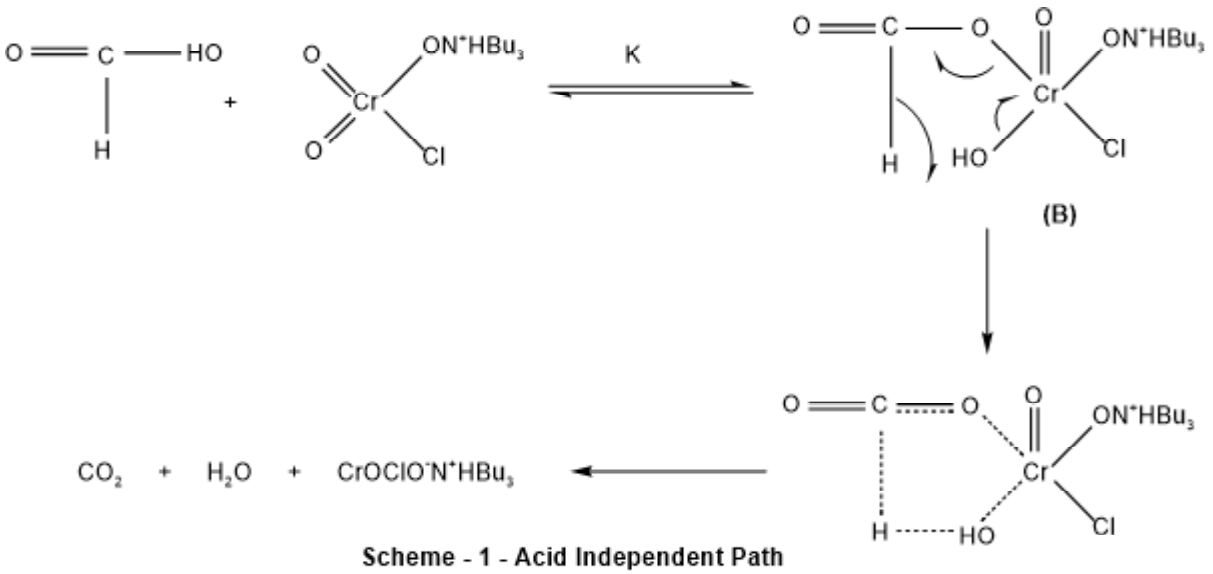

Scheme - 1 - Acid Independent Path

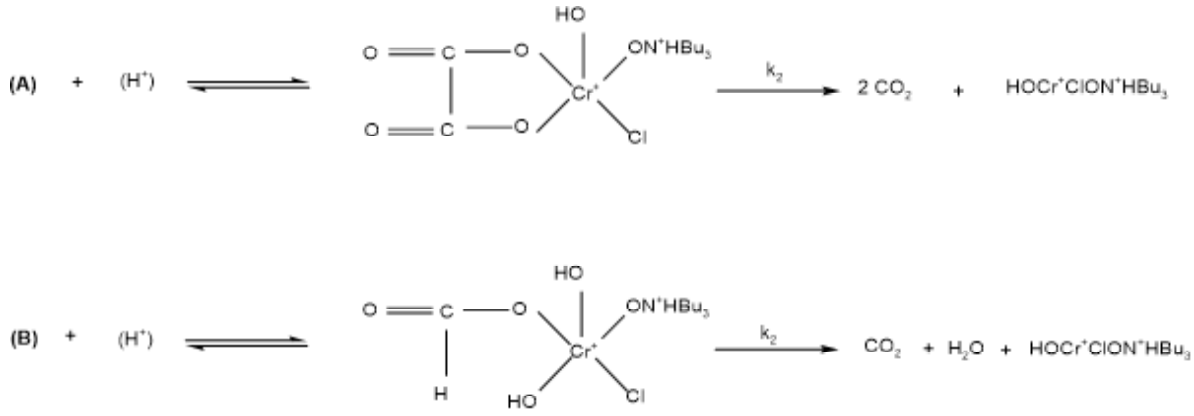

Scheme - 2 - Acid Dependent Path

It is of interest to compare here the mode of oxidation of organic acids by PFC[28], QFC[29], PBC[30], BTEACC[31] and TBACC. The oxidation by PFC, QFC, PBC and TBACC presented a similar kinetic picture, i.e. Michaelis Menten type kinetics, with respect to the reductants. However, the oxidation by BTEACC exhibited a first order dependence with respect to the reductants. It seems that the values of the formation constants for the intermediate compound are very small in the oxidation by BTEACC and is, therefore, not reflected in the rate-laws. Kinetic isotope effects, solvent effects and the dependence on the hydrogen ions are of similar nature in all these reactions, for which essentially similar mechanisms have been proposed.

Conclusions

The reaction is proposed to proceed through a hydride-ion transfer from acid to the oxidant. The hydride ion transfer mechanism is also supported by major role of cation solvating power of the solvents. Both deprotonated and protonated forms of TBACC are the reactive oxidising species. An α-C-H bond is cleaved in the rate-determining step.

Acknowledgement

Thanks are due to the UGC, New Delhi, India for financial assistance as UGC-BSR Startup Grant to PP and to NET-SRF to PN.

References

1. Corey E.J. and Suggs W.J., 1975, *Tetrahedron Lett.*, 2647.
2. Guziec F.S. and Luzio F.A., 1980, *Synthesis*, **(VII),** 691.
3. Bhattacharjee M.N., Choudhuri M.K., Dasgupta H.S., Roy N. and Khathing D.T., 1982, *Synthesis*, **7**, 588.
4. Balasubramanian K. and Prathiba V., 1986, *Indian J. Chem.*, **25B**, 326.
5. Ghammamy S. and Marazee M., 2005, *J. Serb. Chem. Soc.*, **70(5)**, 687.
6. Rao A., Purohit T., Swami P., Purohit P. and Sharma P.K., 2016, *Eur.Chem. Bull.*, **5(5),** 189.
7. Kamla, Pramila N., Priyanka P. and Sharma V. 2021, *Rasayan J. Chem.*, **Special Issue,** 217.
8. Inaniyan Y., Tak P., Naga P. and Purohit P., 2022, *Res. J. Chem. Environ.*, **26(9)**, 26.
9. Tak P., Inaniyan Y., Pramila N. And Purohit P., 2022, *J. Adv. Sci. Res.*, **13(4)**, 45.
10. Wiberg K.B. and Stewart R. 1956, *J. Am. Chem. Soc.*, **78**, 1214.
11. Perrin D.D., Armarego W.L. and Perrin D. R., 1966, Purification of Organic Compounds, Pergamon Press, Oxford.
12. Brown H.C., Rao G.C. and Kulkarni S.U., 1979, *J. Org. Chem.*, **44**, 2809.
13. Bhattacharjee M.N., Choudhuri M.K. and Purakayastha S., 1987, *Tetrahedron*, **43**, 5389.
14. Vadera K., Yajurvedi D., Purohit P., Mishra P. and Sharma P.K., 2010, *Prog. React. Kinet. Mech.*, **35**, 265.
15. Pohani S., Purohit P., Vyas S. and Sharma P.K., 2012, *J. Indian Chem. Soc.*, 2012, **89(3),** 363.
16. Exner O., 1966, *Collect Chem. Czech. Commun.*, **31**, 3222.
17. Kamlet M.J., Abboud J L M., Abraham M.H. and Taft R.W., 1983, *J. Org. Chem.*, **48**, 2877.
18. Swain C.G., Swain M.S., Pqwel A.L. and Alunni S., 1983, *J. Am. Chem. Soc.*, **105**, 502.
19. Kwart H. and Nickel J.H., 1953, *J. Am. Chem. Soc*., **95**, 3394.
20. Kwart H. and Latimer M.C., 1971, *J. Am. Chem. Soc.*, **93**, 3770.
21. Kwart H. and Slutsky J., 1972, *J. Chem. Soc. Chem. Commun*, **21**, 1182.
22. Banerji K.K., 1988, *J. Org. Chem.*, **53**, 2154.
23. Loonker K., Sharma P.K. and Banerji K.K., 1997, *J. Chem. Res.*, 1663. 24. Bordwell F.G., 1974, *Acc. Chem. Res.*, **5**, 374.
25. Woodward R.W. and Hoffmann R., 1969, *Angew. Chem. Int. Ed. Eng.*, **8**, 781.
26. Littler J.S., 1971, *Tetrahedron*, **27**, 81.
27. Gould E.S., 1964, Mechanism and structure in Organic Chemistry, Holt, Rinehart & Winston Inc., New York.
28. Asopa R., Mathur A. and Banerji K.K., 1992, *J. Chem. Res.*, 1117.
29. Khurana M., Sharma P.K. and Banerji K.K., 2000, *Proc. Indian Acad. Sci.*, **112**, 73.
30. Rathore S, Sharma P.K. and Banerji K.K., 1994, *J. Chem. Res.*, 504
31. Chouhan K. and Sharma P.K., 2004, *Indian J. Chem.*, **43A**, 1434.

Conference Alerts

1) IEEE-2023 The 7th International Conference on Green Energy and applications (ICGEA-2023)
March 10-12, 2023, Singapore
Website : http://www.icgea.org

2) 22nd International Conference on Medicinal and Pharmaceutical Chemistry
March 15-16, 2023, Vancouver, Canada
Contact : pharmaceuticalchemistry@annualamericacongress.org

3) World Summit on Organic and Inorganic Chemistry
March 15-16, 2023, London, UK
Contact : contact@globalconferencemeet.com

4) PITTCON Conference and Exposition
March 16-22, 2023, Philadelphia, PA, USA
Contact : info@pittcon.org
expo@pittcon.org
program@pittcon.org

5) International Conference on Chemistry and Applied Sciences
March 20-21, 2023, Rome, Italy
Contact : info@conference2go.com

6) 4th Global Summit on Catalysis and Chemical Engineering
April 13-14, 2023, Rome, Italy
Website : https://catalysis.mindauthors.com/

7) International Conference on Environmental Chemistry and Engineering
April 22, 2023, Belagavi, Karnataka, India
Contact : info@sciencesociety.co

8) 3rd International Conference on Materials Chemistry and Environmental Engineering
May 18, 2023, Stanford, USA
Website : https://www.confmcee.org

9) 3rd Edition of International Conference on Green Chemistry and Renewable Energy (Green Chemistry 2023)
May 22-23, 2023, Tokyo, Japan
Contact : info@conference2go.com

10) International Conference on Chemistry, Chemical Engineering and Biology
May 24-26, 2023, Bangkok, Thailand
Website : https://www.icccb.net/

11) 36th Kuala Lumpur International Conference on Chemical, Biological, Environmental and Natural Resources (CBENR-23)
May 30-June 1, 2023, Kuala Lumpur, Malaysia
Website : http://cbmsr/org/conference.php?slug=CBENR-23@catDid=307

12) 3rd Edition of Chemistry World Conference
June 14-15, 2023, Rome, Italy
Website : https://chemistryworldconference.com/

13) 13th International Chemistry Conference on "Novel Approaches and Innovations in Chemistry Research"
June 28-29, 2023, Paris, France
For registration contact : finance@conferenceseries.com

RNI No. MAHENG / 2017 / 74063
VOLUME 7 (Issue 1) January - June 2023

ISSN No. 2581-5911
BI-ANNUAL SUBSCRIPTION : Rs. 2000/-

G P GLOBALIZE RESEARCH JOURNAL OF CHEMISTRY

VOLUME 7 (Issue 1) January - June 2023
BI-ANNUAL 2023

GAURANG PUBLISHING

GAURANG PUBLISHING GLOBALIZE PRIVATE LIMITED

1, Plot-72, P.M.M.M. Marg, Tardeo, Mumbai-400034. **Tel.:** 022 23522068 **(M) :** +91 9969392245
Email : gpglobalize@gmail.com | **Web :** www.gpglobalize.in

CIN No. U22130MH2016PTC287238 | UAN - MH19D0008178